# NAVAL POSTGRADUATE SCHOOL
## Monterey, California




# THESIS

**COMPARISON OF TRAJECTORIES GENERATED BY THE NOAA OIL SPILL MODEL TO TRAJECTORIES PRODUCED USING HF RADAR-DERIVED CURRENTS IN MONTEREY BAY**

by

Margaret A. Smith

September, 1997

| | |
|---|---|
| Thesis Advisor: | Jeffrey D. Paduan |
| Second Reader: | Mary L. Batteen |

**Approved for public release; distribution is unlimited.**

# REPORT DOCUMENTATION PAGE

*Form Approved*
*OMB No. 0704-0188*



| 1. AGENCY USE ONLY *(Leave blank)* | 2. REPORT DATE | 3. REPORT TYPE AND DATES COVERED |
|---|---|---|
| | September, 1997 | Master's Thesis |

**4. TITLE AND SUBTITLE** COMPARISON OF TRAJECTORIES GENERATED BY THE NOAA OIL SPILL MODEL TO TRAJECTORIES PRODUCED USING HF RADAR-DERIVED CURRENTS IN MONTEREY BAY

**5. FUNDING NUMBERS**

**6. AUTHOR(S)** Smith, Margaret A.

**7. PERFORMING ORGANIZATION NAME(S) AND ADDRESS(ES)**
Naval Postgraduate School
Monterey, CA 93943-5000

**8. PERFORMING ORGANIZATION REPORT NUMBER**

**9. SPONSORING / MONITORING AGENCY NAME(S) AND ADDRESS(ES)**

**10. SPONSORING / MONITORING AGENCY REPORT NUMBER**

**11. SUPPLEMENTARY NOTES**
The views expressed in this thesis are those of the author and do not reflect the official policy or position of the Department of Defense or the U.S. Government.

**12a. DISTRIBUTION / AVAILABILITY STATEMENT**
Approved for public release; distribution is unlimited.

**12b. DISTRIBUTION CODE**

## 13. ABSTRACT *(maximum 200 words)*

HF radar-derived surface current data was examined for use in oil spill trajectory prediction in Monterey Bay. Trajectories produced by the NOAA/HAZMAT On-Scene Spill Model, using different combinations of surface currents and winds, were compared to trajectories generated using HF radar-derived surface currents. Currents examined included output from the NOAA circulation model and canonical-day averages of the HF radar-derived current maps, either as spatially constant but temporally varying currents (time file) or spatially varying two-hourly current patterns (grids). Results from OSSM using the NOAA circulation model currents did not compare favorably with HF radar-derived trajectories inside Monterey Bay. OSSM produced realistic overall trajectory patterns throughout the Bay using the canonical-day grid current files and, to a lesser degree, canonical-day time file currents. Both OSSM and HF radar-derived trajectories show sensitivity to release time. In the afternoon, trajectories display rapid southeastward flow. At night, currents are weaker. The week's worth of direct surface current data used in this study was found to be representative of the seasonal summertime pattern in Monterey Bay and provided realistic current patterns for use in OSSM for initial trajectory prediction in lieu of real-time HF radar-derived surface currents.

| 14. SUBJECT TERMS | 15. NUMBER OF PAGES |
|---|---|
| HF radar-derived surface currents, oil spill trajectory prediction, NOAA On-Scene Spill Model (OSSM) | 112 |
| | 16. PRICE CODE |

| 17. SECURITY CLASSIFICATION OF REPORT | 18. SECURITY CLASSIFICATION OF THIS PAGE | 19. SECURITY CLASSIFI- CATION OF ABSTRACT | 20. LIMITATION OF ABSTRACT |
|---|---|---|---|
| Unclassified | Unclassified | Unclassified | UL |

NSN 7540-01-280-5500

Standard Form 298 (Rev. 2-89)
Prescribed by ANSI Std. 239-18

**Approved for public release; distribution is unlimited**

# COMPARISON OF TRAJECTORIES GENERATED BY THE NOAA OIL SPILL MODEL TO TRAJECTORIES PRODUCED USING HF RADAR-DERIVED CURRENTS IN MONTEREY BAY

Margaret A. Smith
Lieutenant Commander, United States Navy
B. S., Jacksonville University, 1988

Submitted in partial fulfillment of the
requirements for the degree of

**MASTER OF SCIENCE IN METEOROLOGY AND PHYSICAL OCEANOGRAPHY**

from the

**NAVAL POSTGRADUATE SCHOOL**
**September, 1997**

Author: Margaret A. Smith
Margaret A. Smith

Approved by: Jeffrey D. Paduan
Jeffrey D. Paduan, Thesis Advisor

Mary L. Batteen
Mary L. Batteen, Second Reader

Robert H. Bourke
Robert H. Bourke, Chairman, Department of Oceanography

## ABSTRACT

HF radar-derived surface current data was examined for use in oil spill trajectory prediction in Monterey Bay. Trajectories produced by the NOAA/HAZMAT On-Scene Spill Model, using different combinations of surface currents and winds, were compared to trajectories generated using HF radar-derived surface currents. Currents examined included output from the NOAA circulation model and canonical-day averages of the HF radar-derived current maps, either as spatially constant but temporally varying currents (time file) or spatially varying two-hourly current patterns (grids). Results from OSSM using the NOAA circulation model currents did not compare favorably with HF radar-derived trajectories inside Monterey Bay. OSSM produced realistic overall trajectory patterns throughout the Bay using the canonical-day grid current files and, to a lesser degree, canonical-day time file currents. Both OSSM and HF radar-derived trajectories show sensitivity to release time. In the afternoon, trajectories display rapid southeastward flow. At night, currents are weaker. The week's worth of direct surface current data used in this study was found to be representative of the seasonal summertime pattern in Monterey Bay and provided realistic current patterns for use in OSSM for initial trajectory prediction in lieu of real-time HF radar-derived surface currents.

## TABLE OF CONTENTS

## ACKNOWLEDGEMENT

I would like to thank Professor Paduan for his expertise and guidance throughout this thesis. Additionally, I would like to thank Glen Watabayashi at NOAA/HAZMAT for providing the On-Scene Spill Model software, digitized file of Monterey Bay and the output from the NOAA circulation model as well as answering all my questions about running the model and setting up the related files. Finally, I want to express my heartfelt thanks to Mike Cook of the NPS Oceanography Department for his assistance with my computer programing.

# I. INTRODUCTION

Monterey Bay, located within the Monterey Bay National Marine Sanctuary, is a highly sensitive and dynamically complex ocean environment (Figure 1). The Bay has a unique biological diversity of marine life. The economics of the coastal communities are dependent on its biological productivity, which is critical to fishing industries as well as local tourism. There is the additional presence of the deep Monterey Submarine Canyon just offshore of Moss Landing which leads to a complex shelf bathymetry in the Bay. With these unique biological and physical environments–and the presence of various academic and research facilities including Moss Landing Marine Lab, Long Marine Lab at Santa Cruz, Monterey Bay Aquarium Research Institute, Naval Postgraduate School and Hopkins Marine Station–Monterey Bay is an area of increasing focus in marine science.

Ocean surface currents in Monterey Bay are the primary contributors in the movement and distribution of material floating in the Bay. Patterns in the surface currents suggest regions of convergence and divergence. Convergence areas indicate where material floating on or near the surface will concentrate and collect, such as nutrients, associated biological organisms and spilled oil or other hazardous material. Additionally, waves and winds influence the movement of objects floating on the ocean surface.

This study compares trajectories for this open-ocean coastal environment computed using the National Oceanic and Atmospheric Administration's (NOAA) On-

Scene Spill Model (OSSM), run with the surface current patterns calculated by NOAA's finite-element circulation model, against trajectories computed from HF radar-derived surface currents. HF radar-derived surface current maps better describe the complicated spatial and temporal patterns associated with the Bay. Oil spill trajectories computed using these measured currents as input in OSSM should, therefore, provide a more realistic analysis of the possible oil movement. Additionally, already inherent in these surface current maps is most of the wind forcing from the sea breeze and waves. This study takes advantage of the extensive HF radar-derived current and moored wind measurements in Monterey Bay in order to assess the performance of NOAA's spill response protocol, and to suggest ways that OSSM in particular might by revised to better utilize existing measurements.

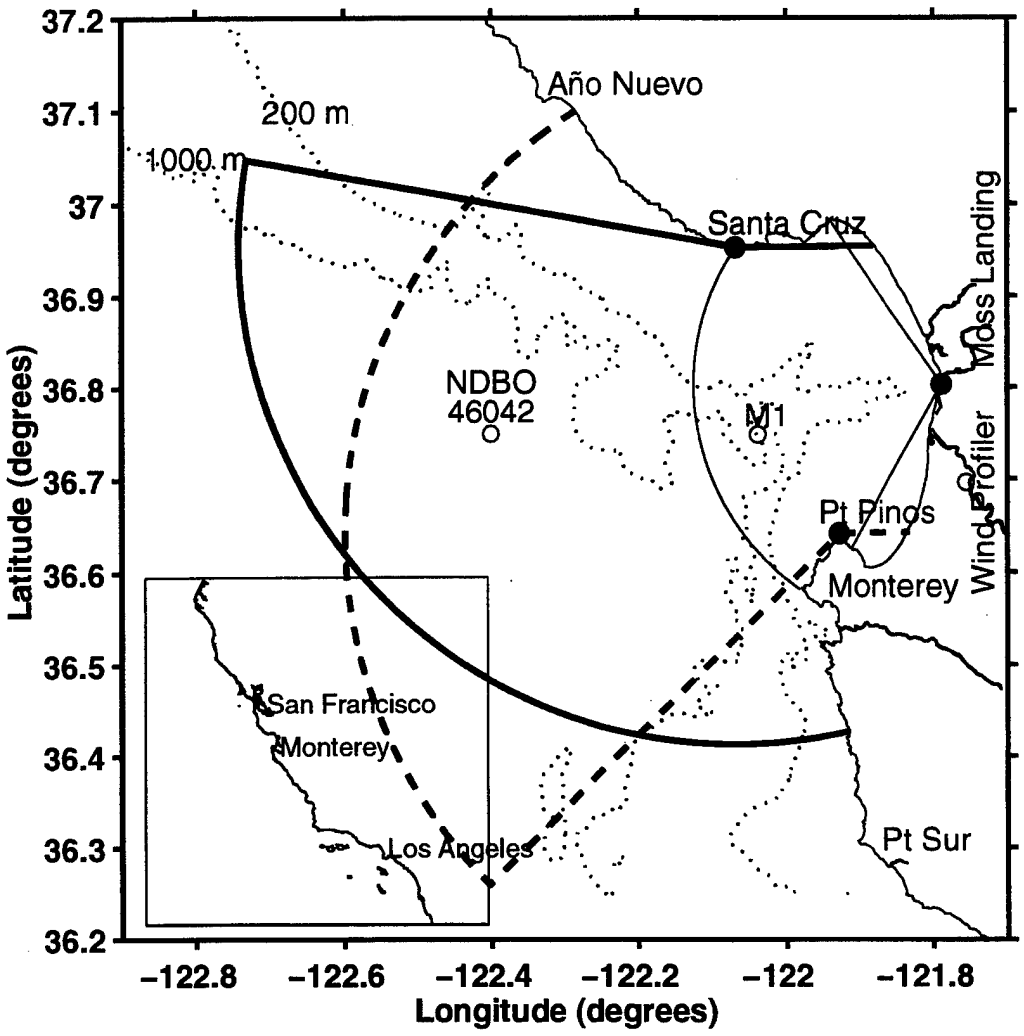


**Figure 1.** Map of Monterey Bay showing bathymetry and locations of the HF radar network, current and wind buoys and the vertical wind profiler (after Paduan and Rosenfeld, 1996).

# II. BACKGROUND

## A. HAZARDOUS SPILL CONTAINMENT

Because of the environmentally sensitive nature of Monterey Bay, the ability to accurately predict and monitor the movement of an accidental discharge of oil or other hazardous waste in the Marine Sanctuary is critical. Oil spill monitoring and assistance in U.S. territorial waters is the responsibility of the National Oceanic and Atmospheric Association Hazardous Material Response and Assessment Division (NOAA/HAZMAT) based at Seattle, Washington. To assist in this process, they have developed a portable On-Scene Spill Model (OSSM) (Torgrimson, 1984). This model accepts a variety of databases, such as climatological winds, modeled currents and tidal data, and uses that information with real-time data, such as buoy winds, forecasted winds and local circulation patterns. All of the environmental data is considered with oil/petroleum characteristics and behavior to predict the movement and concentration of spilled oil or other hazardous material during an emergency.

### 1. Factors Influencing Movement of Spills

In oil spill trajectory modeling, surface winds and ocean surface currents are the primary predictors of oil movement (Overstreet and Galt, 1995; Galt, 1994). In Monterey Bay, wind patterns are driven by the large scale synoptic flow as modified by coastal influences. The large scale offshore winds can be divided into summer and winter patterns. In the summer, the subtropical anticyclone is centered near 40°N and winds are generally out of the north northwest with little synoptic activity to vary this. In the winter,

synoptic activity increases and the offshore subtropical high is weakened and shifted to near 30°N (Nuss, 1996). Along the coast mesoscale meteorological effects become significant influences in actual wind direction. In Monterey Bay the largest coastal wind effect is the sea breeze circulation (Foster, 1993). The sea breeze sets up in response to the differential heating of the Salinas Valley in the east and the ocean to the west (Stull, 1988). The direction of the wind flow is also complicated by the presence of coastal mountain ranges. North of Monterey Bay, the Santa Cruz mountains extend from San Francisco south to Santa Cruz. To the south of the Bay the Salinas Valley extends from Moss Landing to King City and is bounded to the west by the Santa Lucia coastal mountain range (Figure 2). The net effect is to steer the sea breeze to the southeast down the Salinas Valley (Foster, 1993). The sea breeze initially begins along the coast and then extends over water. As the land cools in the evening, the process reverses, first inside the Bay and finally along the coast (Hsu, 1988; Stull, 1988). However, an offshore flow, or land breeze, is seldom seen in this area (Foster, 1993).

Another consideration in oil spill trajectory analysis is the ocean surface current. Monterey Bay has a complicated shelf bathymetry, particularly the deep Monterey Submarine Canyon. Outside Monterey Bay, ocean currents are dominated by the California Current System, which has been variously described as either a southward meandering jet or as a mesoscale eddy field embedded in a southerly flow (Strub et al., 1991). The system becomes most heterogeneous during the late spring through early fall during the upwelling season when cold filaments are observed to be drawn offshore. Associated cyclonic eddies are located southwest of capes and inshore of the main

southward current producing an offshore flow of cold water. Paired counter-rotating eddies are often associated with these features (Strub et al., 1991; Rosenfeld et al., 1994).

The upwelling centers affecting Monterey Bay are located to the north and south at Pt Año Nuevo and Pt Sur, respectively (Figure 1). There is a suggestion of a persistent warm anticyclonic eddy feature outside the Bay and to the south (Rosenfeld et al., 1994). By the end of the summer upwelling period a 20 to 30 $cms^{-1}$ southward current is present outside Monterey Bay. By October, upwelling is reduced as a result of the decrease in the overall wind stress and the nearshore surface current comes under the influence of the northward flowing Davidson Current (Bakun and Nelson, 1991; Chelton, 1984). The flow between Pt Año Nuevo and Pt Conception is variable in October but, by January, the Davidson Current is well established south of Pt Sur (Chelton, 1984).

The circulation patterns within Monterey Bay have been studied and mapped with an HF radar network (Paduan and Rosenfeld, 1996). This shows the late summer and fall circulation to have a southward flow outside the mouth of the Bay of approximately 20 $cms^{-1}$ mean speed. Inside the Bay the five month average shows a single circulation cell with cyclonic rotation centered 15 km northwest of Moss Landing and an anticyclonic circulation cell is suggested between Moss Landing and the Monterey Peninsula with weak currents, less than 3 $cms^{-1}$. A predominately northward mean flow exists along the coast at 5 to 7 $cms^{-1}$.

## 2. Physical Oil Processes

A comparison of oil behavior versus Lagrangian trajectories is difficult because of the complex behavior of spilled oil. As a result, the modeling of oil movement has

become a compilation of algorithms and various rules of thumb. True oil behavior is a complicated interaction between its chemical characteristics and the physical processes of the environment.

Spilled oil characteristics which influence its movement include pour point, density, surface tension and viscosity. The pour point is the temperature below which the oil will congeal. Density indicates whether the oil will sink or float. The surface tension and viscosity of the oil influences how it will flow, whether in thin filaments or droplets. Additionally, the spilled oil can be a mix of various chemical constituents, each with its own evaporation characteristics. (Overstreet and Galt, 1995)

The physical processes affecting spilled oil movement include ocean current circulation with its associated divergence and convergence areas as well as wave and wind effects. Oil closely follows the surface circulation pattern with the divergence and convergence areas indicating where oil will concentrate. Small capillary waves will tend to compress the oil from all directions thus inhibiting its spread (Galt, 1994). Stokes drift results in a small movement of the oil in the wave direction (Gill, 1982; Pond and Picard, 1989). Wind-driven surface gravity waves have the largest effect by "pushing" the oil on top of the water in the direction of the wind. This differential oil-water slip is similar to the Stokes drift. Oil movement due to this differential oil-water slip has been measured to be between 0.7 to 1.4 percent of the wind velocity (Galt, 1994). Additionally, some oil dispersion is related to wave breaking. The turbulence drives the oil under the water surface causing the oil to sink. This oil tends to reappear when the surface becomes calm. Lastly, Langmuir cells form. These bands of convergence and divergence orient

along the direction of wind flow, complicating the downwind movement of oil, and inhibit oil movement due to compressional wind stresses. As a rule of thumb, total oil movement due to wind and waves is approximately three percent of wind speed, in the direction of the wind, superimposed on the surface current field, although other studies have indicated this could be as low as one percent depending on the weathering of the oil. (Torgrimson, 1984; Galt, 1994)

Other physical oil characteristics are not represented well in trajectory analyses. Nearshore processes such as longshore currents and rip currents are not included. Although simple tidal height effects are included, tidal current effects in coastal areas like Monterey Bay are not well represented. Battisti and Clarke (1982) calculated that just outside the Bay barotropic M2 tides are on the order of 4 $cms^{-1}$ along shore and 0.3 $cms^{-1}$ cross shore, but Petruncio (1993, 1996) has shown that tidal currents five times larger than this occur in portions of Monterey Bay, such as over the head of the canyon, due to internal tides.

## B. HF RADAR-DERIVED SURFACE CURRENTS

Ocean surface currents can be evaluated remotely by HF radar. Ocean surface waves have wavelengths comparable to HF frequencies (3 to 30 Hz in the electromagnetic frequency spectrum). Using the principle of Bragg backscatter, large peaks are present in the spectral return due to resonance with ocean waves whose wavelengths are one-half the wavelength of the incident HF. These peaks correspond to the combination of the surface waves flowing over the ocean surface current,

propagating radially to or from the radar. The Doppler shift of these peaks from the incident HF frequency reflects the motion of the surface gravity waves plus the underlying ocean current. Factoring out the speed of the gravity waves in deep water, $c^2=g\lambda/2\pi$, where g is the gravitational acceleration and $\lambda$ is the wavelength of the ocean waves. The surface current estimate is an average down to, approximately, 1 m based on the depth of influence of the surface waves. (Barrick et al., 1977; Stewart and Joy, 1974)

Each backscattered energy spectrum will have large spectral peaks, but in practice many observations are averaged over a large area to improve the statistics. A single radar observation bin is on the order of 1 to 3 km wide and 1 hour in duration. The resolution of approaching or receding (radial) current speeds is 4 $cms^{-1}$. The range is 50 or 60 km from each radar (Paduan et al., 1995; Barrick et al., 1977; Figure 1). Surface current trajectories previously calculated using the HF radar-derived data closely resemble actual trajectories from drifter studies in the Bay (Paduan et al., 1996).

### 1. HF Radar Network in Monterey Bay

Two types of ocean surface current detecting HF radar systems have been operated in Monterey Bay. One is the Ocean Surface Current Radar (OSCR) which uses a phased array pointing method of determining direction. The other system determines direction by using the different beam patterns created by co-located looped orthogonal antennas. This second type, named Coastal Ocean Dynamics Application Radar (CODAR) initially developed by the NOAA Wave Propagation Laboratory, was further developed by Codar Ocean Sensor, LTD. The second generation of CODAR-type HF radars is called SeaSonde. Each CODAR has two crossed looped orthogonal antennas

plus a monopole antenna in its center with known different beam patterns as a function of angle. This system compares the relative amplitudes of the returned energy of the various co-located antennas. The ratio of returned signal strength is used to determine the direction from which the signal originated (Barrick et al., 1977; Paduan and Rosenfeld, 1996; Paduan et al., 1995).

Two CODARs owned by NOAA were installed around Monterey Bay in 1992: one at Hopkins Marine Station near Monterey at the south end of the Bay; and one at Moss Landing (MBARI). These were the older generation CODAR systems. In 1993 and 1994 HF radar coverage increased to three SeaSonde systems: one operated by Stanford University at Granite Canyon Marine Laboratory; one operated by NPS at Pt Pinos at the southern tip of Monterey peninsula; and one operated by NOAA at the Long Marine Laboratory at the University of California at Santa Cruz. An older CODAR system was still in use at Moss Landing. At the time of this study, in September 1994, the HF radar system around Monterey Bay consisted of two SeaSonde systems (Pt Pinos and Santa Cruz) and a CODAR system at Moss Landing (Paduan and Rosenfeld, 1996; Figure 1).

### 2. Comparison of HF Radar-Derived Current Patterns to Oil Spill Trajectories

HF radar-derived current patterns can be considered to be fairly accurate representations of the actual ocean surface current in Monterey Bay. HF radar-derived currents are very near surface. The depth of this current layer measured is less than 1 meter and is dependent upon the waves which are being sampled by the HF radar. For

example, a 25 to 26 MHz signal corresponding to 12 m radar wavelength samples Bragg backscatter from 6 m waves. One "rule of thumb" listed by Barrick et al. (1977) is that the depth of the current layer is approximately $\lambda/2\pi$; Stewart and Joy (1974) estimated the depth of the measured surface current to be $\lambda/8$, where $\lambda$ is the wavelength of the waves sampled. Additionally, Foster (1993) found that the surface current response to the wind (sea breeze) forcing in Monterey Bay was rapid. Stronger winds over a longer period did not significantly strengthen the surface currents.

An evaluation of trajectories was conducted in August 1992 and October 1994 comparing HF radar (CODAR type) velocities with velocities of Argosphere type drifters (Paduan et al., 1996). These drifters are undrogued, 30 cm fiberglass spheres, equipped with batteries, antenna and an Argos transmitter, and were originally designed to follow oil floating on water. The trajectories of the drifters and those derived from the HF radar network were similar. During the August 1992 deployment, both the drifters and the derived trajectories first moved to the southeast in response to the sea breeze and then, within a few kilometers of the coast, turned northward. All beached within two to three days.

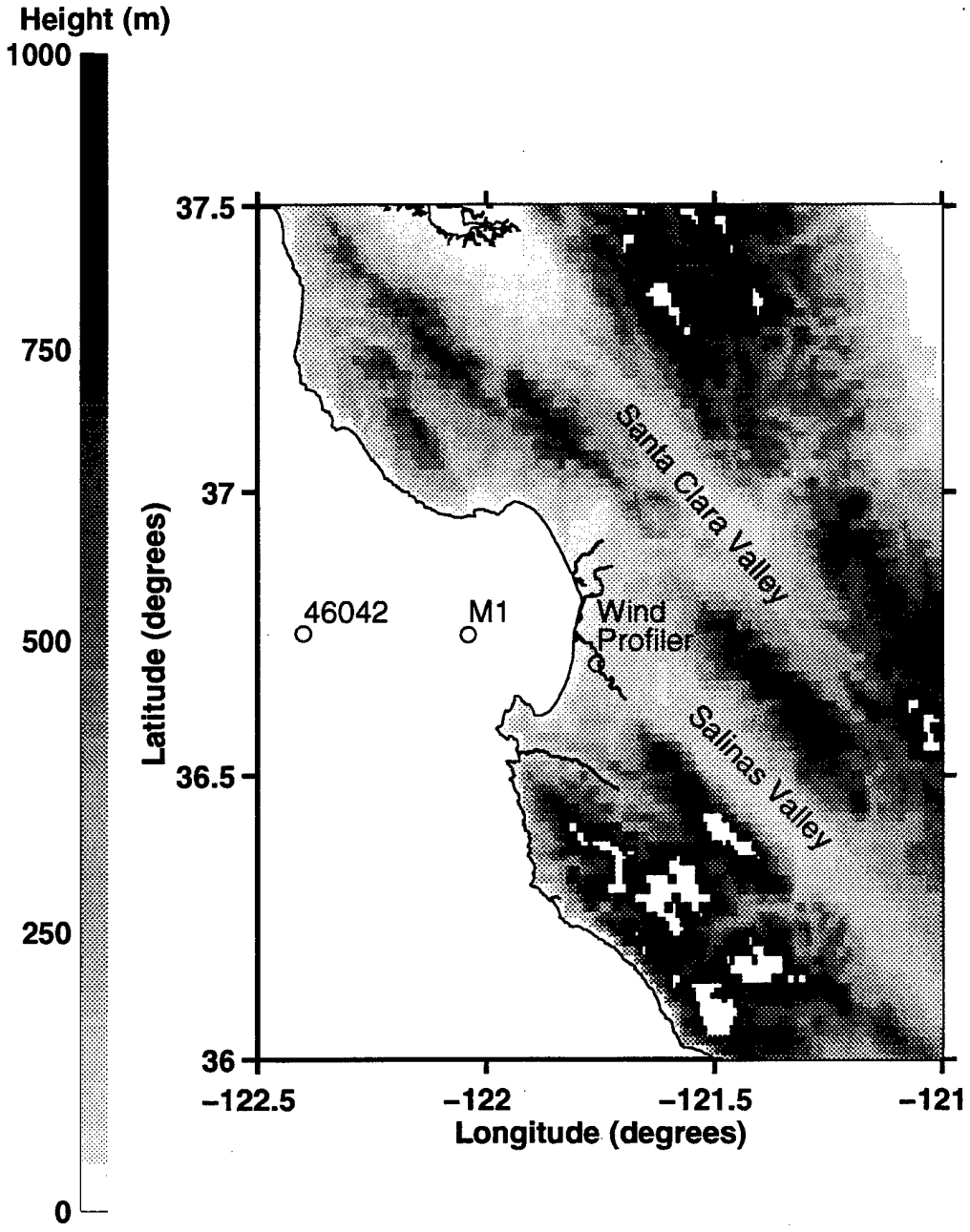


**Figure 2.** Map of Monterey Bay showing topography and locations of moored current and wind buoys and vertical wind profiler (after Boyer, 1997).

# III. METHODS

This study compared trajectories generated from the On-Scene Spill Model, using the NOAA circulation model current and different surface currents produced using HF radar-derived direct measurements, to trajectories produced by the HF radar-derived surface current maps, under different wind conditions. The test period for this study is 0000 PDT 9 September 1994 through 0000 PDT 15 September 1994, chosen because continuous surface current data from all three HF network sites as well as wind data from the two moored buoys and the vertical wind profiler was available. All HF radar-derived surface current data was post processed and not raw data. MATLAB was used to compute trajectories based on HF radar-derived surface current maps.

## A. DATA

### 1. Winds

The wind data was obtained from three sources: two current and wind buoys moored in Monterey Bay and a vertical wind profiler located near the coast (Figures 1 and 2). The NOAA NDBO 46042 mooring buoy is positioned at 36° 48′ N, 122° 24′ W, approximately 48 km due west of Moss Landing, with winds measured at 5 m above MSL. The M1 buoy is maintained by the Monterey Bay Aquarium Research Institute (MBARI) and is positioned at 36° 45′N, 122° 02.4′W, with wind data taken at 3.8 m above MSL. The vertical wind profiler is located at Fritsche Field, at the former Fort Ord, with the surface wind data measured at 53 m above MSL (Foster, 1993). Both

moored buoys recorded in PDT. The vertical wind profiler recorded in GMT and was converted to PDT. Only the hourly wind values were used in computations. There were no gaps in wind data for the time period selected. Figure 3 is the time series of the wind data used in both the OSSM- and the MATLAB-computed LE trajectory runs.

The wind time series are dominated by diurnal variations at the M1 buoy and the vertical wind profiler site. These variations are less evident at the NDBO 46042 buoy site. The entire time period selected does not show the usual pattern of coastal sea breeze southeast down the Salinas Valley. The vertical wind profiler recorded a slight mean southerly influence along the coast. This is not seen in either the NDBO nor the M1 buoys. Mean winds were out of the north northwest at NDBO and out of the northwest at M1, which are consistent with previous studies (Foster, 1993). The time period selected represents a compromise between "ideal" sea breeze patterns and good HF radar coverage.

### 2. Surface Currents

Figures 4 through 18 are surface current maps generated from the HF radar network for 9 through 13 September 1994, in four hourly intervals. The general flow of the surface current is southward outside the mouth of Monterey Bay. Inside Monterey Bay, these figures show an outflow from the Bay during the night, 0000 PDT through 0400 PDT. By 0800 PDT, the flow has turned northeastward. 1200 PDT shows a northeastward to eastward flow of the surface current toward the coast. The 1600 PDT maps display the strong southeastward flow in response to the sea breeze maximum at this time. By 2000 PDT, the flow is weakening and shifting southward and by 0000 PDT

the flow is out of the Bay once more. This overall nearly diurnal, anti-cyclonic rotation throughout the Bay is the response to the sea breeze forcing (Foster, 1993). These maps also display the day to day variation which occurs throughout this time period. Figures 4 and 7 show a strong nighttime outflow for 9 and 10 September 1994. By 12 and 13 September 1994, this nighttime outflow has lessened (Figures 13 and 16). Also suggested in these surface current maps is a cyclonic eddy feature in the northern part of Monterey Bay and an anti-cyclonic eddy feature outside the Bay.

## B. MODEL OUTPUT

### 1. On-Scene Spill Model

The On-Scene Spill Model (OSSM) was developed for use by NOAA/HAZMAT for oil spill response and designed to be taken to the site of the spill for on-scene prediction of oil movement to aid in clean up and recovery (Torgrimson, 1984). It is a flexible trajectory model capable of importing different databases in order to produce results in various output types and formats depending on need, such as concentration amounts, trajectories and receptor mode analysis.

Inputs generated external to the model include specifically formatted digitized shorelines, ocean surface currents, surface winds, tidal heights and tidal currents. The user can select diffusion, oil type, positions of oil elements and time of release. OSSM can be used with different databases such as climatological wind or current atlases for long term analysis or in the short term with a few days of meteorological wind forecasts,

archived tidal current data and current circulation model output or direct current measurements.

Map files of the coastline must be digitized separately. These are specifically formatted files of 48 lines by 80 columns, corresponding to 80 boxes in the east-west direction and 48 boxes in the north-south direction. For this study, one was provided by NOAA/HAZMAT for the Monterey Bay area.

The model creates Lagrangian element (LE) files which identify spilled material by latitude and longitude, release time, age and pollutant type. Selecting a preset pollutant type inputs a set percentage of constituents defined by half life and observational threshold. These parameters can be modified or new ones created as necessary. The Lagrangian elements themselves (i.e., sources of spilled oil) can be defined as point sources with a set start and stop of discharge; line sources with a set start and stop of discharge or as circular distributions randomly filled with any number of Lagrangian elements.

OSSM provides for oil diffusion and spreading as well. This can be turned on or off. By default a random walk diffusion is set in the model, with the number of steps per hour set for 1 and a horizontal eddy diffusivity constant of $1 \times 10^5$ $cm^2s^{-1}$.

Surface currents, winds, tidal height and tidal currents are included in OSSM trajectory analyses by adding them as grid files, time files or as combinations of both. Grid files are externally created files consisting of up to 960 lines identifying u- and v-components by latitude and longitude. These grids are used to create spatial 2-D patterns. OSSM separates grids into either "current" grids or "wind" grids. Grids designated as

current grids, by default, are assigned a "multiplicative" factor of 1 (a factor of 100 percent) so that the full u- and v-component of each latitude and longitude on the grid is used in the trajectory computation. Grid files defined as containing wind data default to a multiplicative factor of 0.03 (a factor of three percent). Only three percent of the surface wind value at each latitude and longitude on the grid is used in the trajectory computation. OSSM can use up to 12 grid files for each map. Grids are time invariant.

Temporal variation is introduced with time files. Time files are the second type of externally created files that OSSM uses for current and wind input. These formatted files identify u- and v-components by time. OSSM can use up to 10 time files for each map. Time files are spatially invariant and must be attached to a grid. The grid that time files are usually joined to consist of latitude and longitude patterns from zero to one for the u- and v-components. Joining a time file to one of these grids creates a simple time-varying spatial pattern. OSSM also assigns multiplicative factors to time files. Like grid files, current time files default to a multiplicative factor of 1 (a factor of 100 percent) and wind time files default to a multiplicative factor of 0.03 (a factor of three percent) (Torgrimson, 1984; Figure 19).

### 2. NOAA Circulation Model

As the first-guess current field for OSSM in oil spill trajectory prediction, NOAA/HAZMAT uses the output from the circulation model developed by Galt (1980). This model uses a finite element solution as opposed to a finite difference numerical solution usually used in oceanographic studies because of its ease to set up and represent the irregular and complex domains in coastal circulation. The basic flow is considered to

be slow, steady, with friction on the surface and bottom layers, hydrostatic and Boussinesq. These currents are geostrophic and subject to Ekman dynamics and include both baroclinic and barotropic flows (Gill, 1982). Specific boundary conditions will determine individual current flow patterns based on either bathymetry or coastlines. The current flow pattern is then scaled to match actual conditions (Galt, 1980; Han et al., 1980).

This circulation model was run by the NOAA/HAZMAT group for Monterey Bay and the resultant current field was provided. The details of the model set up, such as scale-large or small-and vertical resolution, were not provided. The resultant pattern for Monterey Bay is a constant current to the southwest. This suggests that the model was run on a large scale and a single point was provided for the area encompassing Monterey Bay. This current generally corresponds to the overall circulation outside the Bay, specifically the California Current (Strub et al., 1991; Rosenfeld et al., 1994). However, experiments both inside and outside Monterey Bay have found that drifter trajectories do not follow this overly simplified current, but that they are highly dependent on the local mesoscale features (Paduan et al., 1996; Davis, 1985).

## C. TRAJECTORY COMPUTATIONS

### 1. MATLAB-computed Trajectories

Trajectories calculated from HF radar-derived surface current maps were computed using MATLAB. Figure 20 shows the initial release positions of 25 Lagrangian Elements (LEs) that were used throughout this study. First, radial HF radar

data was converted to u and v vector components on a latitude and longitude grid every two hours (e.g., Figures 4 through 18 show every other map used). The u- and v-component of the nearest grid point to each LE in the 25-point array was taken to represent the current at the LE location each time step. The same was done for the three wind sites, NOAA NDBO buoy, M1 buoy and the vertical wind profiler. These closest wind components, u and v, were multiplied by either 0.01 (one percent winds) or 0.03 (three percent winds) and added to the u and v current components. The position of each LE was advanced with a time step of one hour using data from the two-hourly HF radar-derived current maps. The latitude and longitude position of each LE was saved every two hours. Table 1 lists the various combination of wind factors and release time used with the HF radar-derived currents in this study.

**Table 1.**

| MATLAB-run | Current | Wind | LE Release |
|---|---|---|---|
| 1 | HF radar-derived | none | 0000 PDT |
| 2 | HF radar-derived | three percent | 0000 PDT |
| 3 | HF radar-derived | one percent | 0000 PDT |
| 4 | HF radar-derived | one percent | 1600 PDT |

## 2. OSSM-generated Trajectories

For this study, NOAA/HAZMAT provided the FORTRAN compiled On-Scene Spill Model, a file containing the digitized Monterey Bay coastline and a file containing the circulation model output for Monterey Bay. The On-Scene Spill Model calculates trajectories by taking the closest u- and v-components of the current and wind to each Lagrangian Element (LE) and then moves each element forward in time. Positions were

computed in one hour increments and plotted every two hours. Lagrangian element files corresponding to the Figure 20 initial release positions were created with each LE defined as a point discharge source of a conservative substance. All OSSM grid files, both current and wind, were assigned a multiplicative factor of 1. All time files containing surface current data were assigned a multiplicative factor of 1 and time files containing winds were assigned a factor of 0.01 or 0.03. No directional offset was applied to the wind; dispersion was set to zero; and oil characteristics such as evaporation and weathering effects were ignored.

Tidal height and tidal currents are not separately considered in the OSSM-generated LE trajectories. Although tidal heights are important when oil is beached and subsequently subjected to re-floating, in this study the trajectories are stopped once they beach. Tidal currents are not explicitly included as input to the oil spill model, although their influence may be felt where the HF radar-derived canonical currents are used as described below.

Three type of currents fields were used as input to OSSM. First, the model output provided by NOAA/HAZMAT was used to simulate the first-guess field that would be used by that group were there an actual spill within the Monterey Bay National Marine Sanctuary. That current "field" consists of a constant flow to the southwest throughout the region. In addition to these currents, attempts were made to incorporate the actual currents measured by the HF radar network, within the framework of the latest version of OSSM. Because the model is not capable of directly accepting the spatially and temporally varying data, the observations were distilled into canonical, or average, daily

variations that were either constant in space with an appropriate time variation applied, or were constant in time with observed spatial variations (in order to incorporate this pattern variability through time, the model was run forward two hours and restarted with a new grid file and updated LE positions).

The canonical-day currents represent averages of the HF radar-derived surface current maps from 0000 PDT 9 September 1994 through 2200 PDT 14 September 1994 of those grid points containing current radial data at least 50 percent of the time. Figure 21 presents the mean surface current pattern for the entire study period while Figures 22 through 33 present the 12 two-hourly canonical-day surface current maps. As described above, two types of OSSM-formatted files were created from the canonical-day current maps: canonical-day grid currents and a canonical-day time file of the currents. The 12 canonical-day grid current files are just the direct conversion of the maps in Figures 22 through 33 into OSSM grid format. The canonical-day time file currents only includes only those grid points inside Monterey Bay between 121.8°W and 122°W. The u- and v-components for each two-hour interval in this area were averaged. Hourly values were produced by interpolation. Figure 34 shows the area used to extract the canonical-day current time series along with the resulting daily current variations repeated for the entire study period. Trajectory runs using these canonical-day time files ran quickly and easily on OSSM. The canonical-day grid files were more complicated; as mentioned above, the model had to be run forward in two-hourly increments for each grid.

Additionally, three wind grids were created to accompany the current grids in the various OSSM simulations in this study: one for the NOAA NDBO buoy, one for the M1

buoy and one for the vertical wind profiler. Each wind grid consisted of three latitude and longitude locations, corresponding to each wind source position with the u- and v-components either zero or one. For example, the M1 wind grid assigns u=1 and v=1 at the latitude and longitude of the M1 buoy and u=0 and v=0 at the other two latitude and longitude grid points. Time files containing the hourly wind data for each wind source was joined to its respective grid creating a simple 2-D surface wind pattern over Monterey Bay. Table 2 lists the separate OSSM trajectory runs.

**Table 2.**

| OSSM-run | Current | Wind | LE Release |
|---|---|---|---|
| 1 | NOAA circulation model | none | 0000 PDT |
| 2 | canonical-day time file | none | 0000 PDT |
| 3 | canonical-day grid | none | 0000 PDT |
| 4 | NOAA circulation model | three percent | 0000 PDT |
| 5 | canonical-day time file | three percent | 0000 PDT |
| 6 | canonical-day grid | three percent | 0000 PDT |
| 7 | canonical-day grid | one percent | 0000 PDT |
| 8 | canonical-day grid | one percent | 1600 PDT |

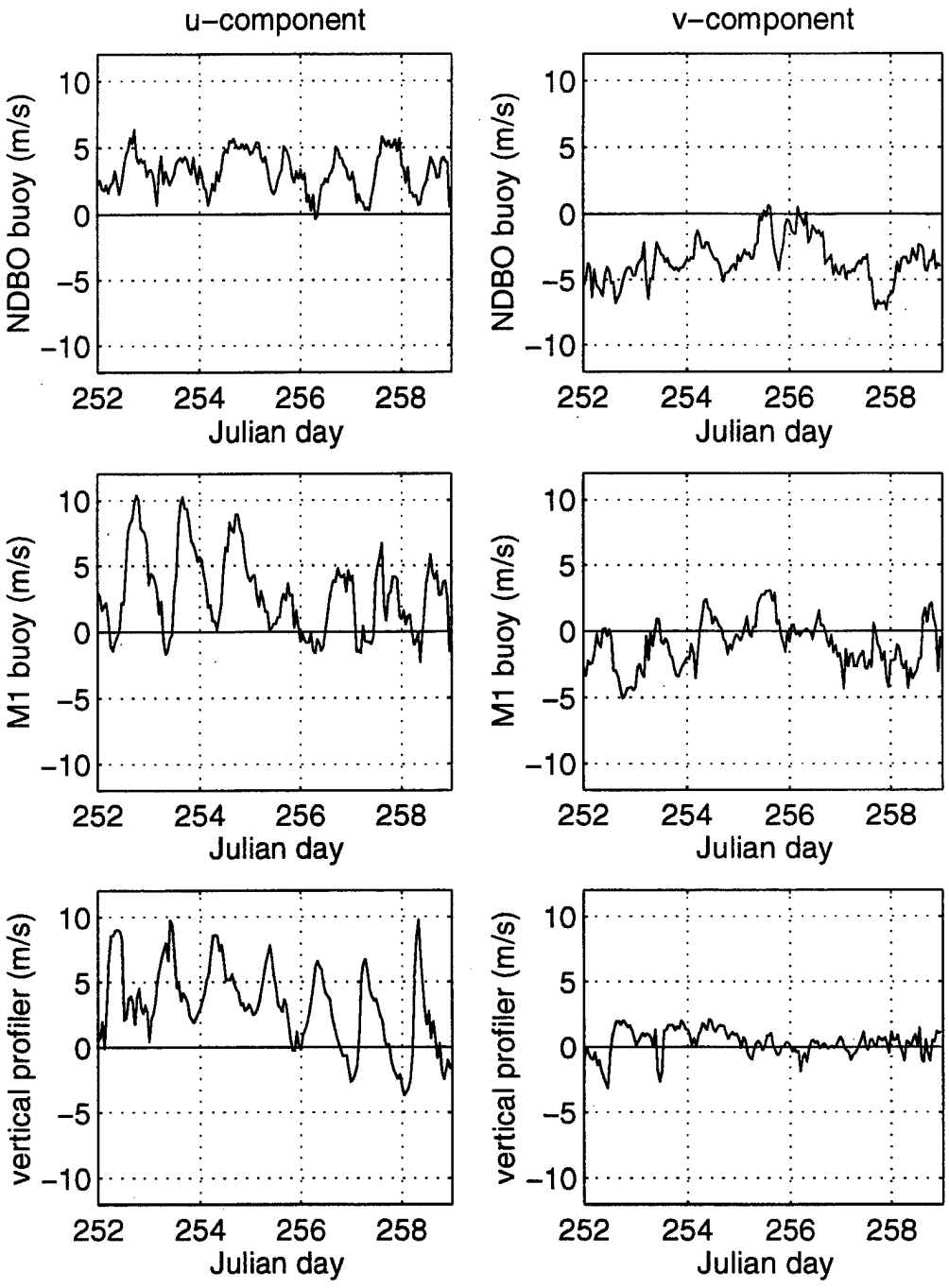


**Figure 3.** Time series of hourly winds from Julian day 252 to 258 (0000 PDT 9 September 1994 to 0000 PDT 15 September 1994) by u- and v-component. Upper panels are the NDBO 46042 buoy winds. Middle panels are the MBARI M1 buoy winds. Lower panels are the vertical wind profiler winds.

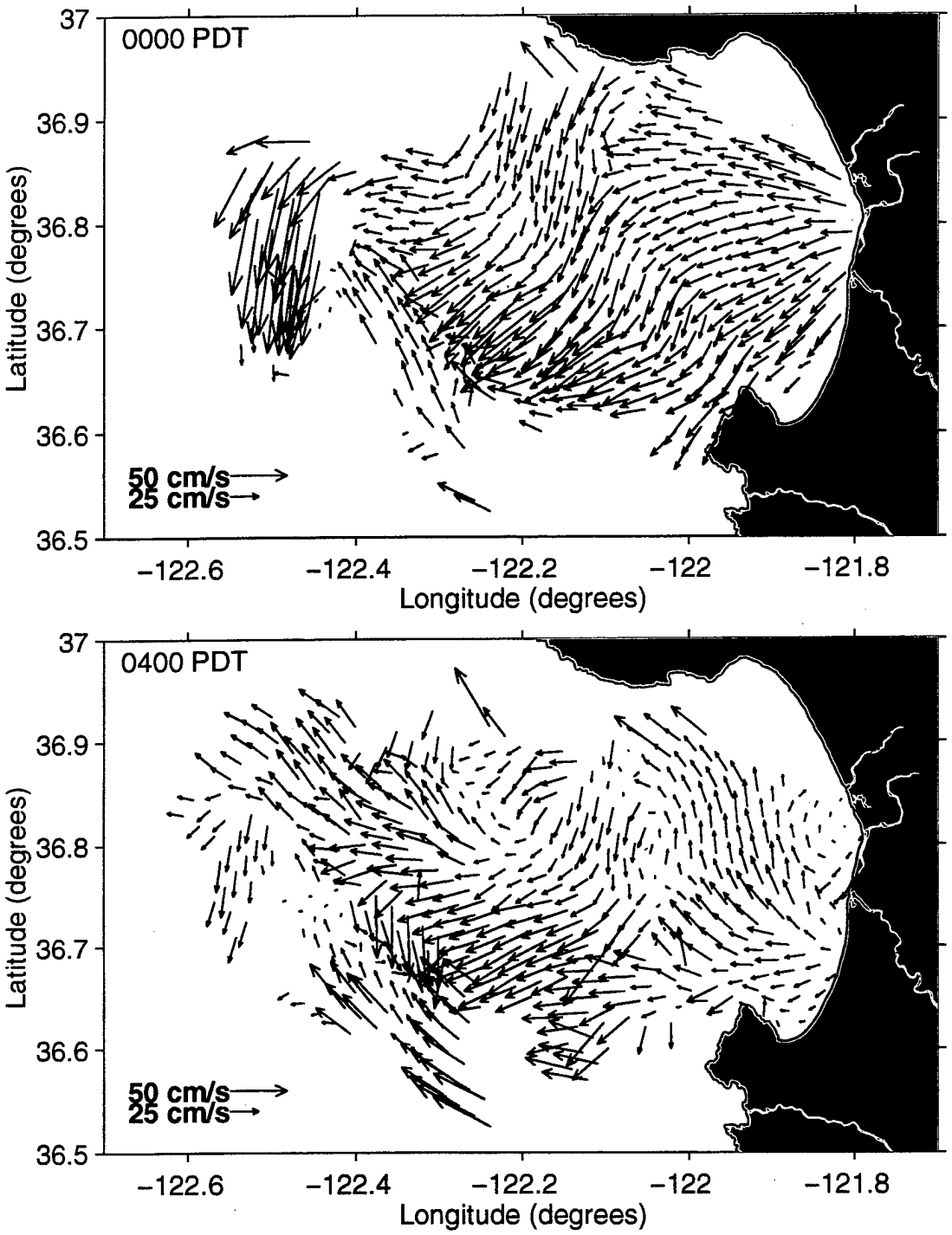


**Figure 4.** HF radar-derived surface current maps for 9 September 1994. Upper panel is 0000 PDT. Lower panel is 0400 PDT.

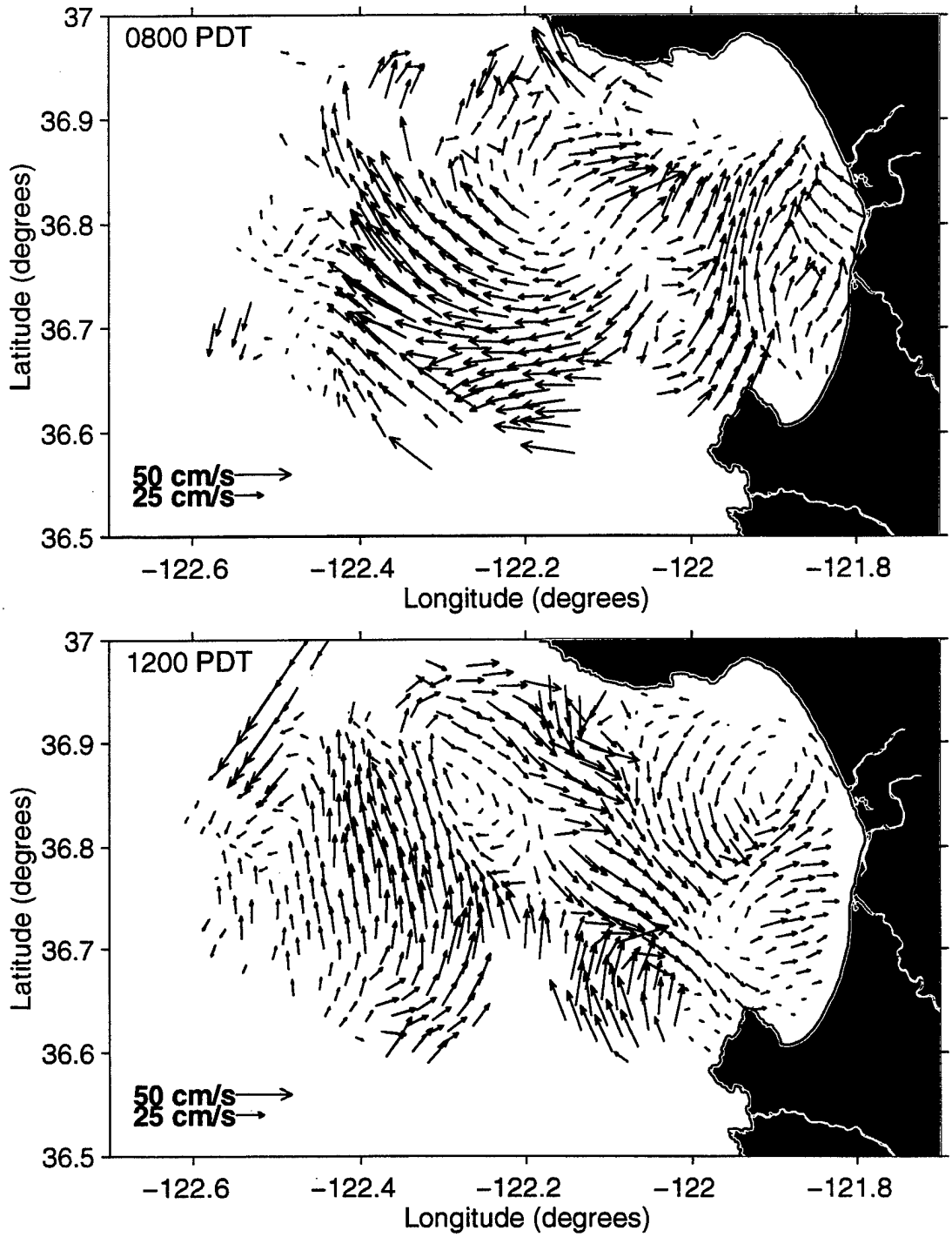


**Figure 5.** HF radar-derived surface current maps for 9 September 1994. Upper panel is 0800 PDT. Lower panel is 1200 PDT.

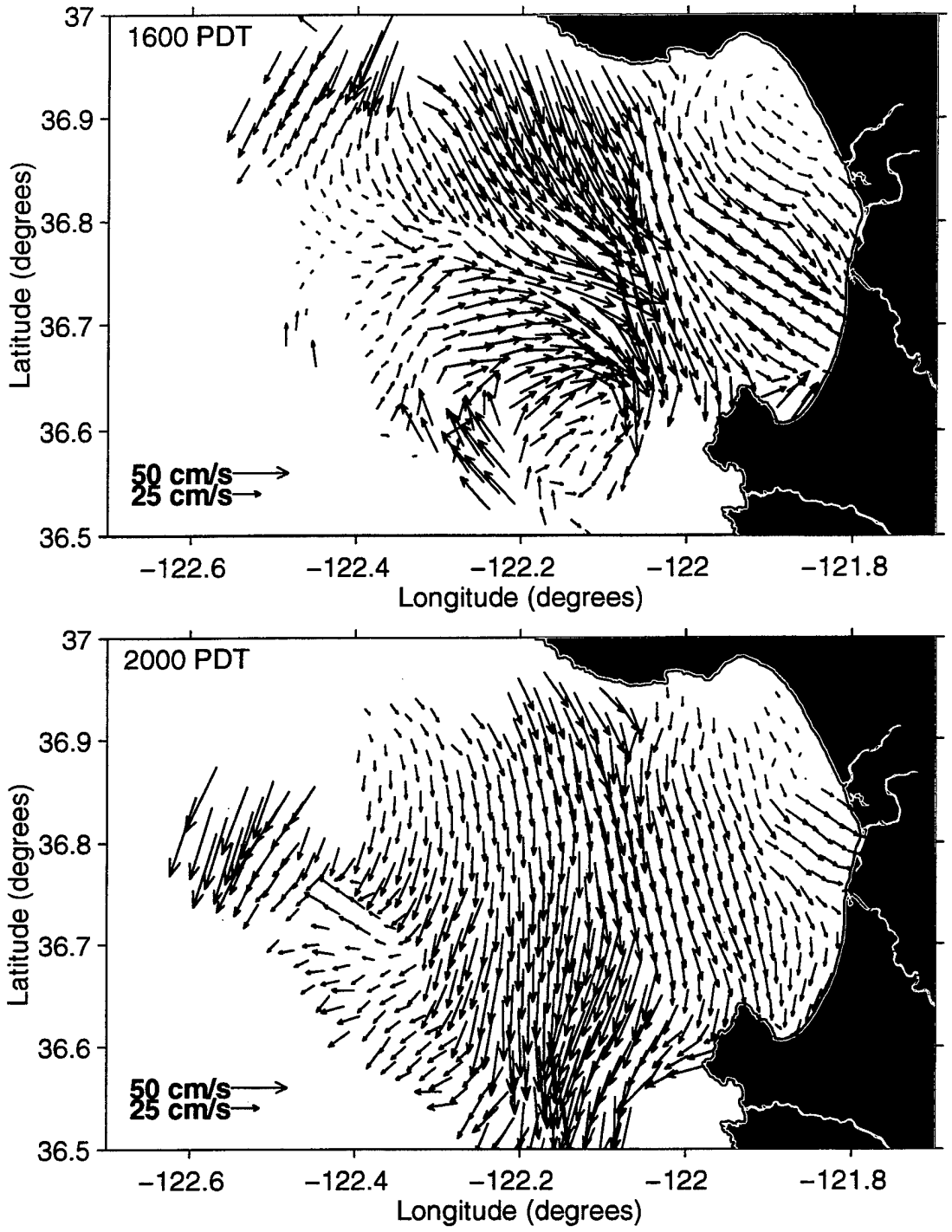


**Figure 6.** HF radar-derived surface current maps for 9 September 1994. Upper panel is 1600 PDT. Lower panel is 2000 PDT.

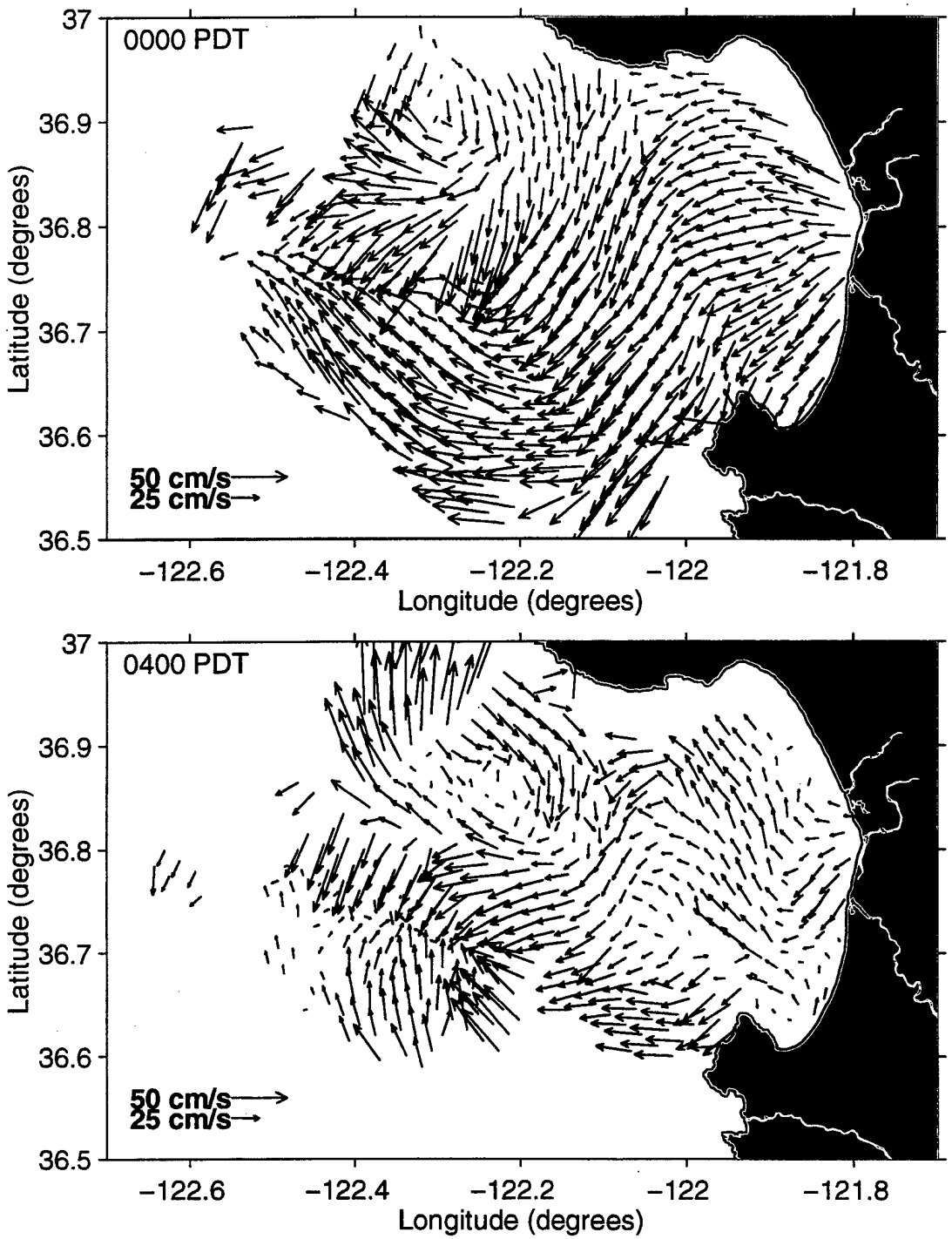


**Figure 7**. HF radar-derived surface current maps for 10 September 1994. Upper panel is 0000 PDT. Lower panel is 0400 PDT.

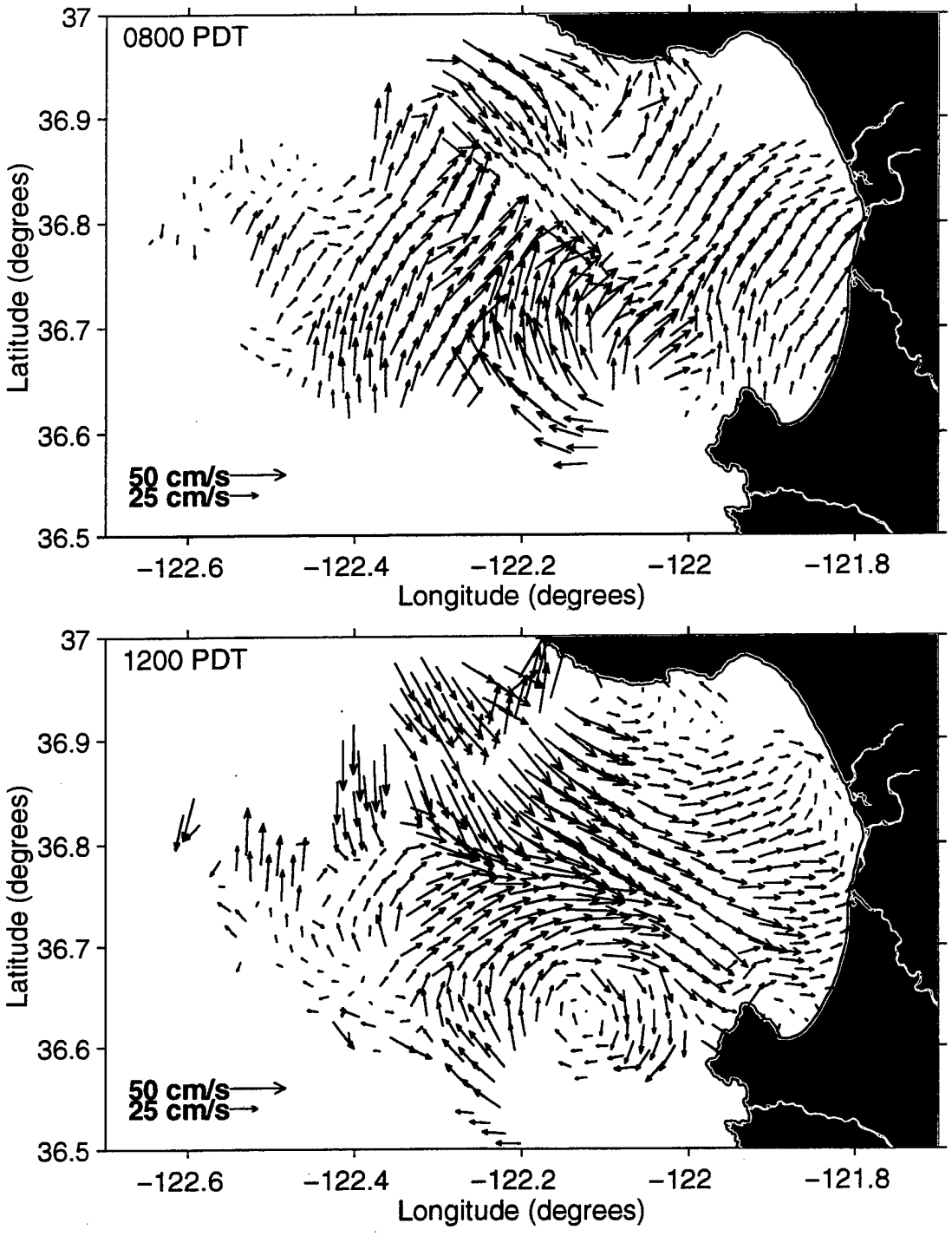


**Figure 8.** HF radar-derived surface current maps for 10 September 1994. Upper panel is 0800 PDT. Lower panel is 1200 PDT.

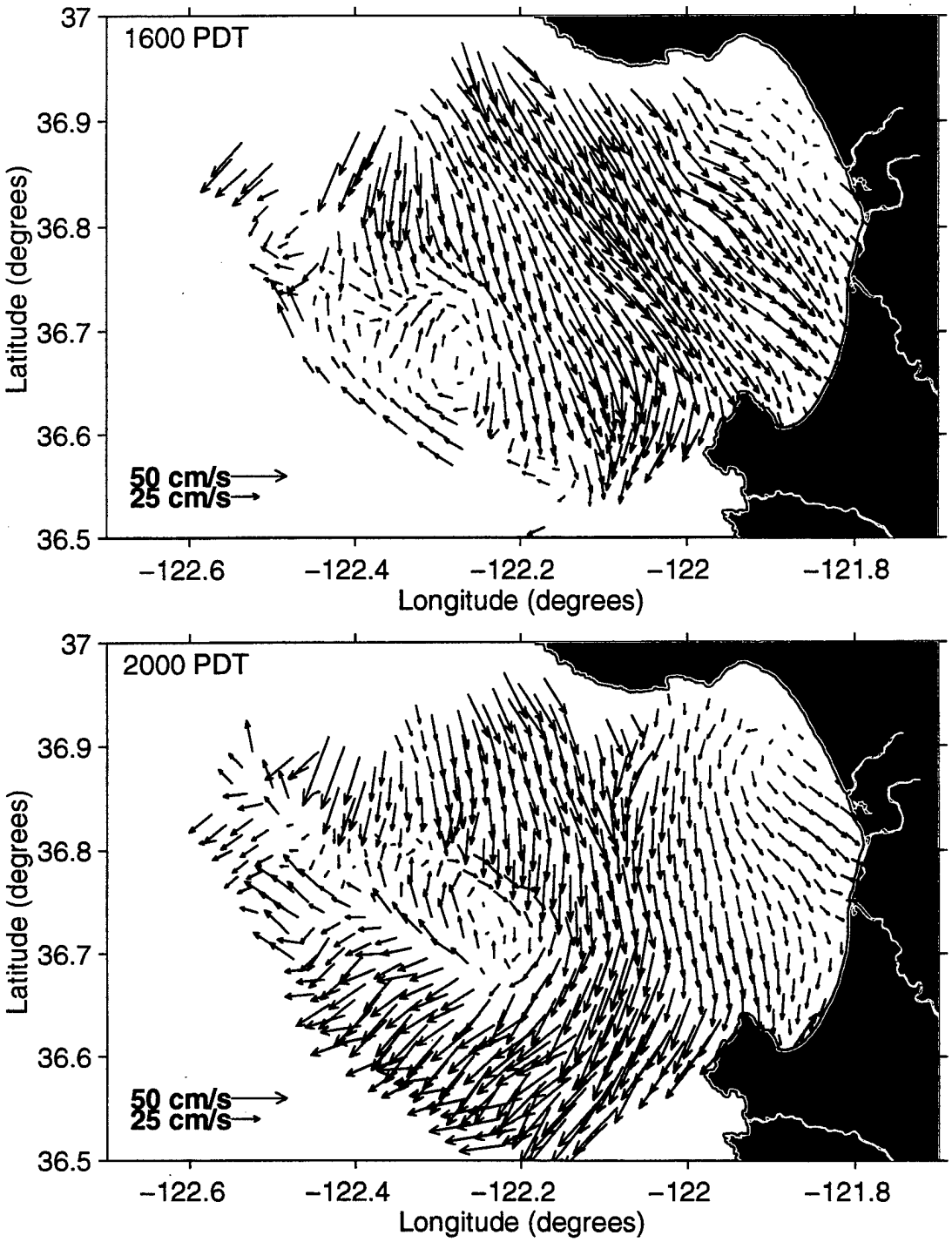


**Figure 9**. HF radar-derived surface current maps for 10 September 1994. Upper panel is 1600 PDT. Lower panelis 2000 PDT.

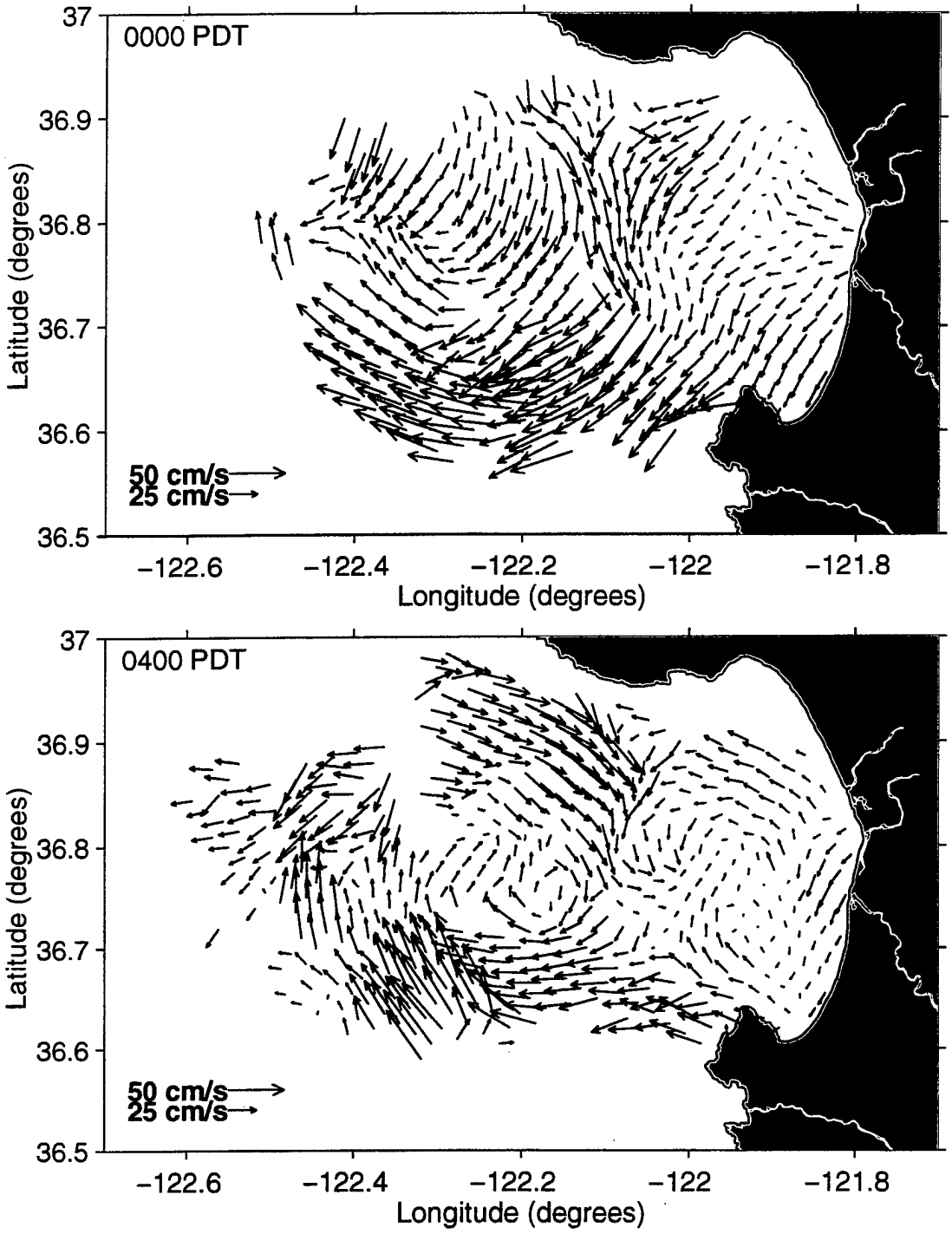


**Figure 10**. HF radar-derived surface current maps for 11 September 1994. Upper panel is 0000 PDT. Lower panel is 0400 PDT.

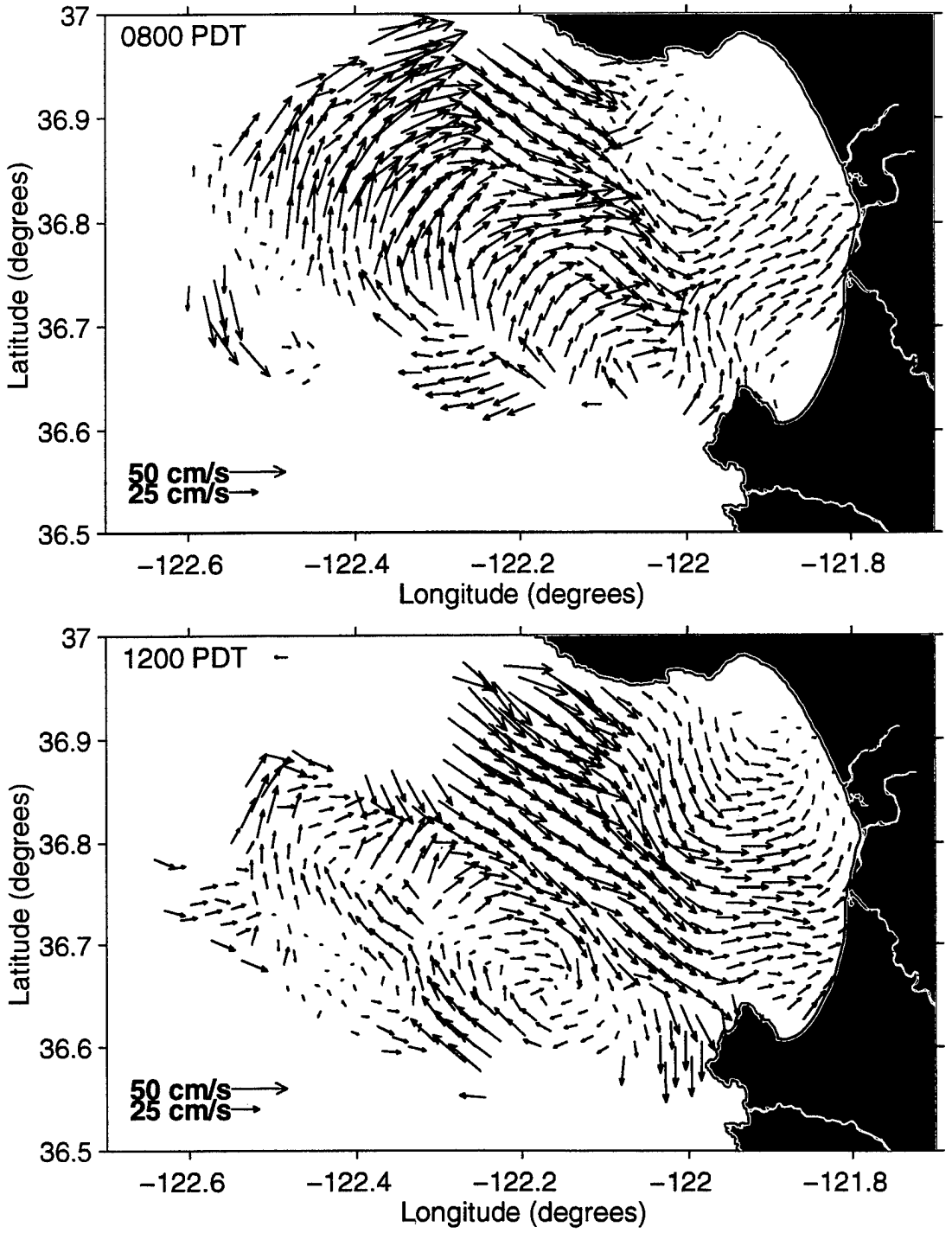


**Figure 11.** HF radar-derived surface current maps for 11 September 1994. Upper panel is 0800 PDT. Lower panel is 1200 PDT.

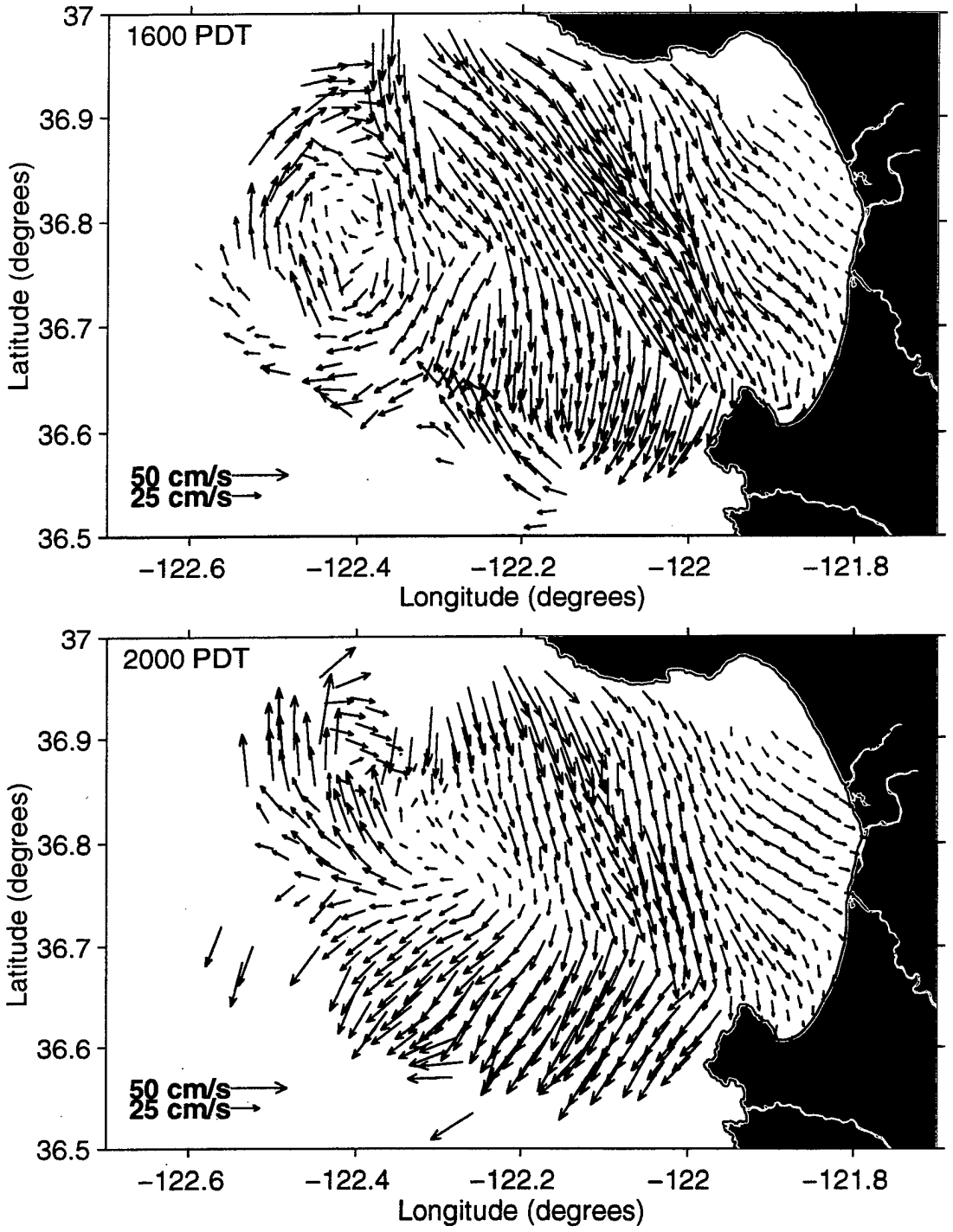


**Figure 12.** HF radar-derived surface current maps for 11 September 1994. Upper panel is 1600 PDT. Lower panel is 2000 PDT.

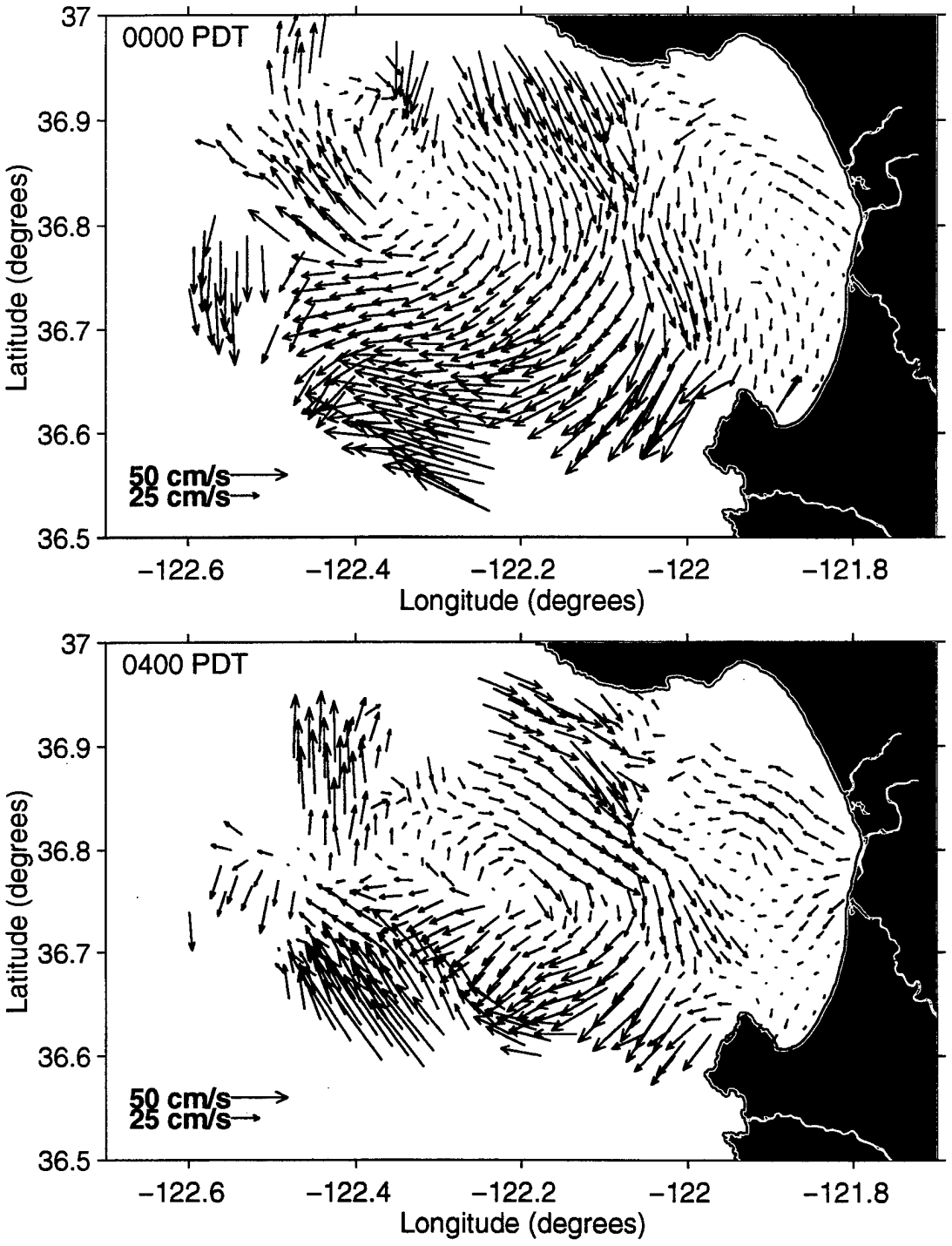


**Figure 13.** HF radar-derived surface current maps for 12 September 1994. Upper panel is 0000 PDT. Lower panel is 0400 PDT.

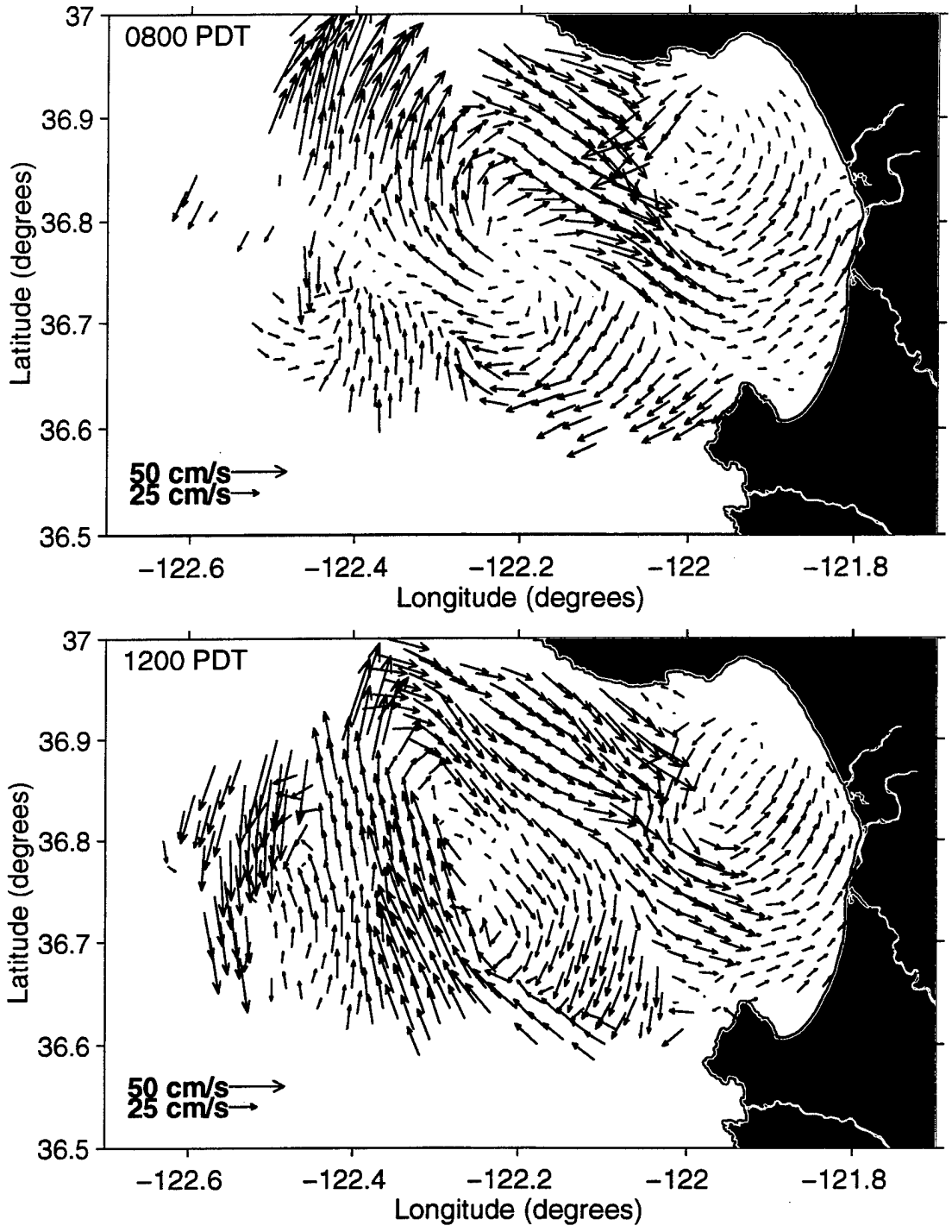


**Figure 14.** HF radar-derived surface current maps for 12 September 1994. Upper panel is 0800 PDT. Lower panel is 1200 PDT.

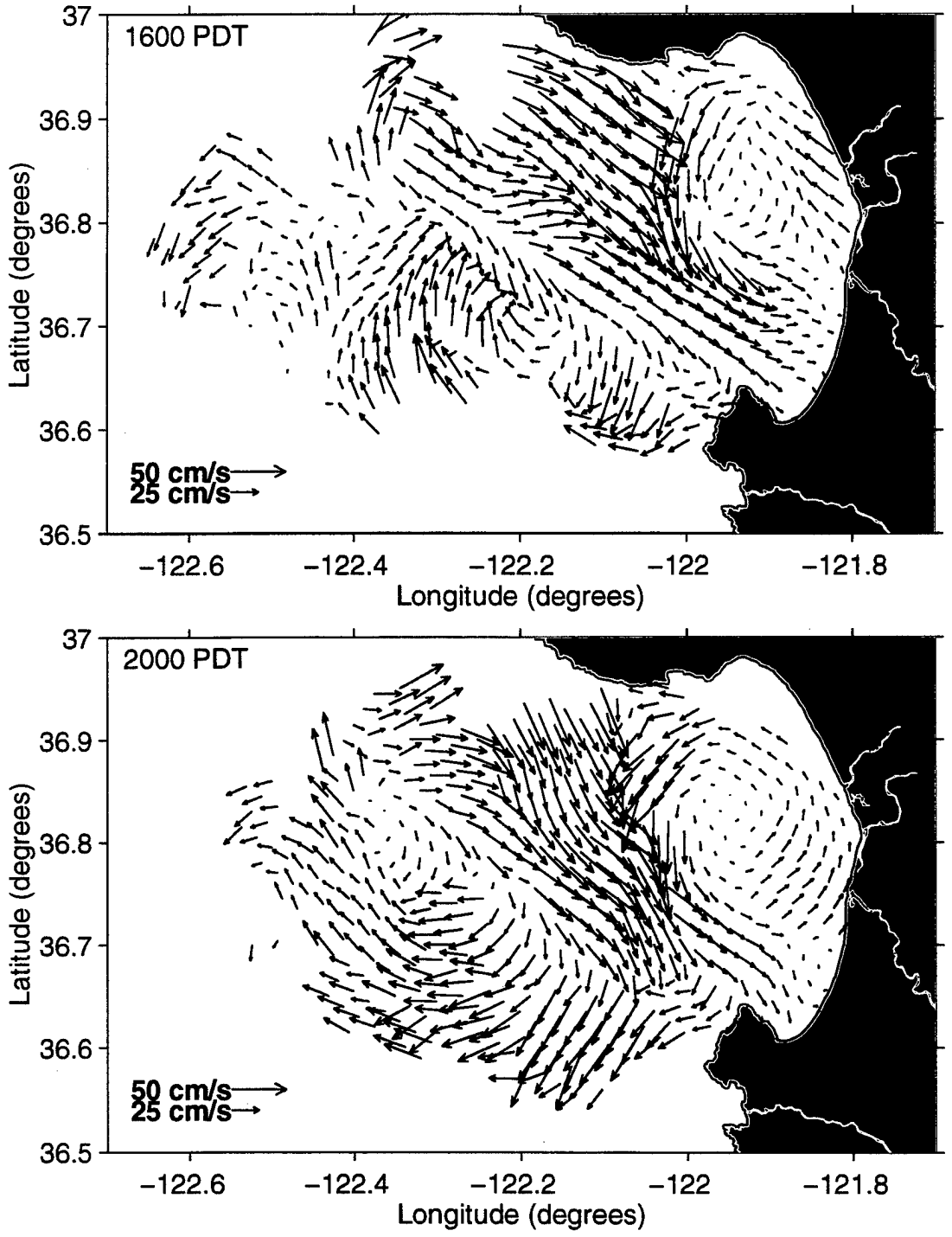


**Figure 15.** HF radar-derived surface current maps for 12 September 1994. Upper panel is 1600 PDT. Lower panel is 2000 PDT.

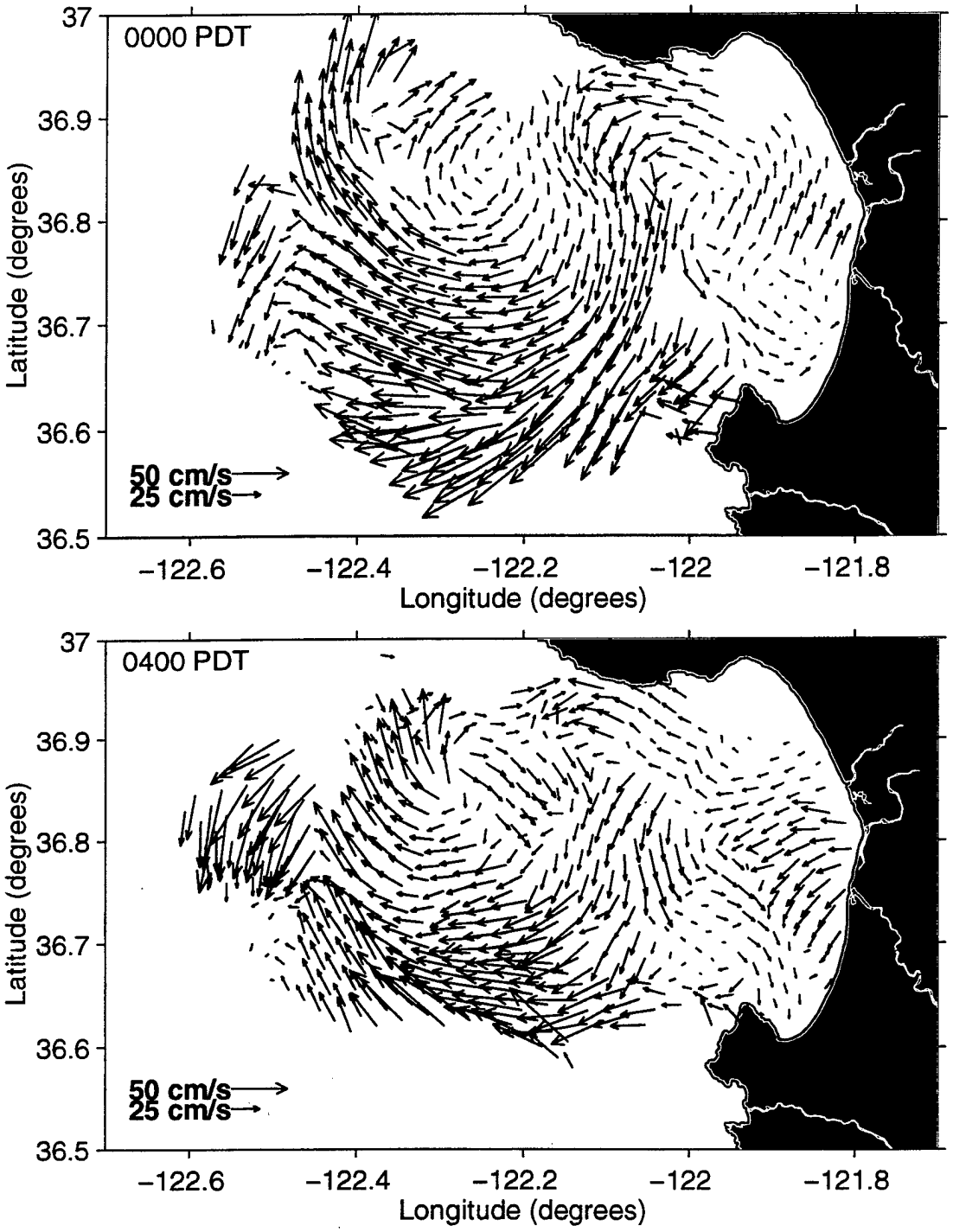


**Figure 16.** HF radar-derived surface current maps for 13 September 1994. Upper panel is 0000 PDT. Lower panel is 0400 PDT.

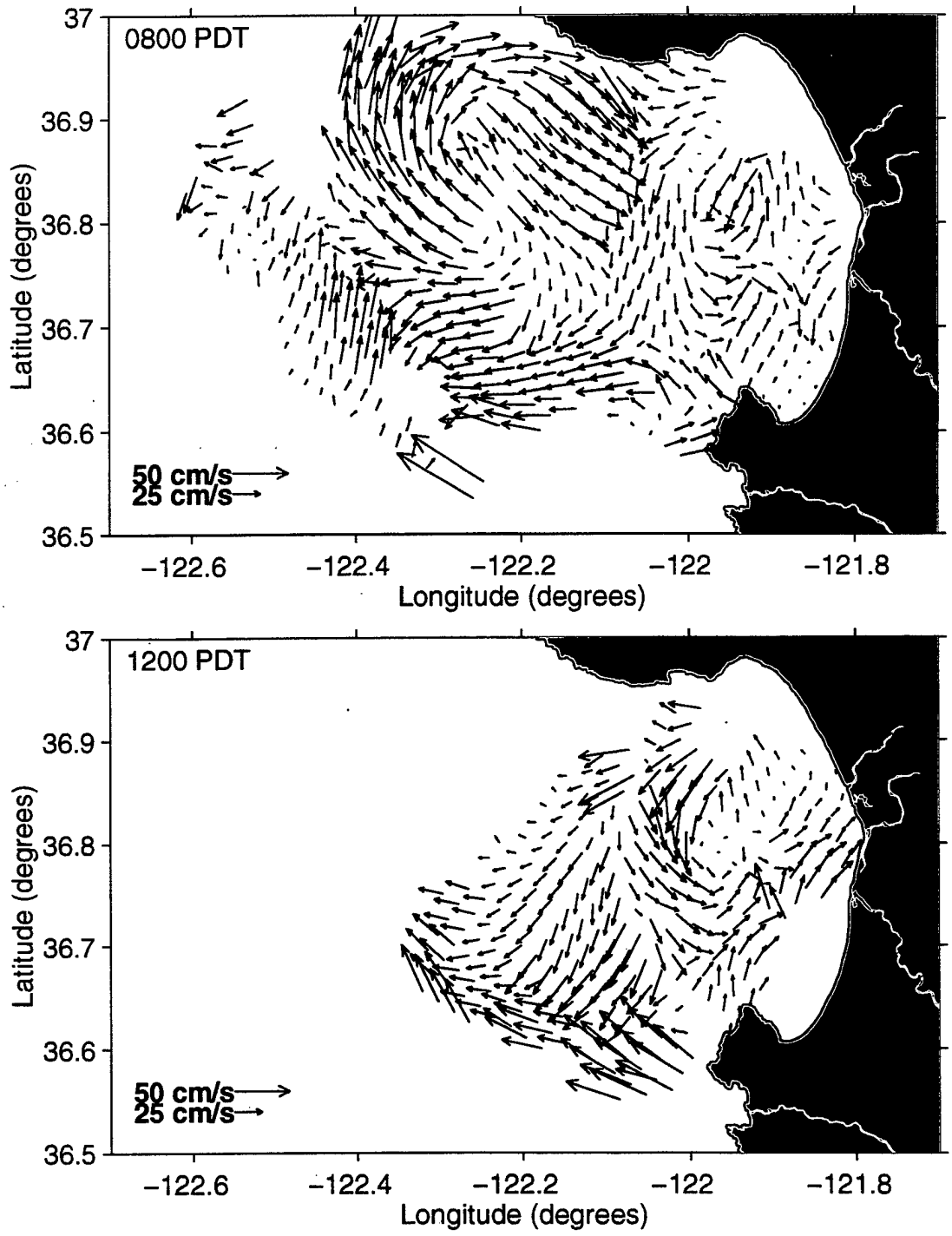


**Figure 17.** HF radar-derived surface current maps for 13 September 1994. Upper panel is 0800 PDT. Lower panel is 1200 PDT.

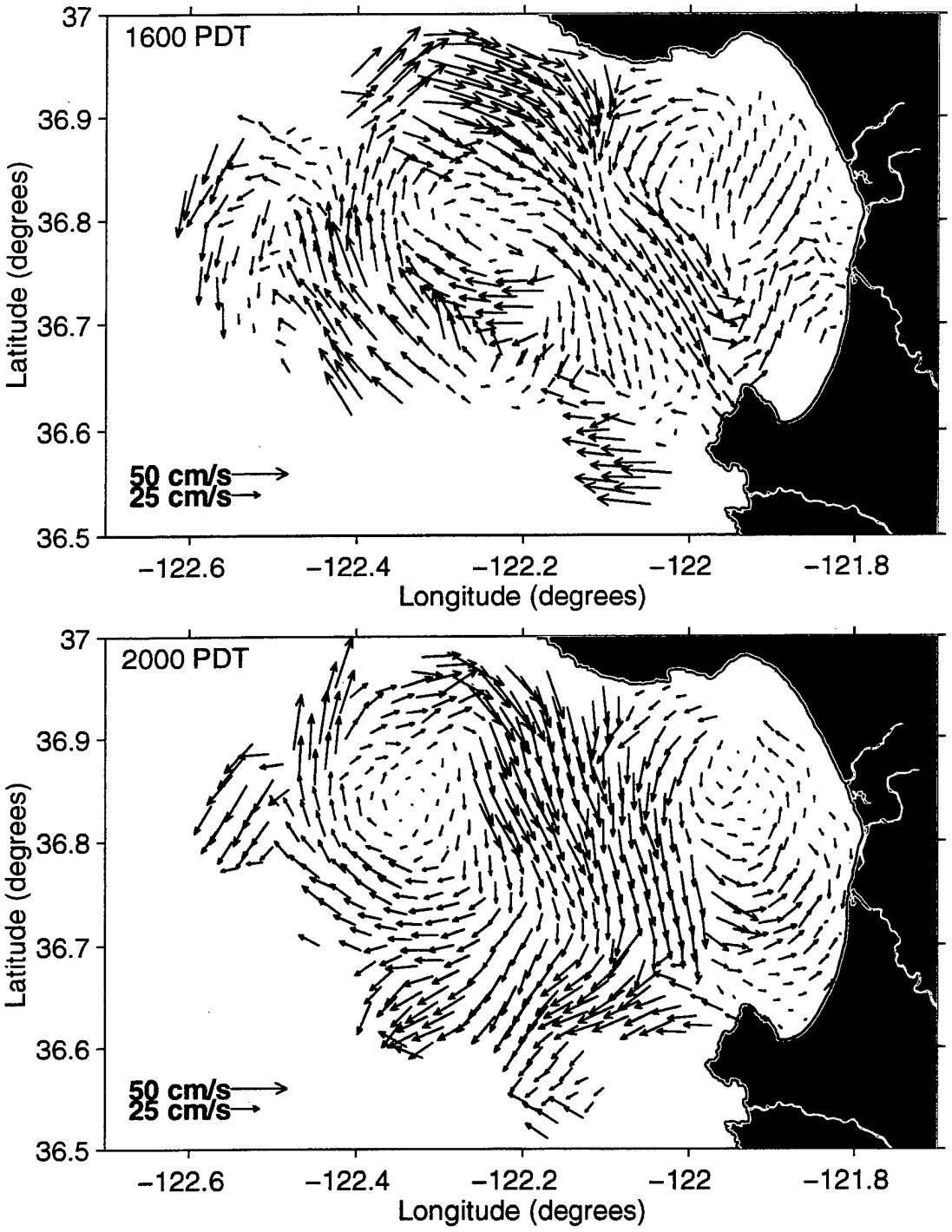


**Figure 18.** HF radar-derived surface current maps for 13 September 1994. Upper panel is 1600 PDT. Lower panel is 2000 PDT.

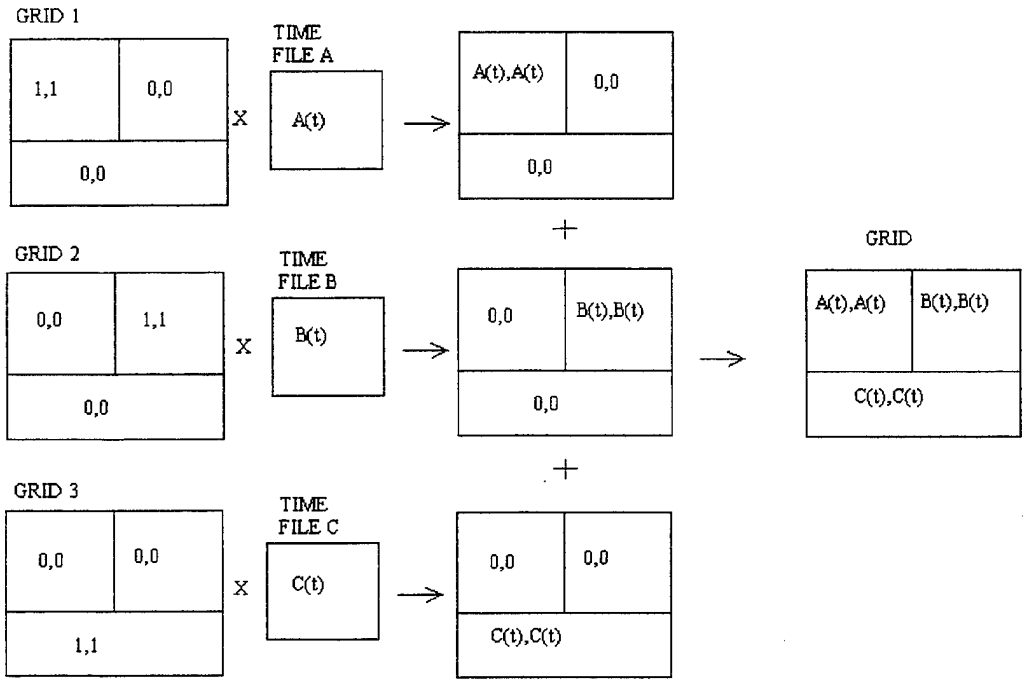


**Figure 19**. Example of joining of grids and time files to create a simple temporally varying spatial pattern.

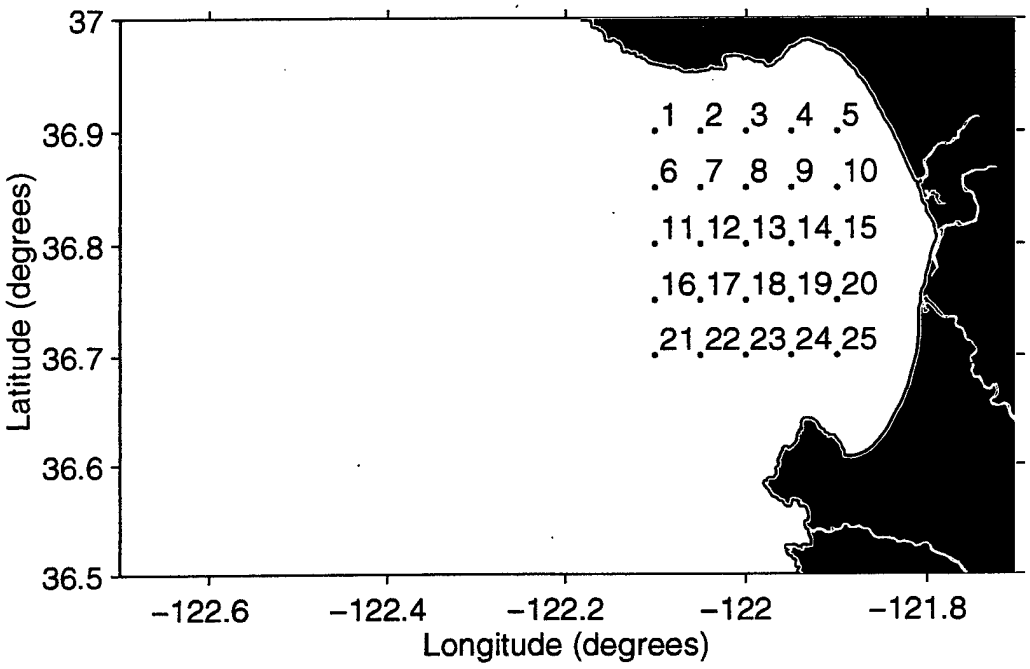


**Figure 20**. Initial release positions used in computing trajectories.

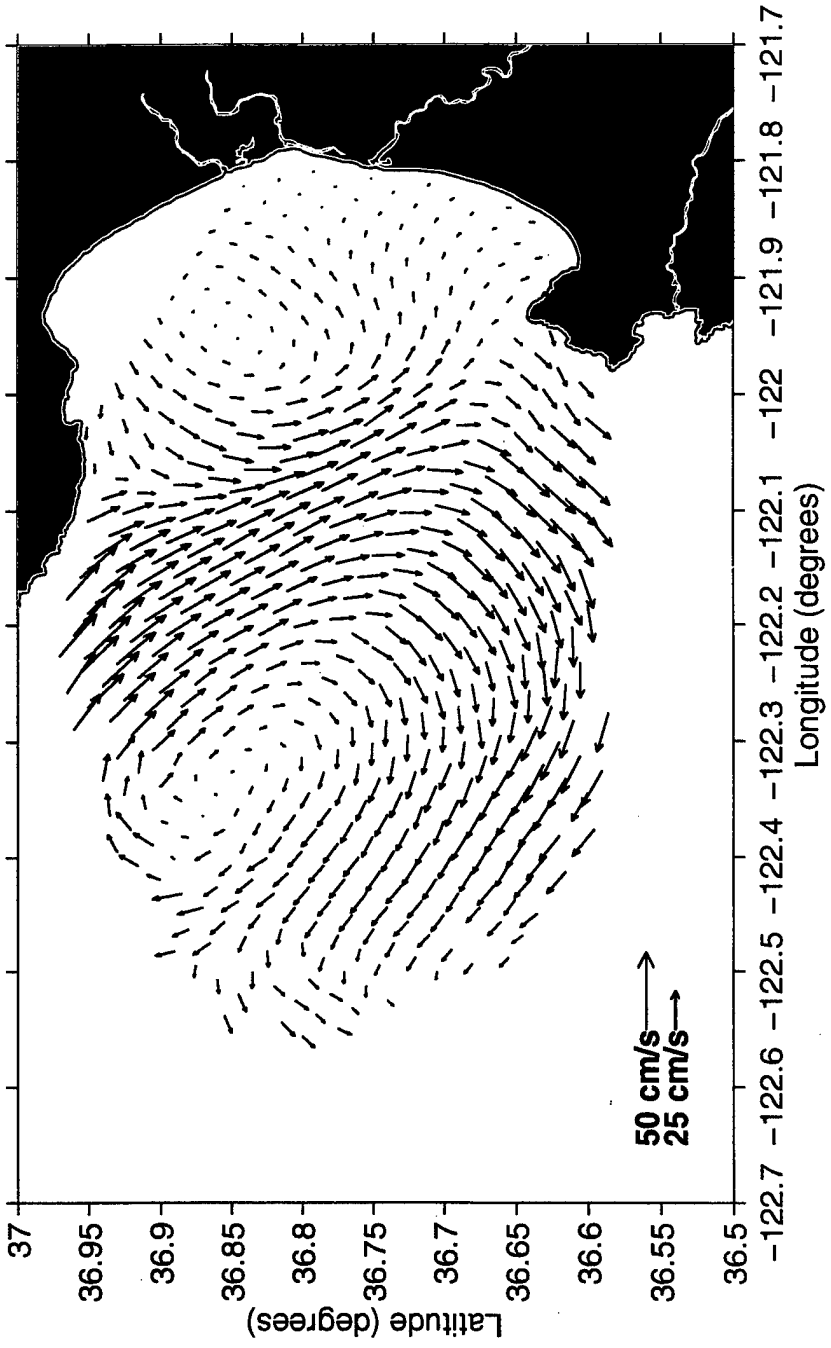


**Figure 21**. Mean surface current map for 9-14 September 1994.

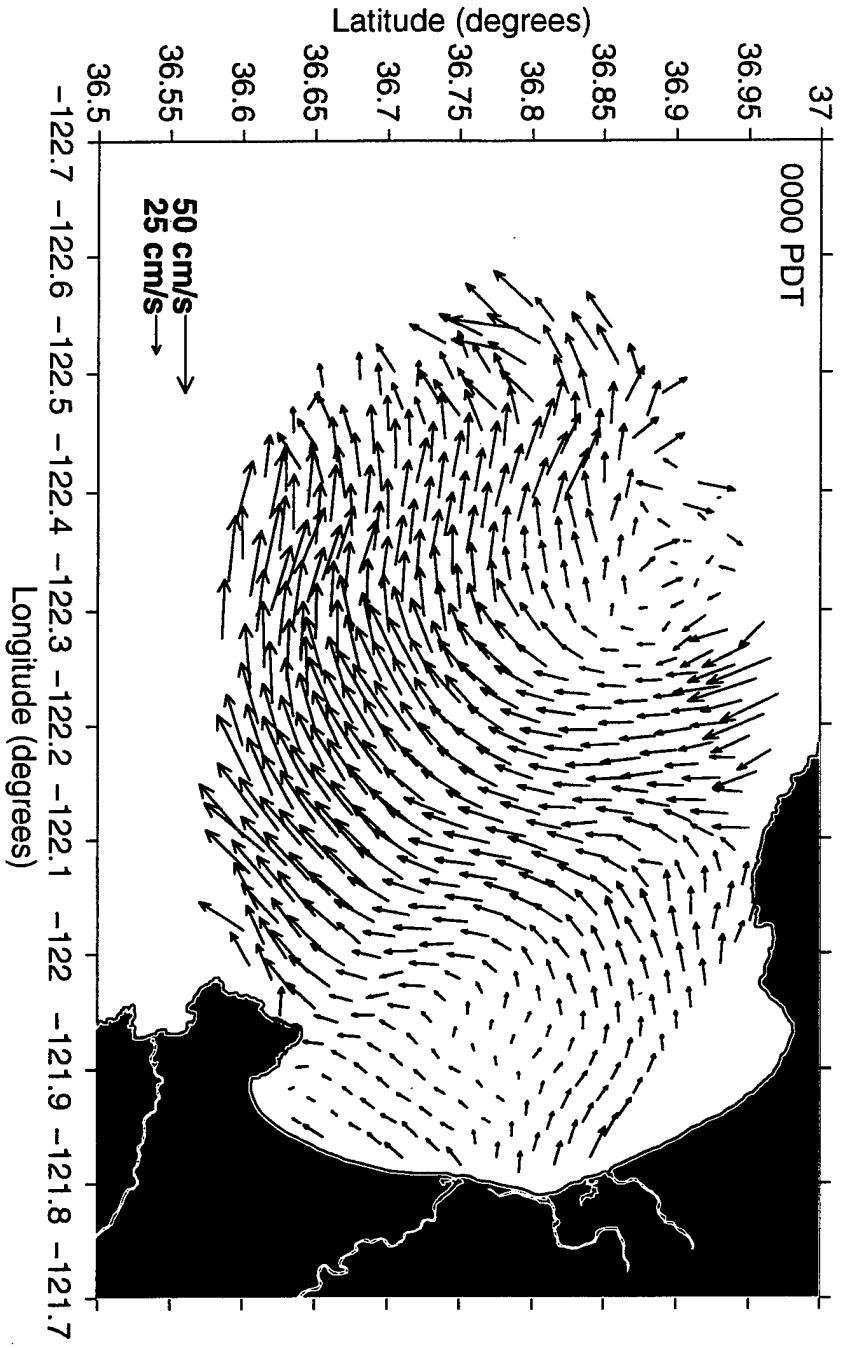


**Figure 22.** Canonical-day surface current map for 0000 PDT for 9-14 September 1994.

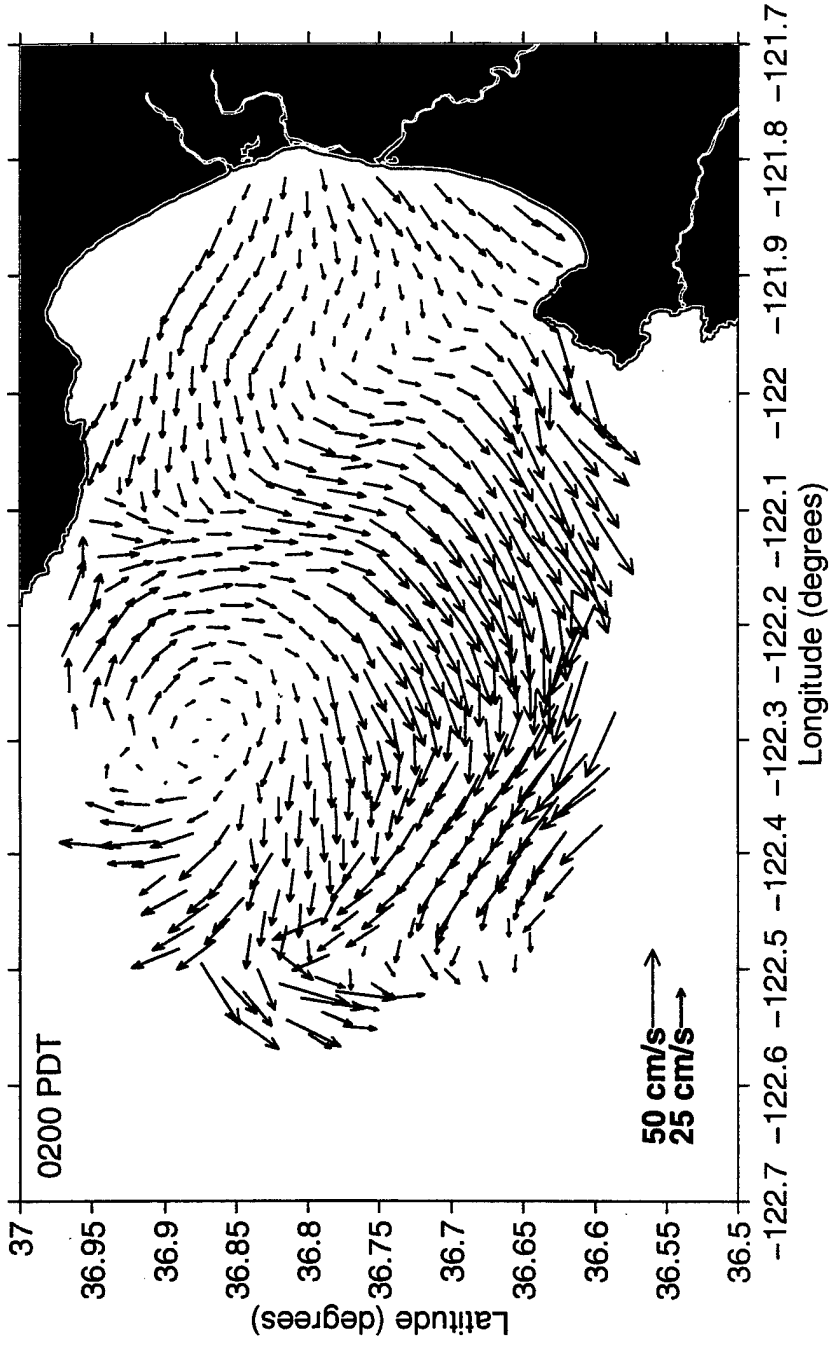


**Figure 23.** Canonical-day surface current map for 0200 PDT for 9-14 September 1994.

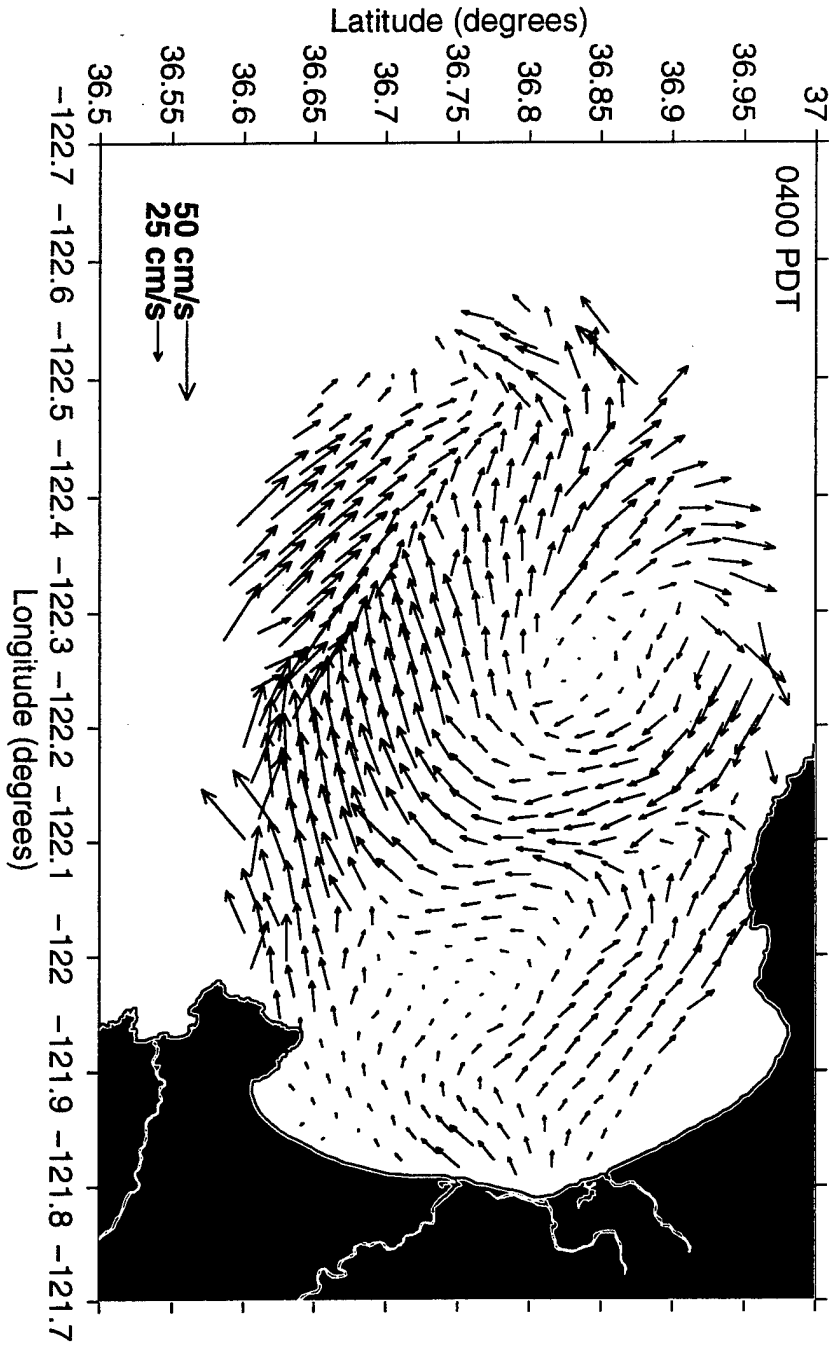


**Figure 24.** Canonical-day surface current map for 0400 PDT for 9-14 September 1994.

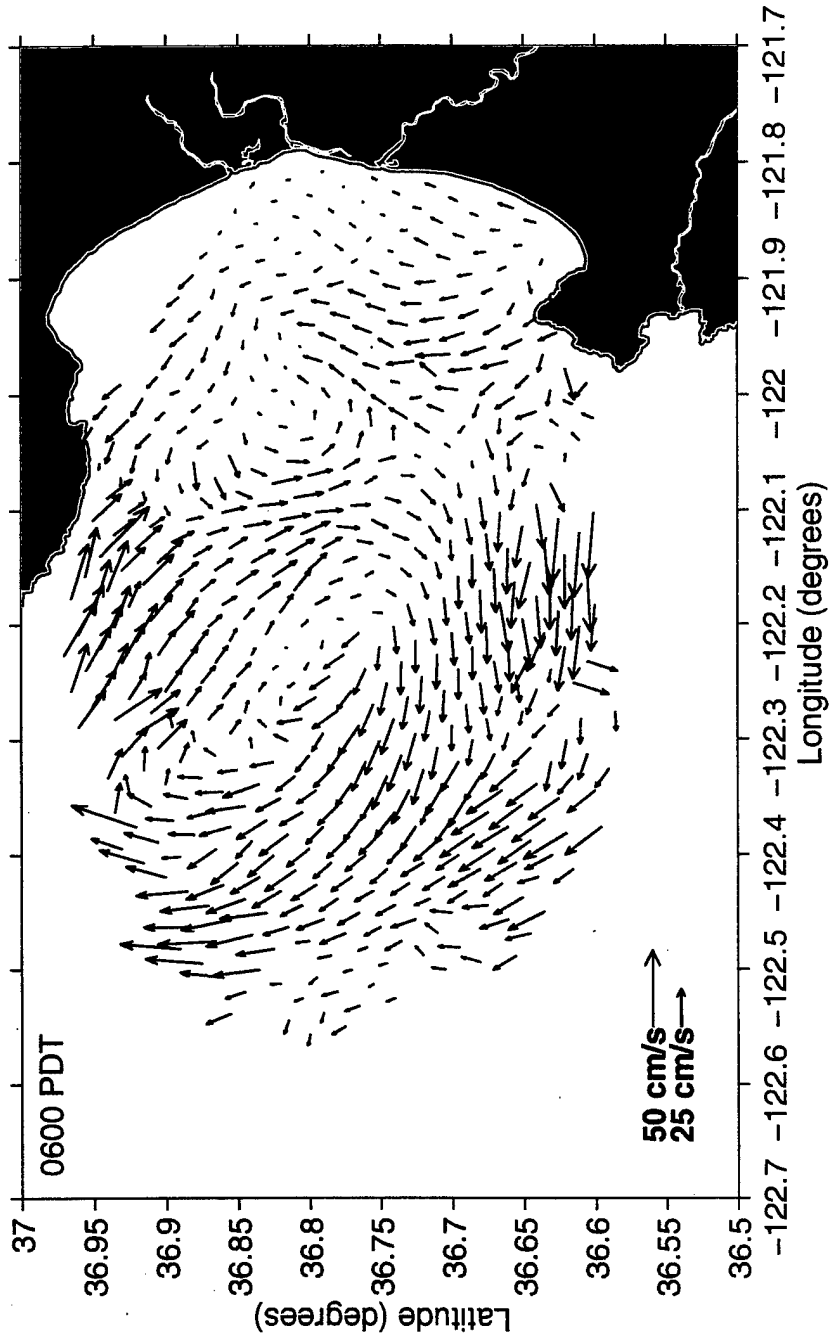


**Figure 25**. Canonical-day surface current map for 0600 PDT for 9-14 September 1994.

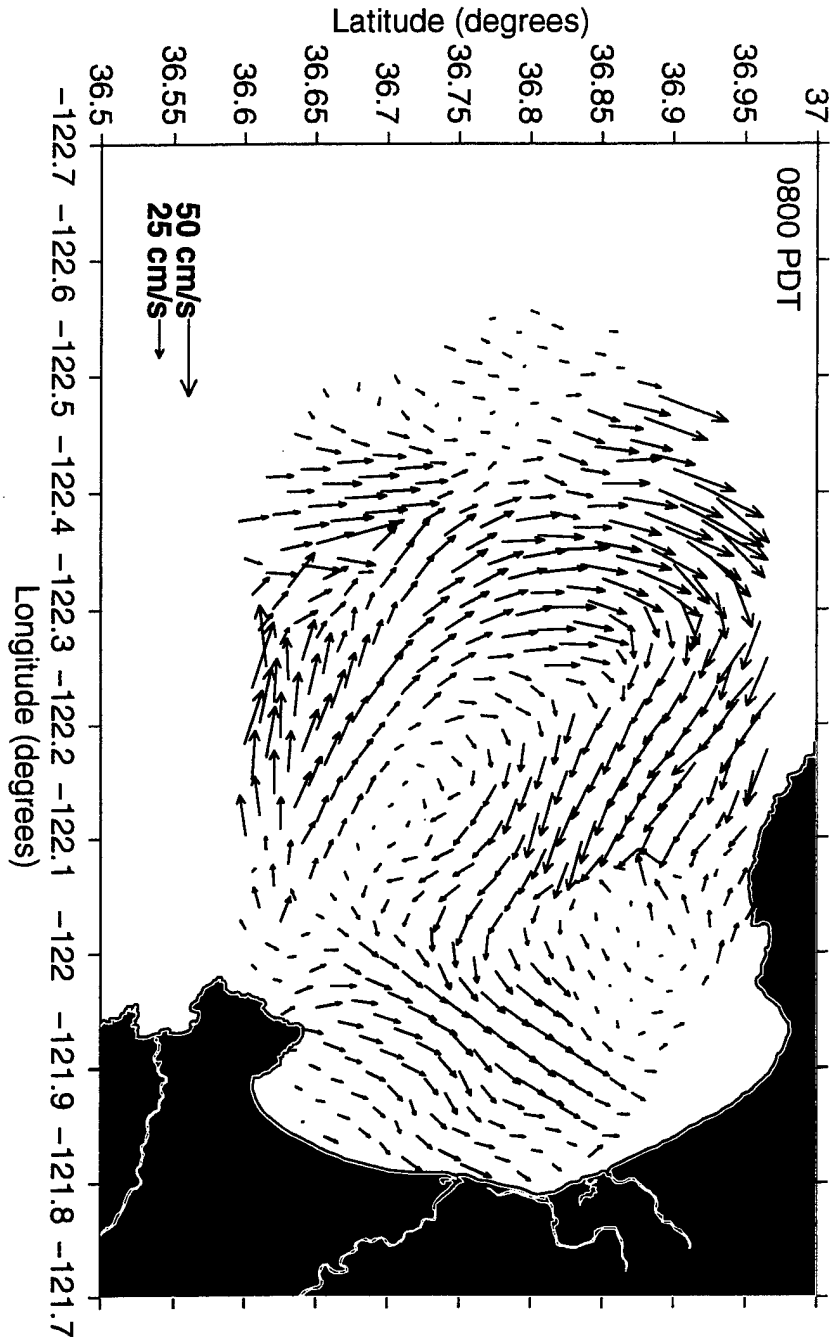


**Figure 26.** Canonical-day surface current map for 0800 PDT for 9-14 September 1994.

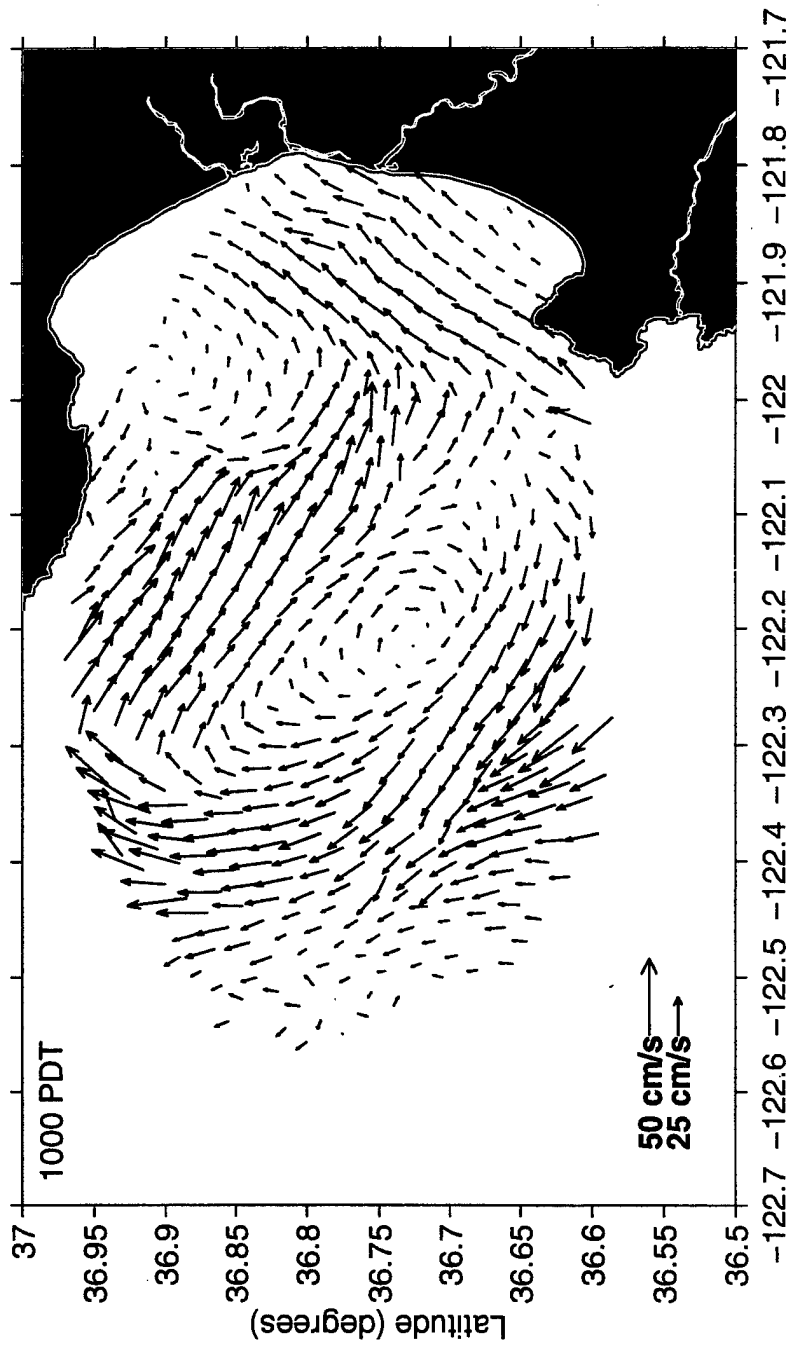


**Figure 27**. Canonical-day surface current map for 1000 PDT for 9-14 September 1994.

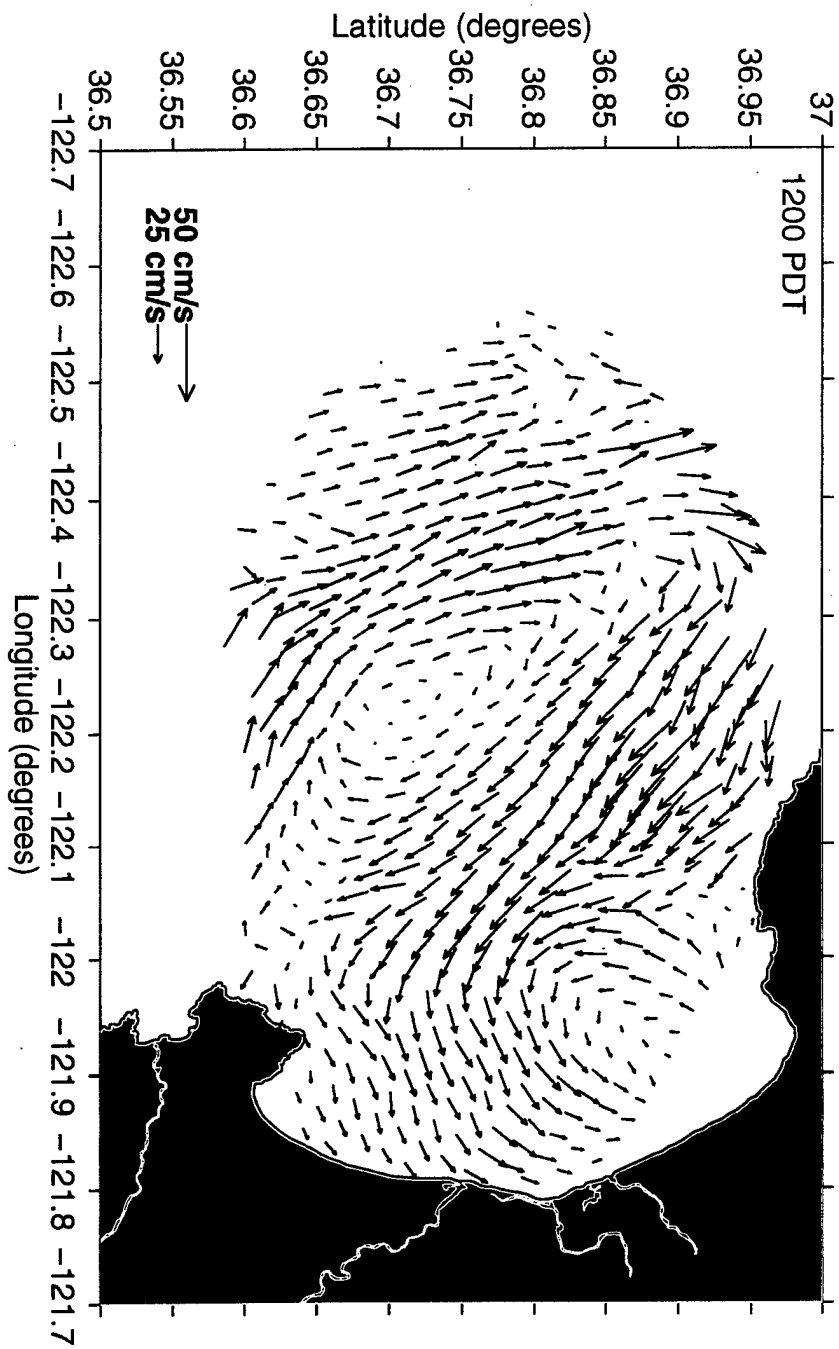


**Figure 28**. Canonical-day surface current map for 1200 PDT for 9-14 September 1994.

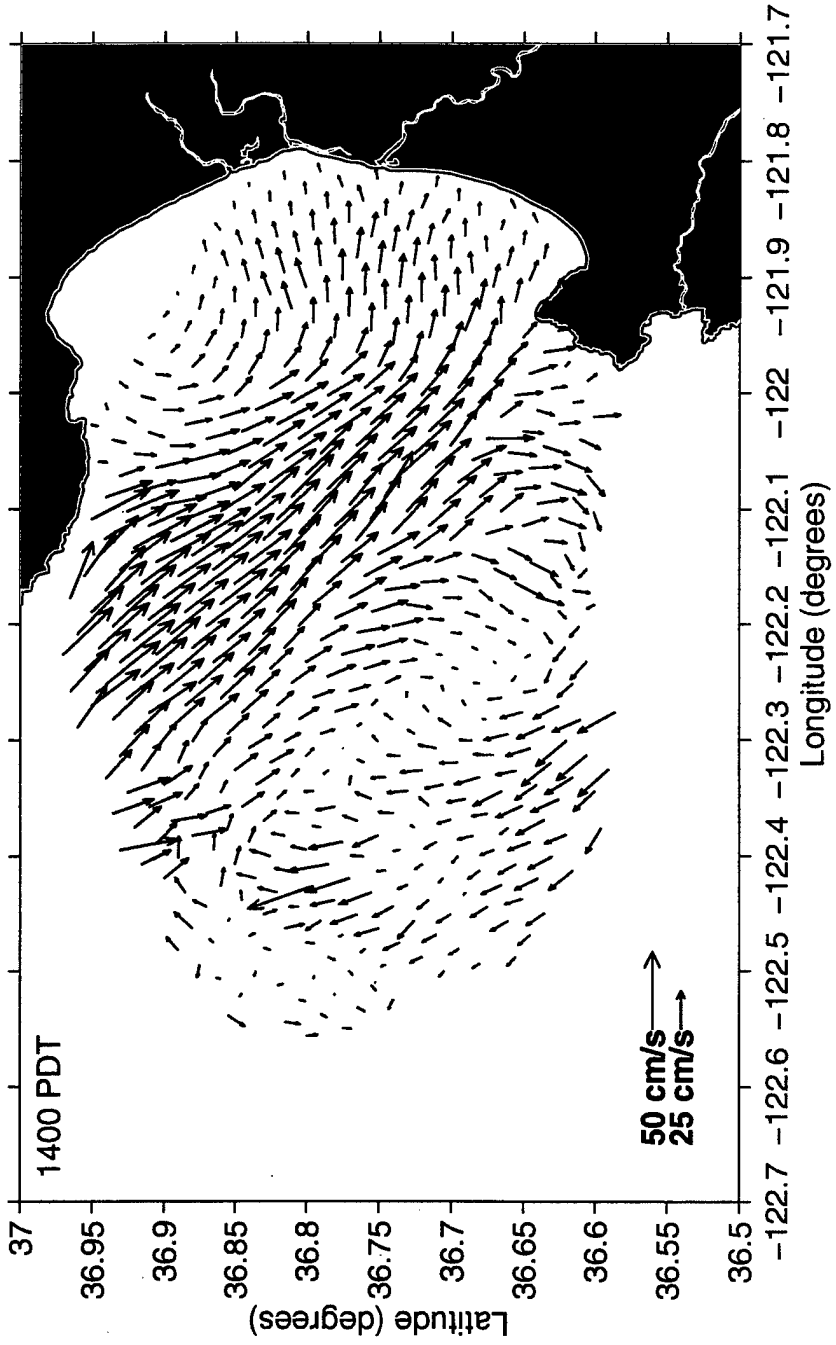


**Figure 29**. Canonical-day surface current map for 1400 PDT for 9-14 September 1994.

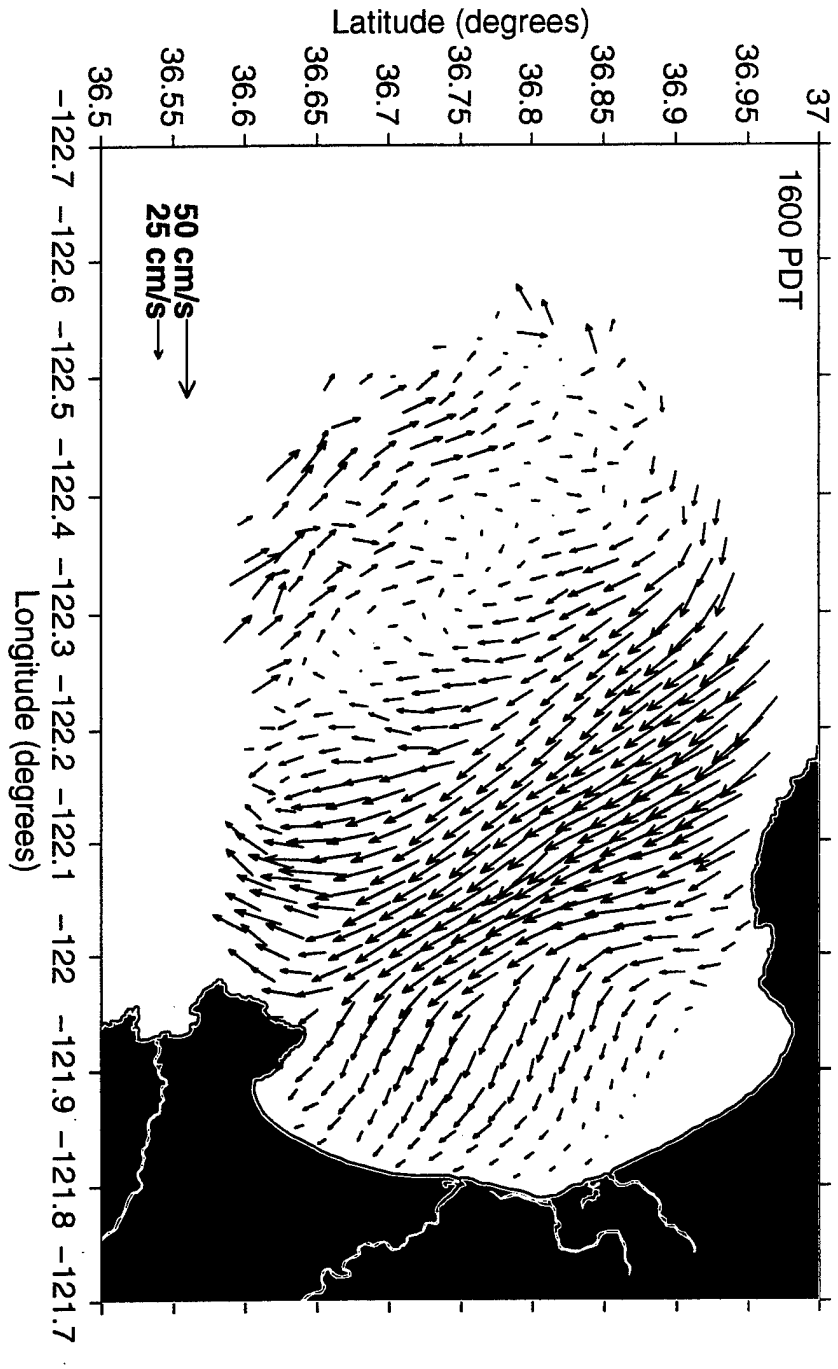


**Figure 30**. Canonical-day surface current map for 1600 PDT for 9-14 September 1994.

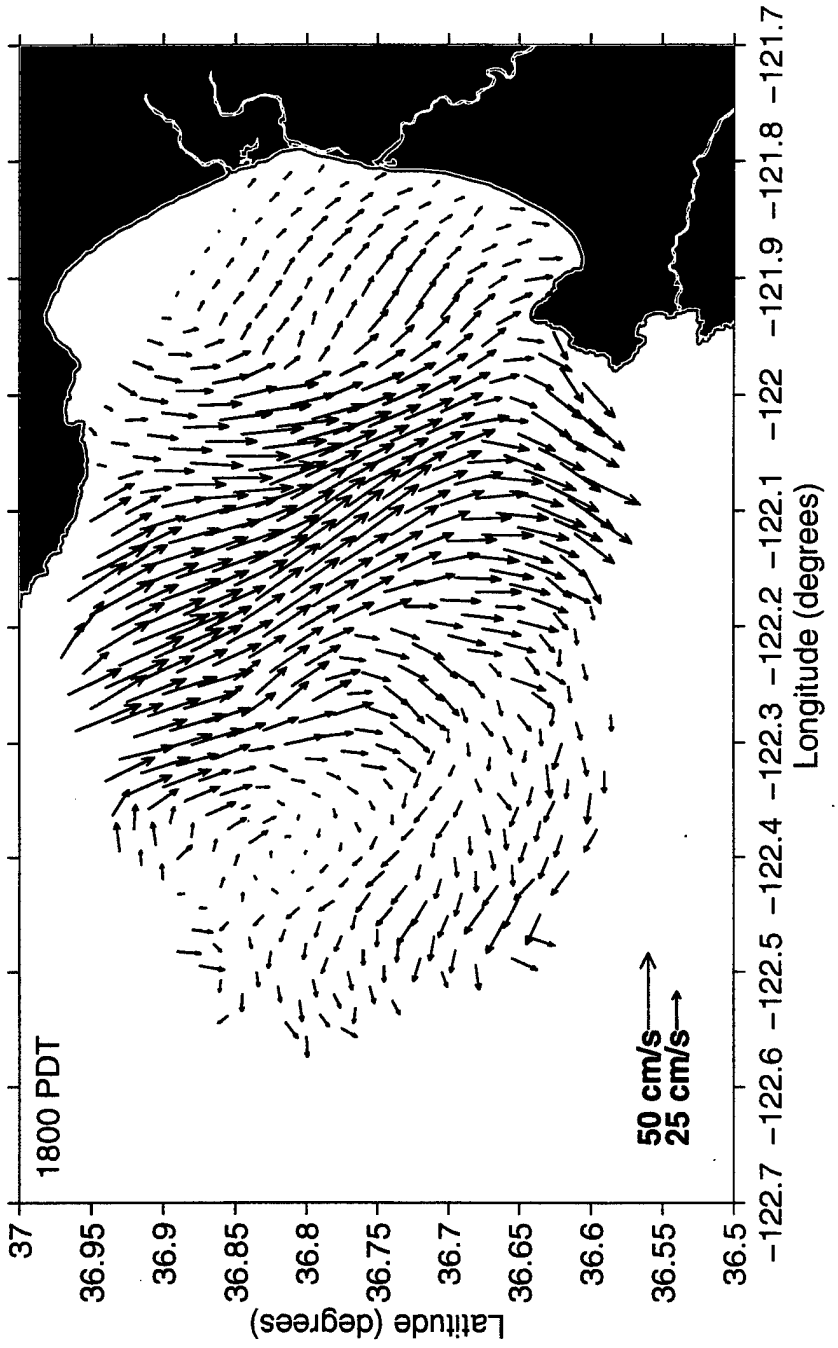


**Figure 31**. Canonical-day surface current map for 1800 PDT for 9-14 September 1994.

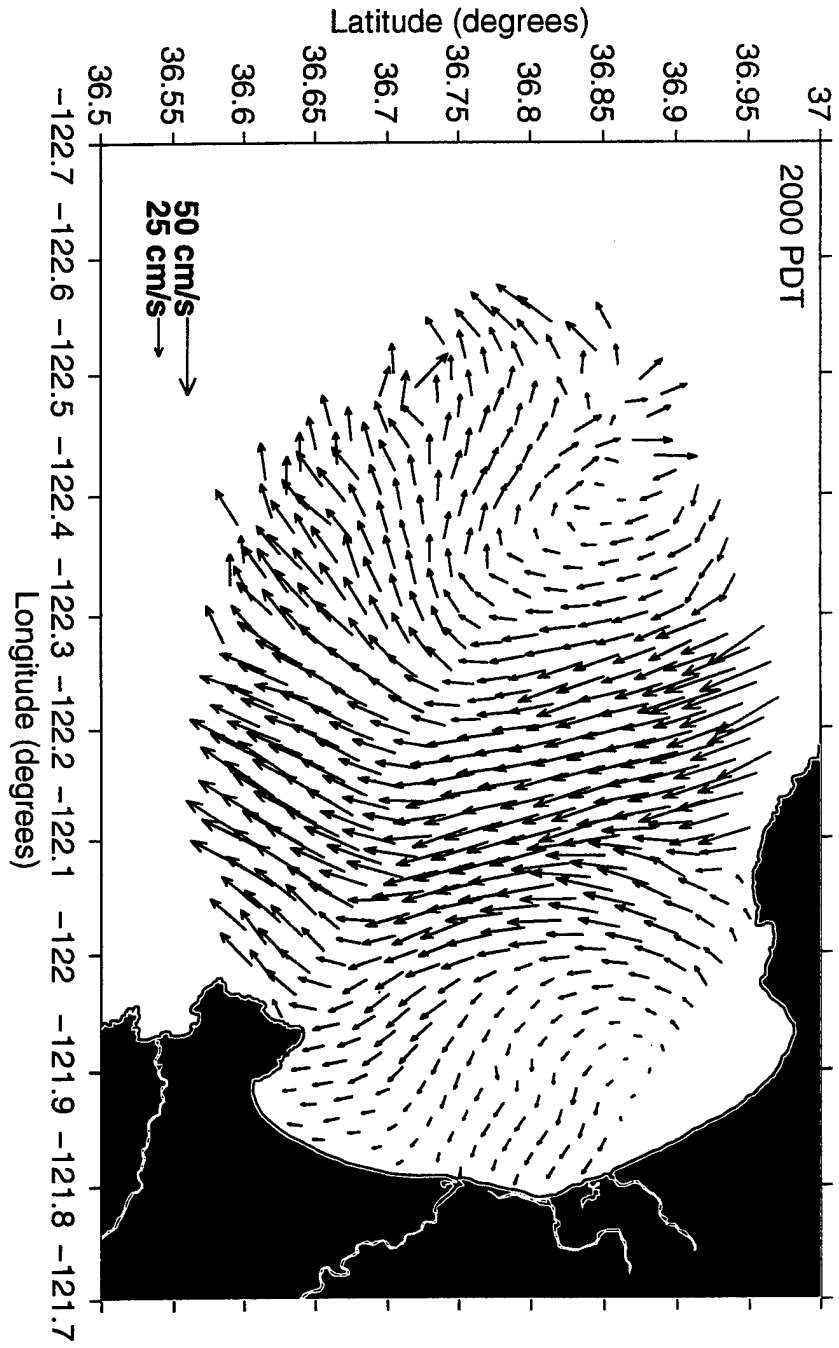


**Figure 32.** Canonical-day surface current map for 2000 PDT for 9-14 September 1994.

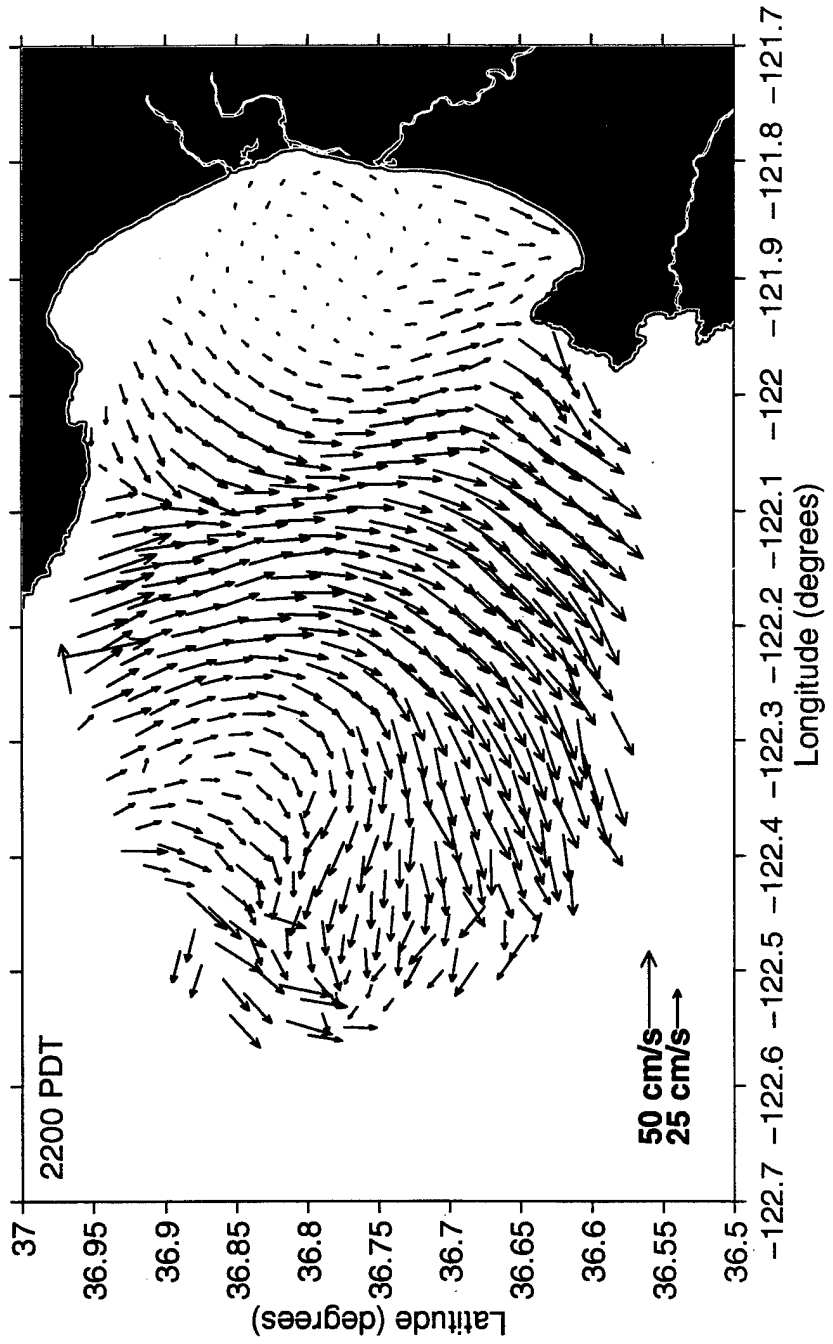


**Figure 33.** Canonical-day surface current map for 2200 PDT for 9-14 September 1994.

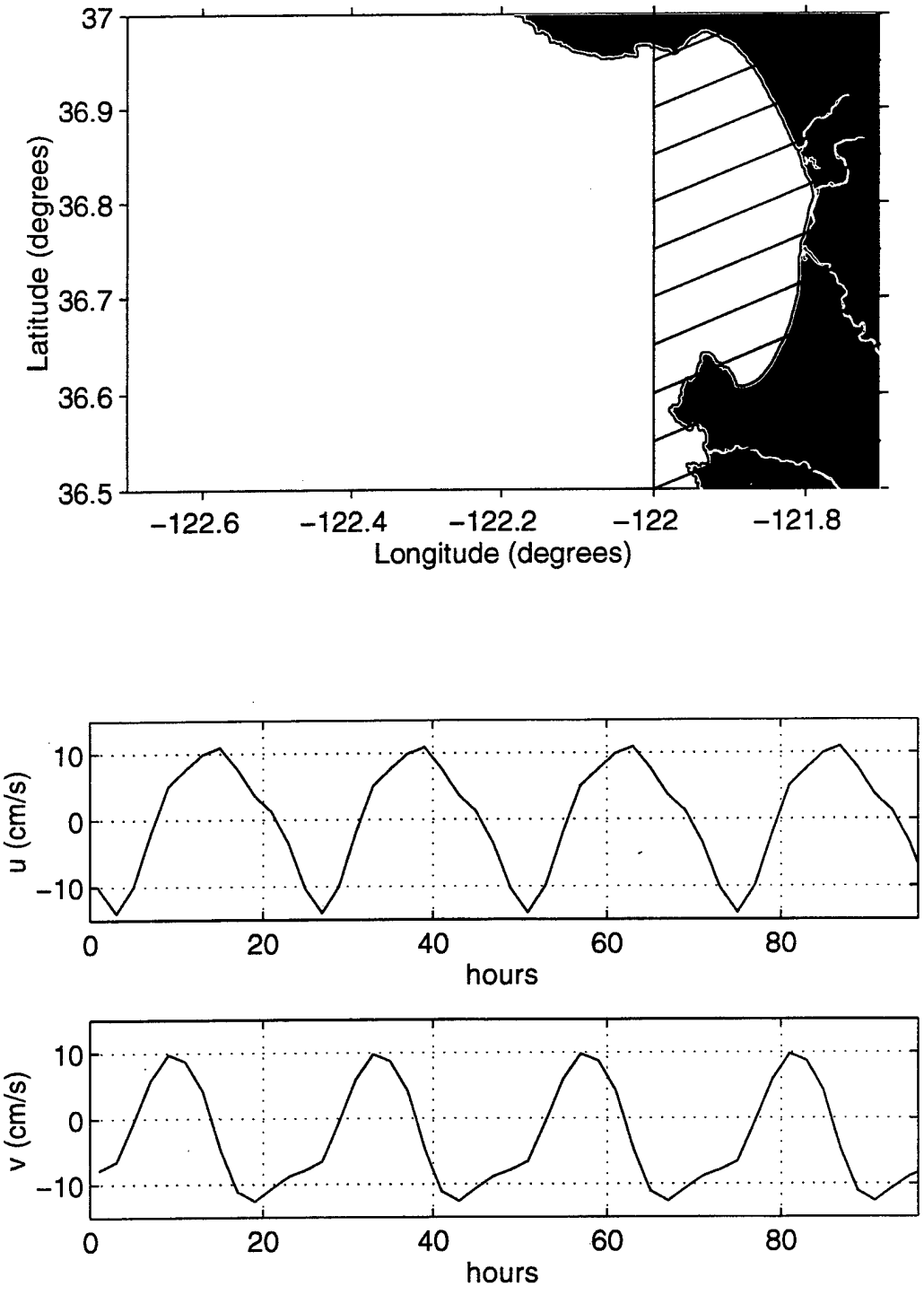


**Figure 34.** Time file of currents derived from the spatial average (hatched area) of the canonical-day surface current maps. Upper panel is Monterey Bay area considered in calculating the average current. Lower panel is the time series of the canonical-day current.

# IV. RESULTS

## A. DESCRIPTIONS OF TRAJECTORIES

Lagrangian Element (LE) trajectories were computed from different surface current patterns with no wind, different surface current patterns with three percent winds and different surface current patterns with one percent wind at separate release times. Tables 1 and 2 list the different cases examined. To view the results, trajectories were plotted for all 25 LEs, a north-south line of LEs along 121.95°W and an east-west line of LEs along 36.8°N. In all cases, symbols are plotted at two-hour intervals along the trajectories.

### 1. Current Only

Figures 35 and 36 are the MATLAB-computed trajectories from the two-hourly HF radar-derived surface current maps. This is assumed to represent the most realistic representation of the actual current trajectory patterns in Monterey Bay. The LEs deployed in the outer portion of the Bay escape, while those deployed in the inner portion of the Bay do not. All but the northernmost LEs show a southeast drift toward the coast with a superimposed anti-cyclonic rotation. The northernmost LEs display an initial northward component. As the trajectories approach the coast they develop a northward component and turn parallel to the beach. The LEs appear to have a large scale cyclonic rotation inside the Bay over this five day time period and a smaller sea-breeze forced diurnal anti-cyclonic rotation superimposed on this. Outside the Bay the LEs which "escape" display a large scale anti-cyclonic pattern. As expected, none of the current-

only trajectories beach. Currents alone cannot beach oil since they must have a zero component perpendicular to the coast as seen in Figure 35. In addition, LE trajectories computed with direct surface current data show the day to day variation which occurs over the five day period.

Figures 37 and 38 are the trajectories generated by OSSM using the NOAA circulation model current. The trajectories display the constant southwest current of the model output. Although this does agree with the overall movement of the California Current well outside Monterey Bay, it does not represent the conditions inside the Bay. All LE trajectories leave the Bay. This suggests the resolution of the circulation model is too large for this area.

Figures 39 and 40 are the trajectories produced by OSSM with the canonical-day current time file. These show an anti-cyclonic diurnal rotation superimposed on a slow southeastward movement. This anti-cyclonic pattern was also described by Foster (1993) and is considered to be dominated by the surface current response to sea breeze forcing. This time file shows a slight drift to the southeast, over the day u has eastward drift of $O(0.001\ ms^{-1})$ and v has southward drift of $O(0.01\ ms^{-1})$. All LE trajectories remain inside the Bay.

Figures 41 and 42 show the OSSM-generated trajectories using the canonical-day current grids. These give the best representation of the actual current patterns in the Monterey Bay for use in the oil spill model. LEs deployed in the outer part of Monterey Bay escape into the California Current. LEs deployed inside the Bay generally show a slight movement toward the coast with an anti-cyclonic rotation superimposed. In the

southern part of the Bay, this rotation is much more pronounced and there is more of a southeastward flow. In the northern part of the Bay, the LEs seem to be "trapped" off the coast and display only slight movement to the north. The plots show that some of the southernmost LEs just make it to the beach but then remain in a northward or southward flow along the coast. The pattern closely follows the mean surface current map generated for the period 9-14 September 1994 (Figure 21). Since each current grid is repeated daily, no day to day variation is seen throughout time period.

### 2. Current with a Three Percent Wind Factor

The addition of a wind factor results in LE trajectories beaching within 2 to 3 days. A three percent wind is used in the comparison between LE trajectories, as this is the default set by OSSM, for comparison between the different surface current patterns. The wind effect is of the same order of magnitude as the surface current. For example, 100 percent of a typical current (10 $cms^{-1}$) is 0.1 $ms^{-1}$ and one percent of a typical wind (10 $ms^{-1}$) is also 0.1 $ms^{-1}$.

Figures 43 and 44 are MATLAB-computed trajectories using HF radar-derived surface currents and three percent wind. The trajectories display a rapid movement. The initial direction of all LEs is toward the south or southeast, then they slow and turn northward near the coast. Only a slight anti-cyclonic rotation is noted. The LEs tend to beach uniformly around the Bay with no preference either toward the north or south.

Figures 45 and 46 show the OSSM-generated trajectories using the NOAA current and a wind factor of three percent. The current is constant and the only variation is due to the wind. The weakening effect of the sea-breeze away from the coast can be seen by

the stronger diurnal variations near the M1 buoy compared to near the NOAA NDBO buoy. However, even with a wind factor of three percent, none of the trajectories remain in the Bay.

Figures 47 and 48 display the trajectory plots produced by OSSM using canonical-day time file currents and a three percent wind factor. These LE trajectories show an anti-cyclonic rotation and travel toward the east and east northeast, due to the combined wind and current. The largest wind effect is seen along the coast, where the sea-breeze is stronger and there is a mean northward wind component. All trajectories beach in either the middle or northern part of the Bay.

Figures 49 and 50 show OSSM-generated trajectories using canonical-day grid currents with a three percent wind factor. Again, this is a more realistic pattern and better represents actual trajectory patterns calculated from direct surface current measurements. The southernmost LEs initially go south, then turn east or northeast. The northernmost LEs travel toward the north or east at first. All LEs which remain within Monterey Bay eventually turn northward as they approach the coast. As seen in the current only case, a large scale cyclonic rotation around the entire Bay is indicated. The anti-cyclonic diurnal rotation is most pronounced in the southern half of the Bay.

## B. SENSITIVITY TO RELEASE TIME

Results from previous drifter experiments in Monterey Bay by Paduan et al. (1996) indicate that trajectories are sensitive to release times. To evaluate the significance of this timing effect, MATLAB-produced trajectories and OSSM-generated

trajectories were initialized at both 0000 PDT and 1600 PDT on 9 Sep 94 to evaluate sensitivity to release time. (Results discussed above with no wind or three percent wind all used LEs released at 0000 PDT.) For these comparisons, OSSM-generated trajectories with canonical-day grid currents and MATLAB-computed trajectories based on the two-hourly HF radar-derived surface currents were combined with a one percent wind effect as opposed to the three percent default in the oil spill model. HF radar-derived currents already include many of the wind effects that this wind factor is meant to represent, such as the sea breeze surface wind forcing (Foster, 1993; Paduan and Rosenfeld, 1996), longshore currents and Stokes drift (Barrick, 1986; Stewart and Joy, 1974). The only wind factor not specifically included in direct surface current measurements is the differential oil-water drift, calculated to be between 0.7 and 1.4 percent of the wind from previous oil spill studies (Overstreet and Galt, 1995; Galt, 1994). Using a three percent wind generally results in the LE trajectories beaching within two to three days, whereas a one percent wind results in beaching in four to five days.

### 1. MATLAB-computed Trajectories

Figures 51 and 52 show the trajectories for the 0000 PDT release. At 0000 PDT both the wind and surface current are generally weak. Initially, the LEs tend to go south in the outer part of the Bay and to the north inside the Bay. Trajectories then go toward the east and begin cycling through anti-cyclonic rotations. The southernmost LEs overall track toward the southeast. The central/northern LEs head east and then north along the coast. Many of the outer Bay LEs escape into the California Current. Figures 53 and 54

display the 1600 PDT-released trajectories. At 1600 PDT the sea-breeze is at a maximum. Initial movement is rapid and toward the south southeast. The outer Bay and southernmost LEs tend to beach further south than in the 0000 PDT release. LEs in the north seem to remain near the initial release positions.

### 2. OSSM-generated Trajectories

Figures 55 and 56 show the 0000 PDT-released trajectories. Initially, only the outer Bay LEs show any real movement, and it is toward the south. Eventually these LEs move toward the southeast and then turn northward at the coast. The LEs inside Monterey Bay show sluggish initial movement but then tend toward the east or the northeast. Except for those LEs which get caught in the southward flowing California Current, nearly all LEs beach in the northern part of the Bay. Figures 57 and 58 are the trajectories associated with a 1600 PDT release. The LEs outside of the Bay initially move to the southeast and the LEs inside the Bay move toward the east. All turn toward the north when they approach the coast. Overall, these LE trajectories beach farther to the north than the LEs released at 0000 PDT.

In all four cases, the same southwestern-most LE's tend to escape Monterey Bay in both the 0000 PDT and 1600 PDT release time runs. Overall, where the trajectories beach are similar in both OSSM runs, whether the LEs are released at 0000 PDT or 1600 PDT. This is most likely a result of the daily repetition of the same current grids, that is, the current pattern at 1000 9 Sep 94 is the same current pattern at 1000 10 Sep 94. The winds do not display a significant day to day variation in this time period (Figure 3). Both OSSM-derived and MATLAB-derived trajectories take longer to beach, four to five days,

as compared to the two to three day beaching noted for many of the drifters in the Monterey Bay experiment (Paduan et al., 1996). This could be either because the wind factor needs to be greater than 1 percent or because many of the trajectories beach in the Northeast corner of the Bay where there is generally poor wind and HF radar coverage, resulting in smaller currents and onshore winds than actually exist in that area.

## C. OSSM-GENERATED VS MATLAB-COMPUTED TRAJECTORIES

### 1. NOAA Provided Current

The OSSM-generated trajectories based on the NOAA circulation model current of LEs outside Monterey Bay are only comparable to the HF radar-derived ones in that the trajectories do not beach. The OSSM results do not show the offshore mesoscale eddy feature suggested in the MATLAB-computed trajectories and previous studies (Rosenfeld et al., 1994; Figure 21). Inside the Bay, the two are not at all comparable. No OSSM LEs beach even with three percent winds. This surface current pattern is not the best to use for Monterey Bay.

### 2. Canonical-day Time File Currents

Outside the Monterey Bay the OSSM generated LE trajectories using canonical-day time file currents do not compare favorably with the MATLAB-calculated ones. Inside the Bay the OSSM LE trajectories tend to beach in the northern part of the Bay, most likely a result of the winds, since the canonical-day time file current trajectories (Figures 39 and 40) have very little actual movement over 24 hours. OSSM results show no evidence of any mesoscale eddy circulation nor the northward flow along the coast as

seen in the MATLAB-calculated trajectories. In the southeast part of Bay, trajectories computed with OSSM based on the canonical-day time files and three percent wind look similar to the MATLAB-computed ones.

### 3. Canonical-day Grid Currents

Use of canonical-day grid currents in OSSM gives the best comparison between HF radar-derived surface current based MATLAB trajectories both inside and outside Monterey Bay. These canonical-day current grids can be considered to represent a typical summer time pattern generated with data from the time period 9-14 September 1994. The mean pattern for the week closely resembles the seasonal pattern for the period August-December 1994 obtained by Paduan and Rosenfeld (1996). The OSSM-generated LE trajectories show mesoscale eddy features both inside and outside Monterey Bay as well as the slight northward current flow along the coast. Not seen in the trajectory patterns computed using canonical-day current grids are the day to day variations noted in the trajectories computed using HF radar-derived surface currents. Figures 4 through 18 are examples of this variation. These figures show the actual surface current patterns every four hours for comparison with the canonical-day maps. The daily variation is particularly pronounced by the strong currents seen 9-10 September 1994 (Figures 4 to 9) and the weaker currents on 12-13 September 1994 (Figures 13 to 18).

## D. ERRORS ASSOCIATED WITH TRAJECTORY ANALYSIS

Various errors are associated with this type of approach to trajectory analysis. Errors occur in the assignment of the closest u and v for both the current and winds as

opposed to interpolation or weighting the data. However, this same approach, assigning the closest u- and v-component vice interpolation, is the mode in which NOAA's On-Scene Spill Model was run. Likewise, both OSSM and the MATLAB program simply used the closest wind site to each LE for the wind u- and v-components. This cannot be considered accurate in the northern part of the Bay where no local winds are included. Errors in the current field also occur when there is insufficient radial observations, when the direction finding algorithms cannot resolve angular directions and when there are maximum range fluctuations due to atmospheric and sea state conditions. This last is not considered significant in this study as the more distant points are generally not a danger for beaching.

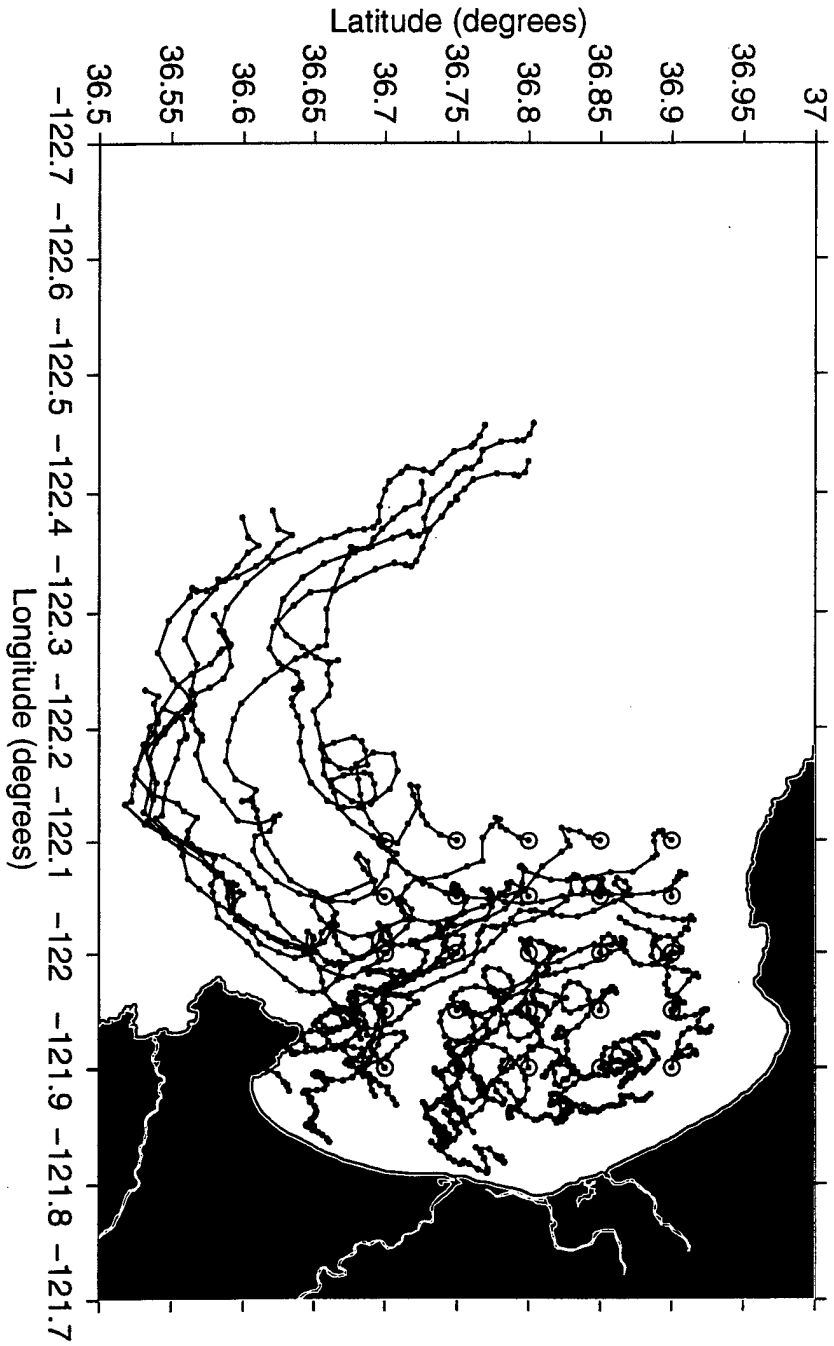


**Figure 35**. Trajectories for all 25 LEs computed from HF radar-derived surface current maps only. 120 hours plotted (each symbol represents two hours).

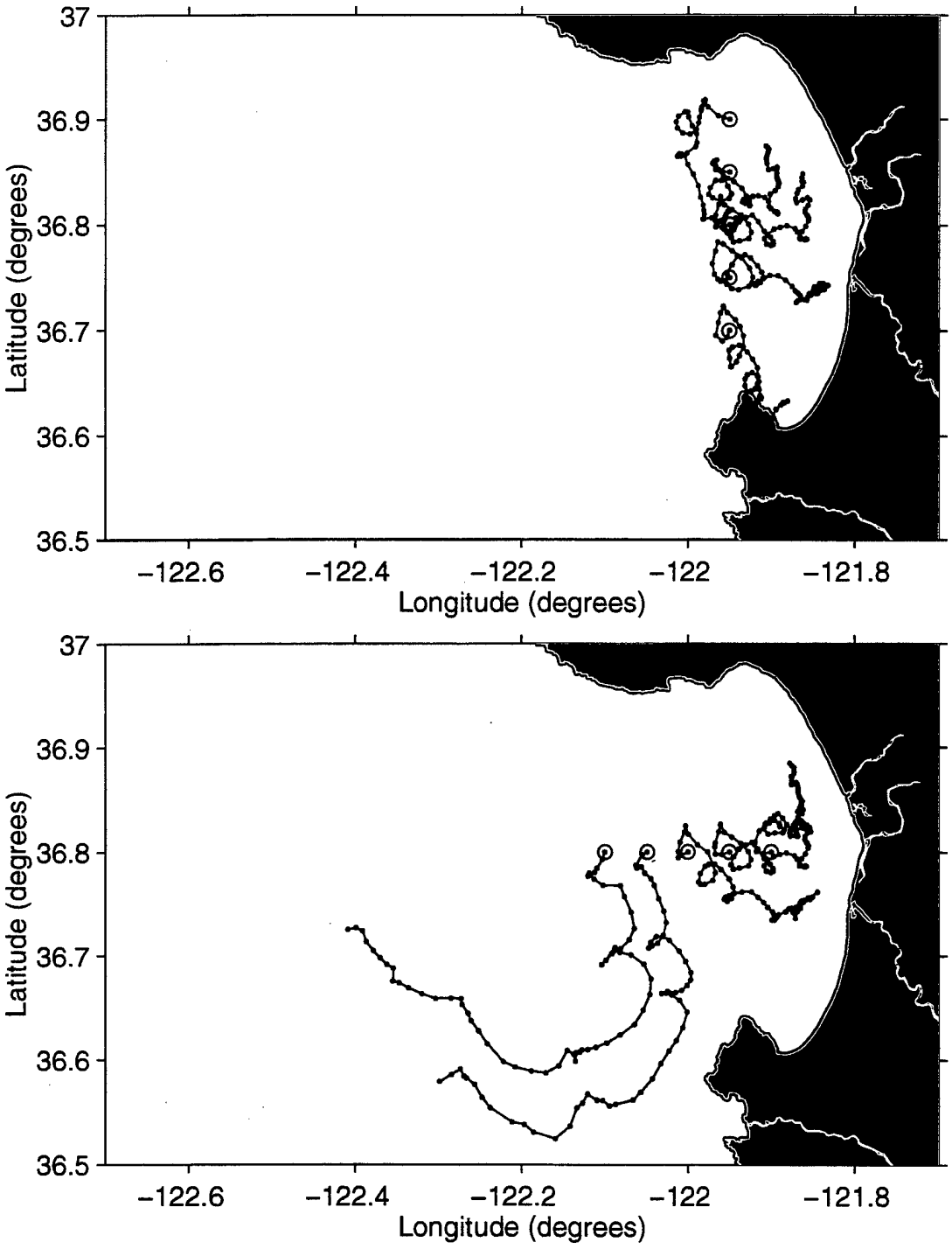


**Figure 36.** Trajectories for selected LEs computed from HF radar-derived surface current maps only. 120 hours plotted (each symbol represents two hours). Upper panel displays LEs along 121.95°W. Lower panel displays LEs along 36.8°N.

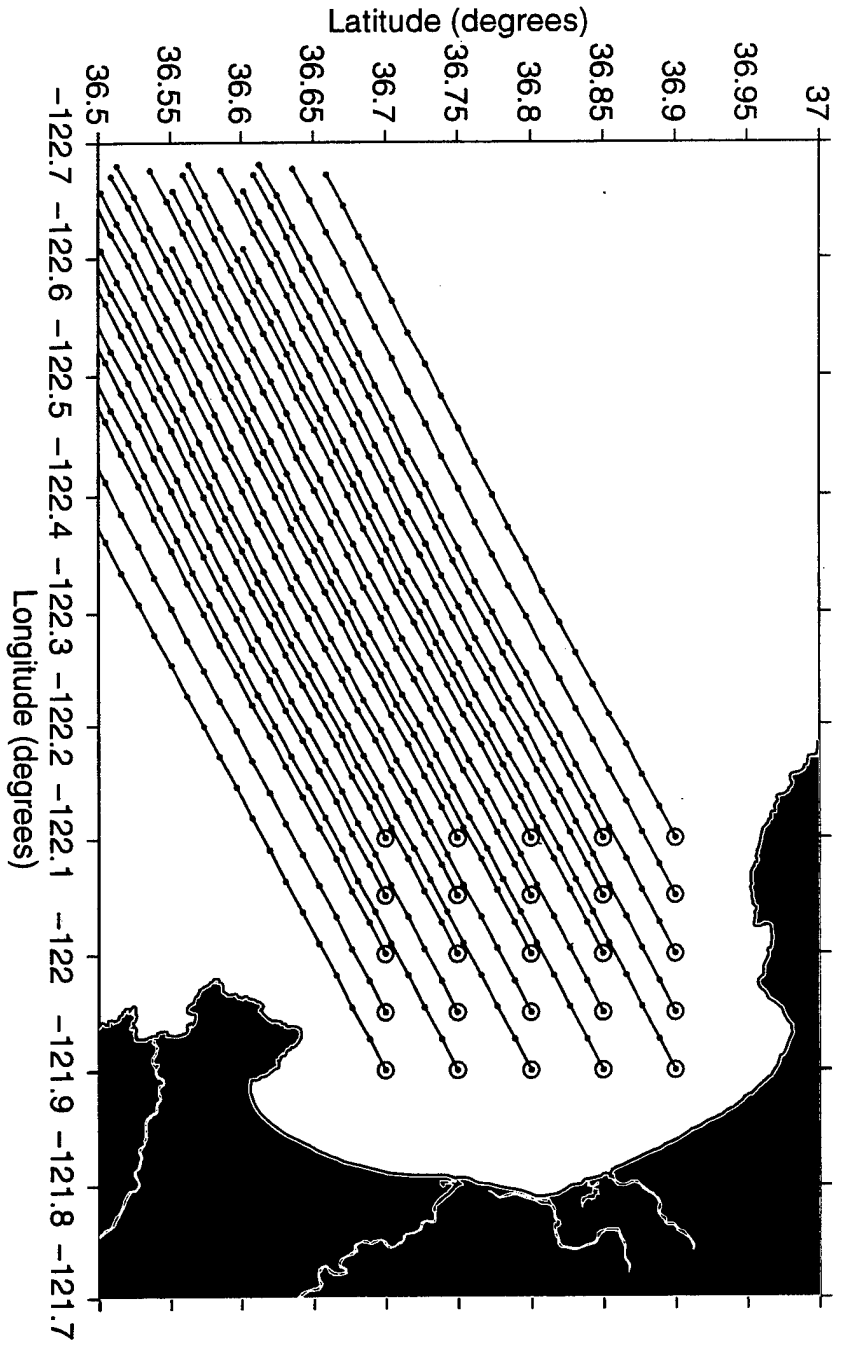


**Figure 37.** Trajectories for all 25 LEs produced from OSSM using NOAA circulation model currents only. 52 hours plotted (each symbol represents two hours).

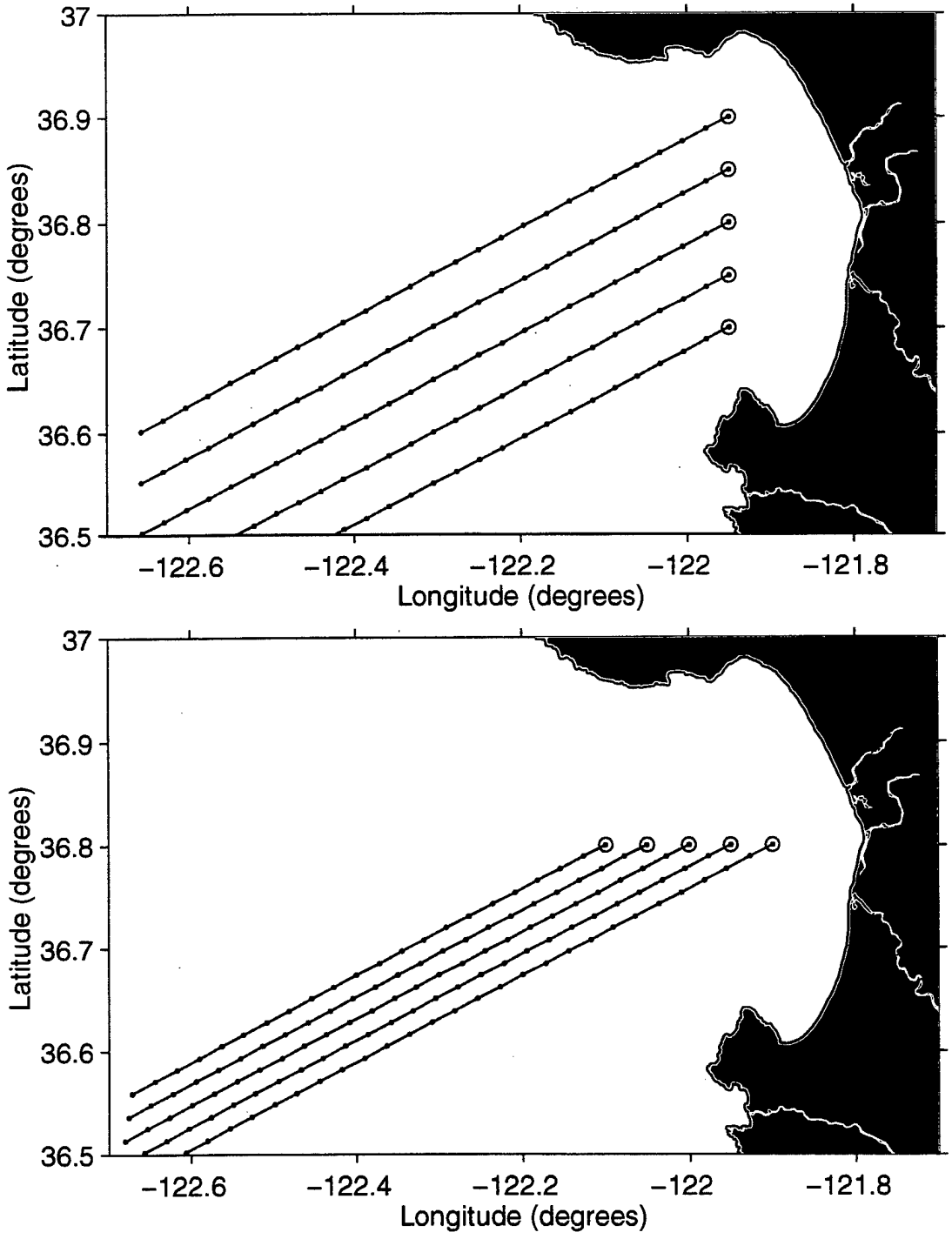


**Figure 38.** Trajectories for selected LEs produced from OSSM using NOAA circulation model currents only. 52 hours plotted (each symbol represents two hours). Upper panel displays LEs along 121.95°W. Lower panel displays LEs along 36.8°N.

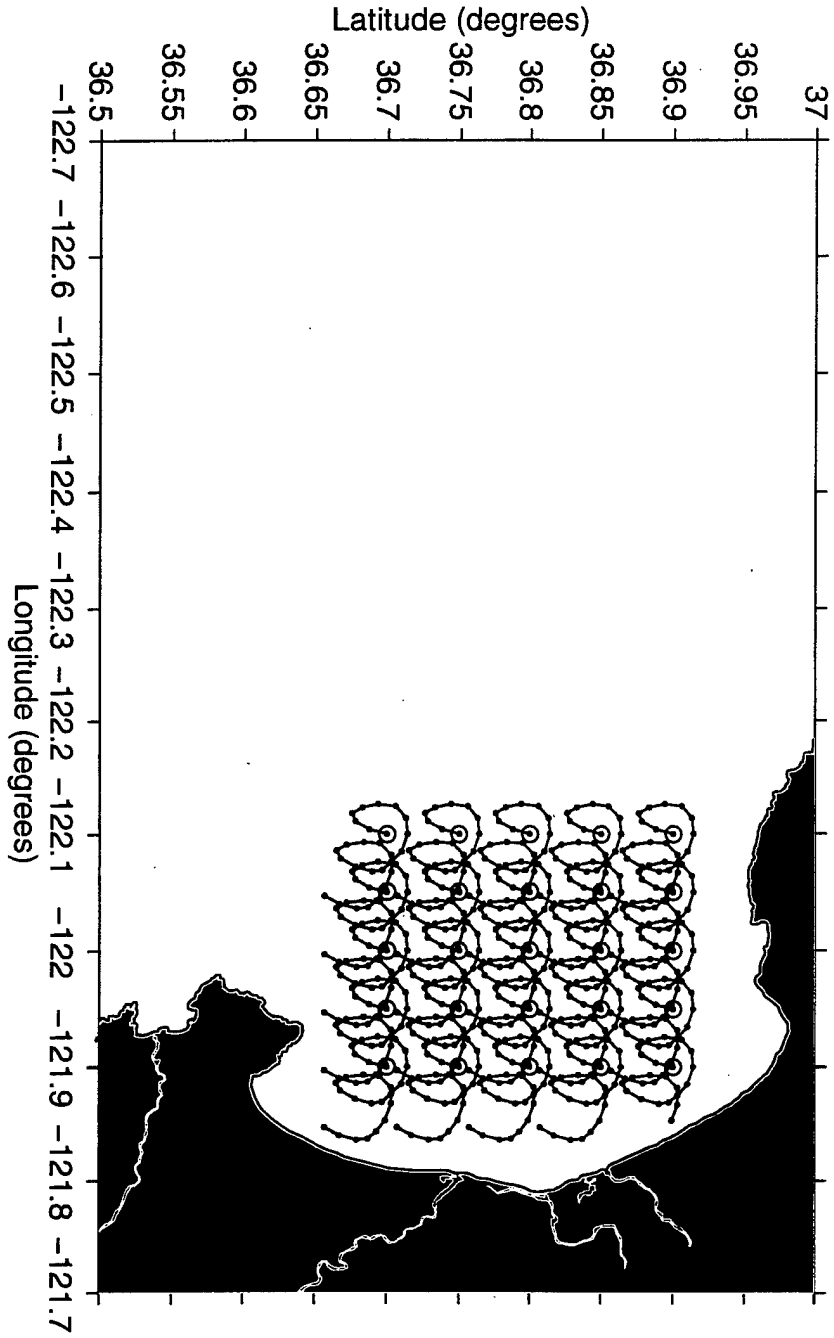


**Figure 39**. Trajectories for all 25 LEs produced from OSSM using canonical-day time file currents only. 52 hours plotted (each symbol represents two hours).

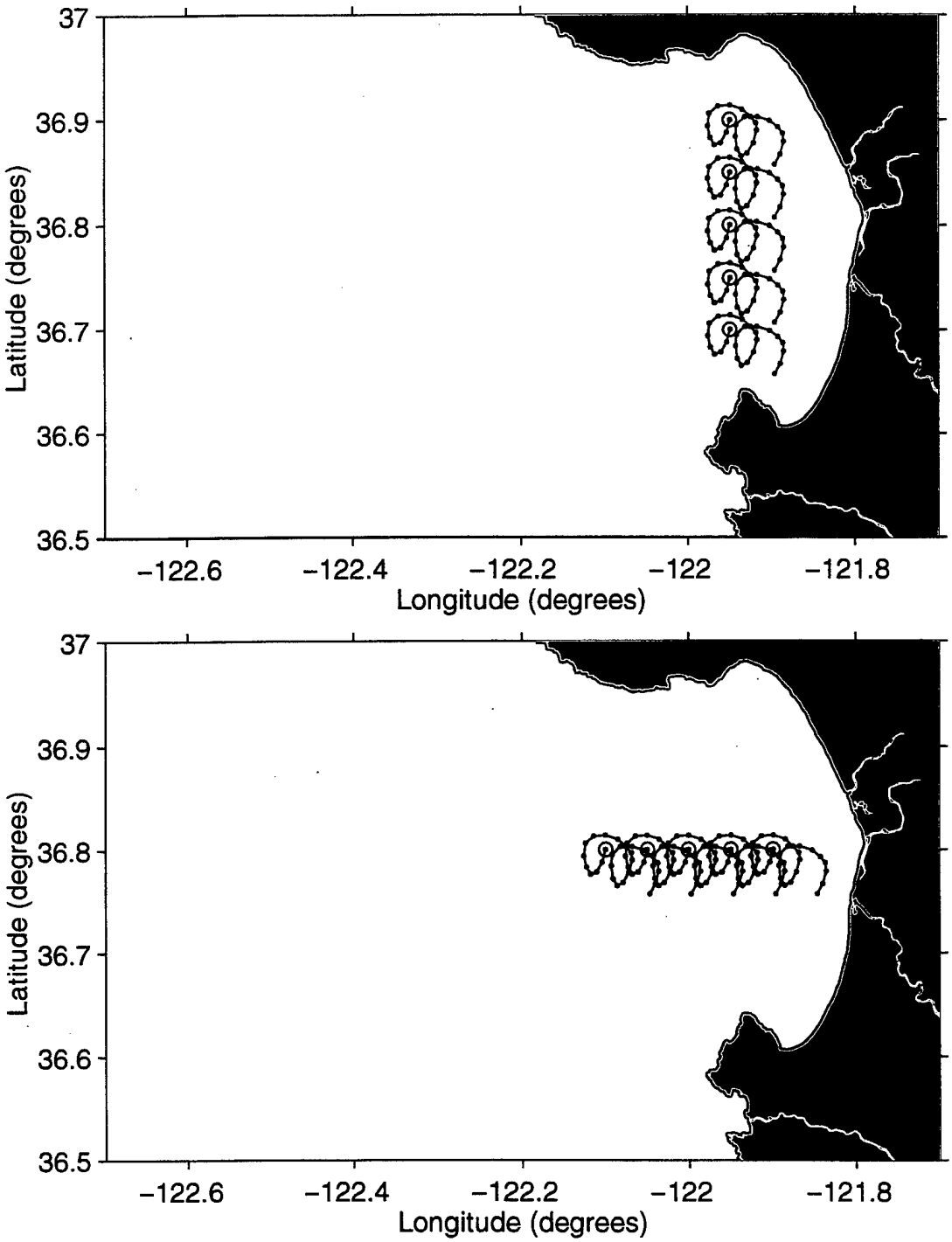


**Figure 40**. Trajectories for selected LEs produced from OSSM using canonical-day time file currents only. 52 hours plotted (each symbol represents two hours). Upper panel displays LEs along 121.95°W. Lower panel displays LEs along 36.8°N.

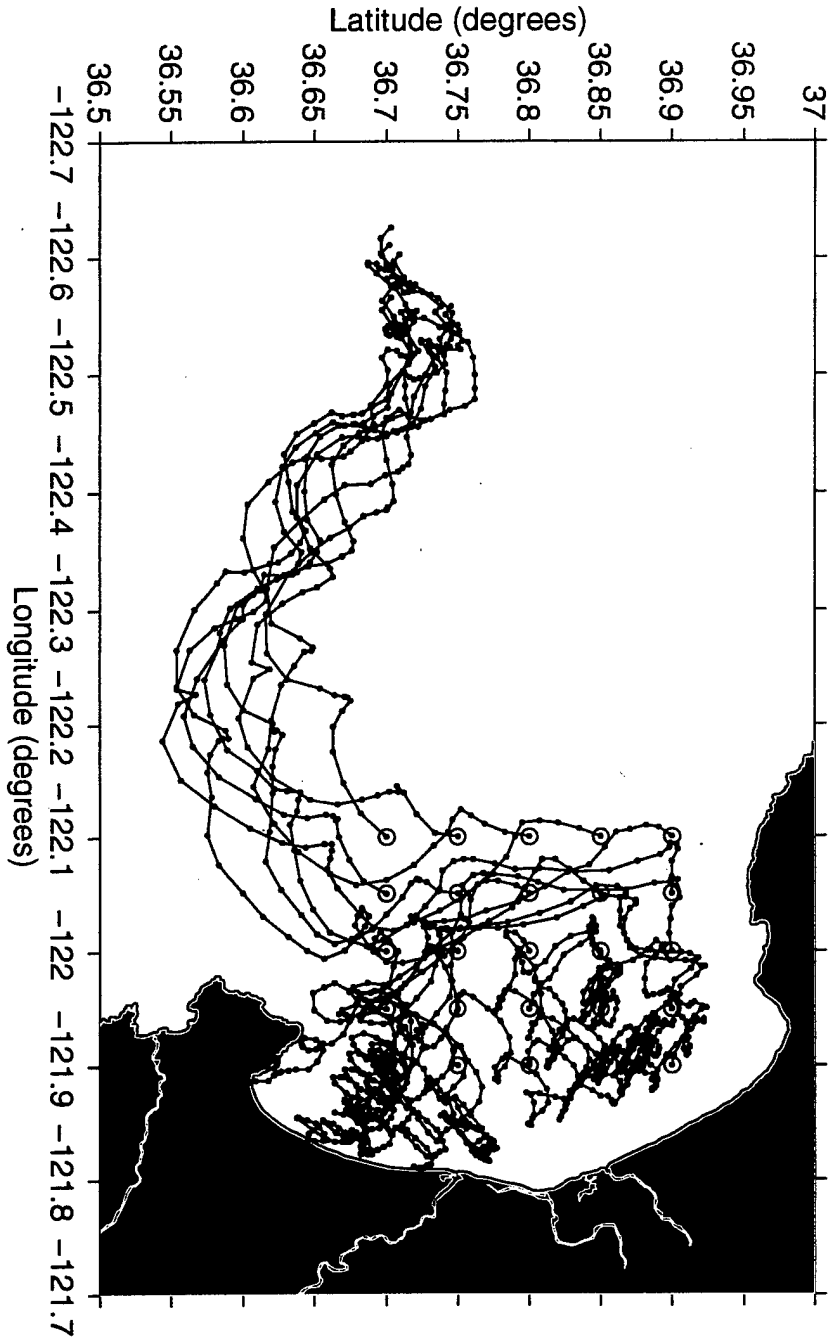


**Figure 41**. Trajectories for all 25 LEs produced from OSSM using canonical-day grid currents only. 120 hours plotted (each symbol represents two hours).

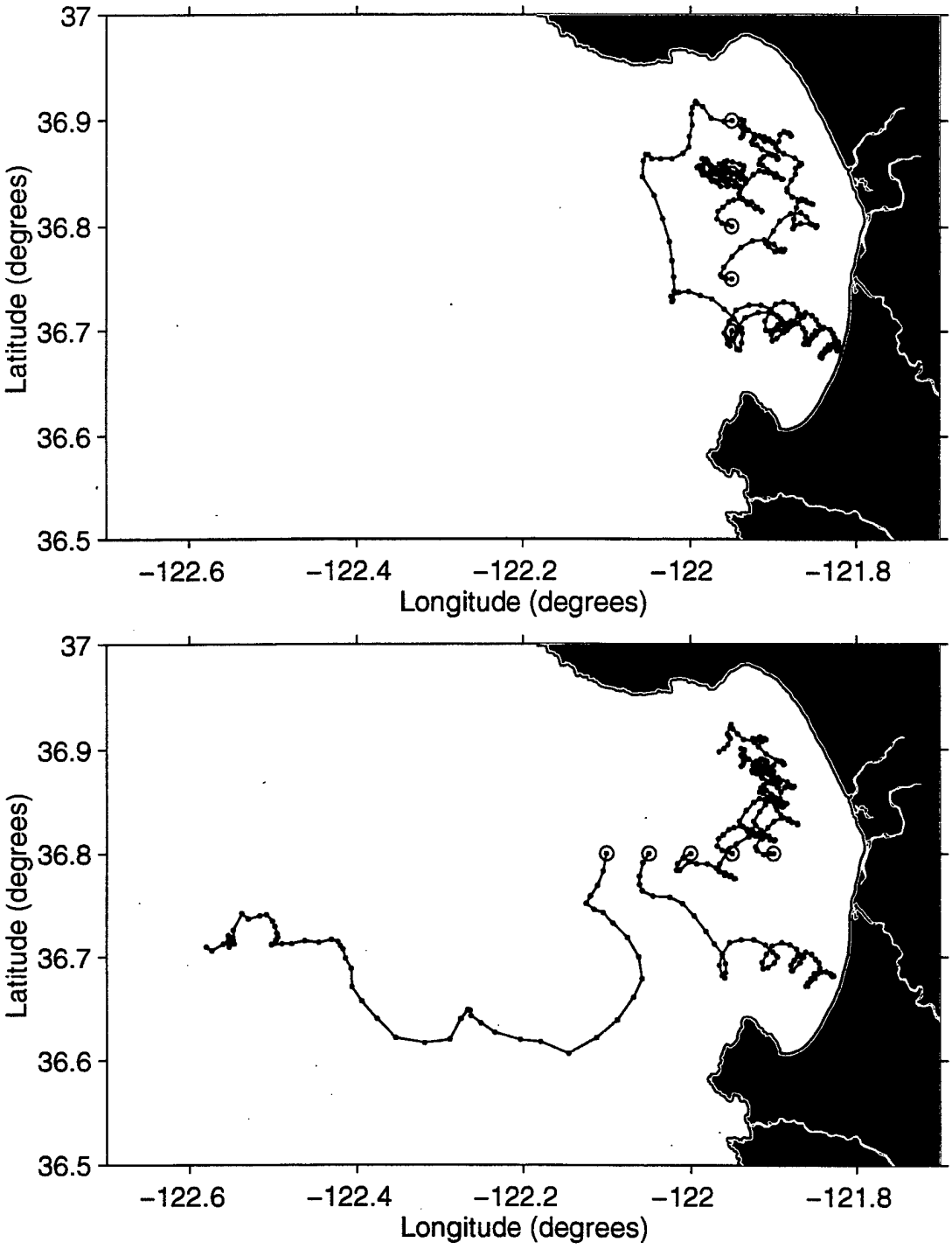


**Figure 42.** Trajectories for selected LEs produced from OSSM using canonical-day grid currents only. 120 hours plotted (each symbol represents two hours). Upper panel displays LEs along 121.95°W. Lower panel displays LEs along 36.8°N.

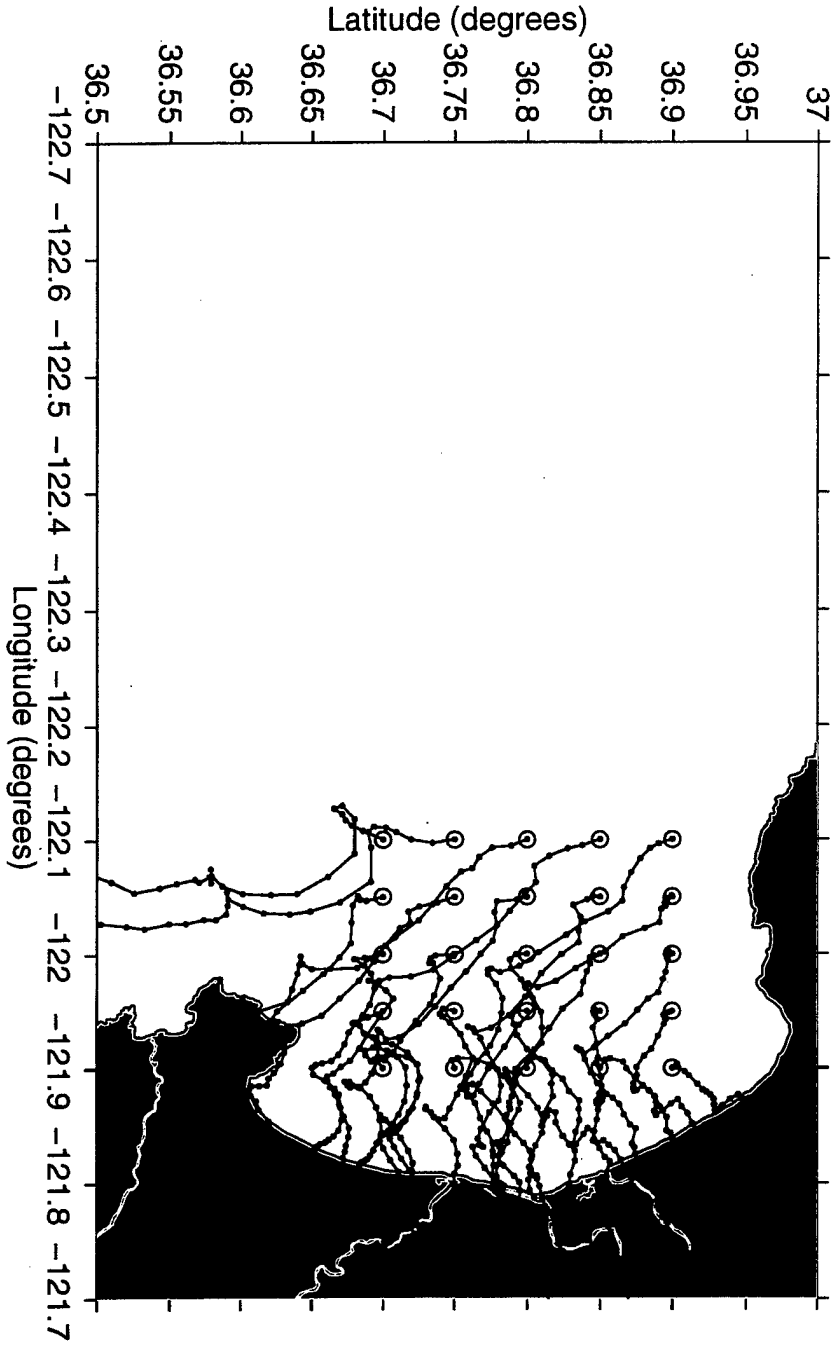


**Figure 43**. Trajectories for all 25 LEs computed from HF radar-derived surface current maps with a three percent wind. 72 hours plotted (each symbol represents two hours).

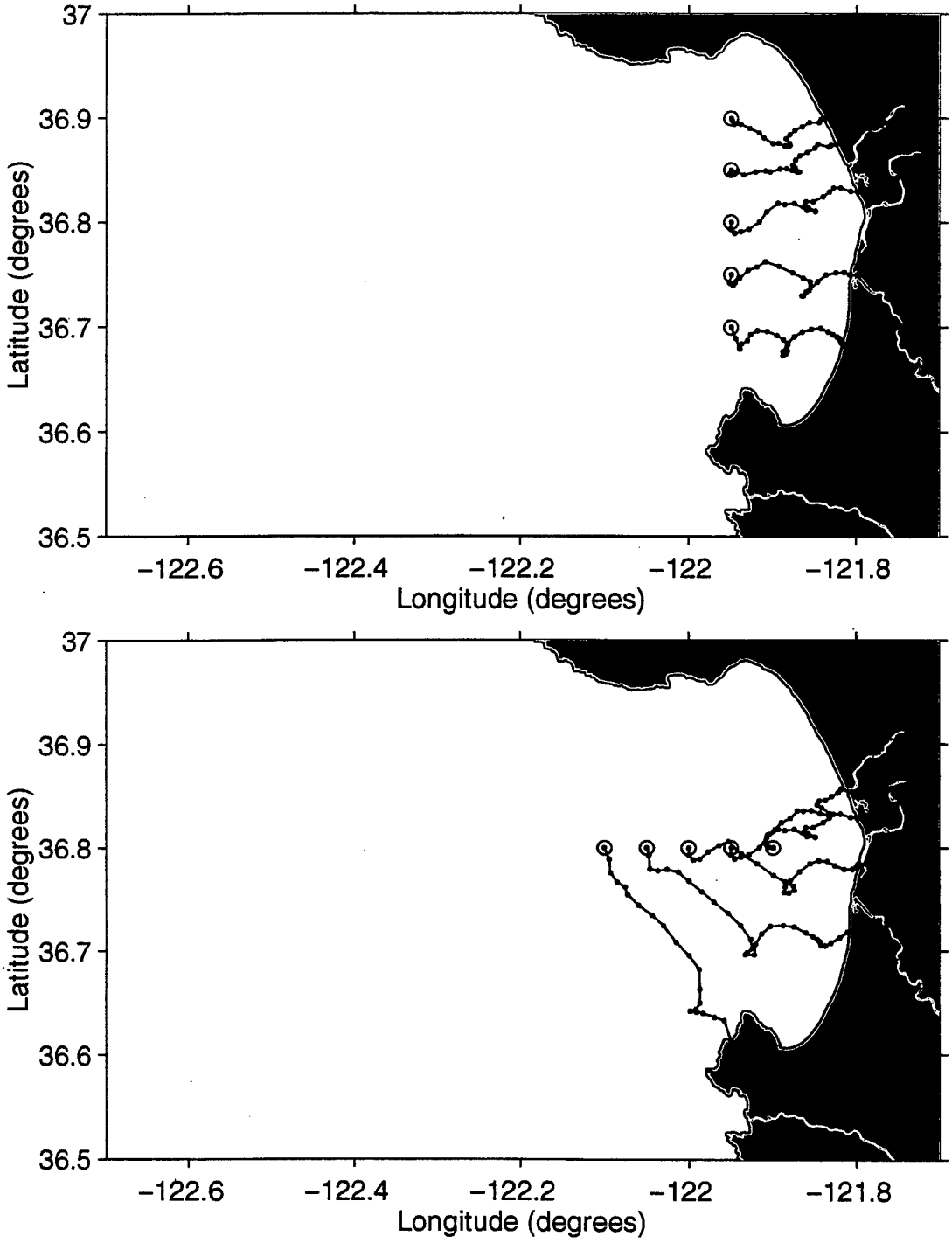


**Figure 44**. Trajectories for selected LEs computed from HF radar-derived surface current maps with a three percent wind. 72 hours plotted (each symbol represents two hours). Upper panel displays LEs along 121.95°W. Lower panel displays LEs along 36.8°N.

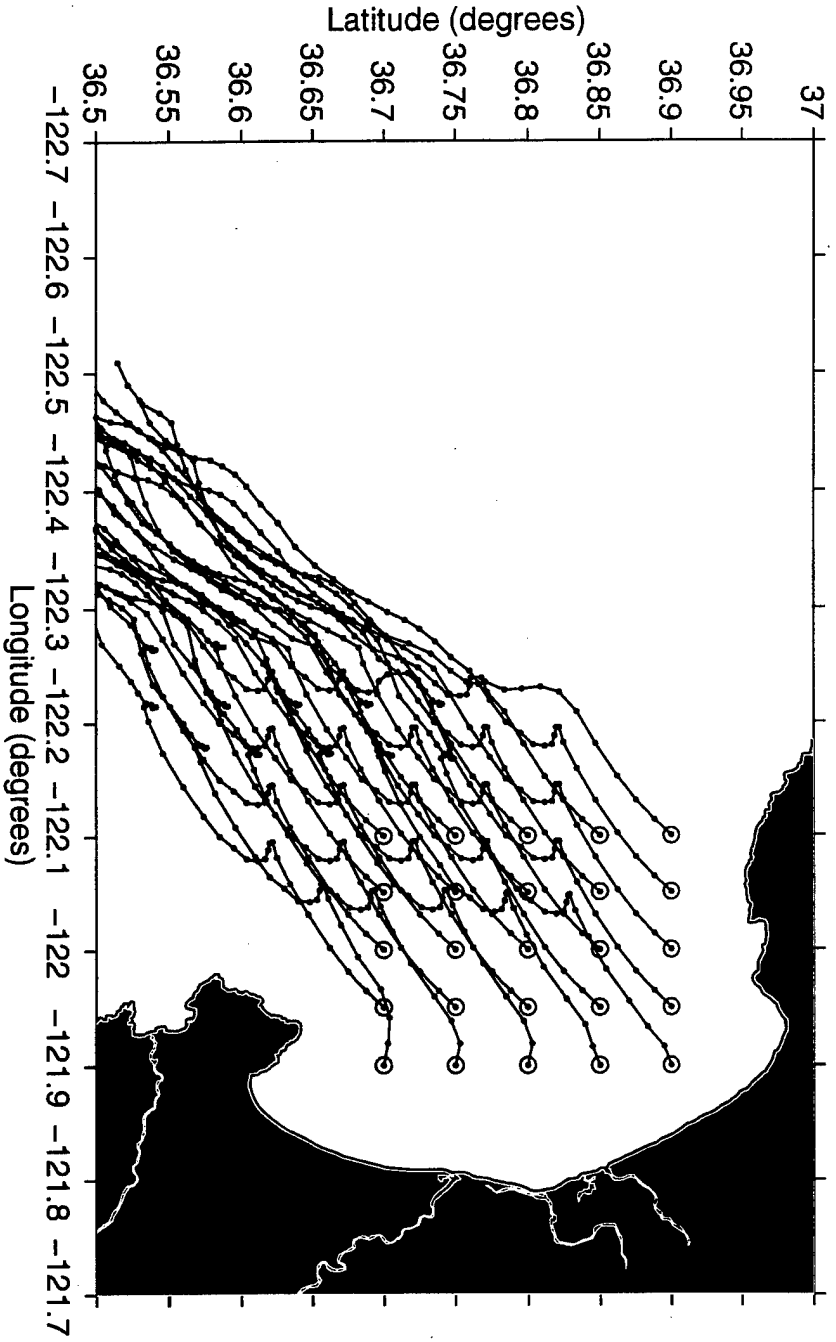


**Figure 45.** Trajectories for all 25 LEs produced from OSSM using NOAA circulation model currents with a three percent wind. 96 hours plotted (each symbol represents two hours).

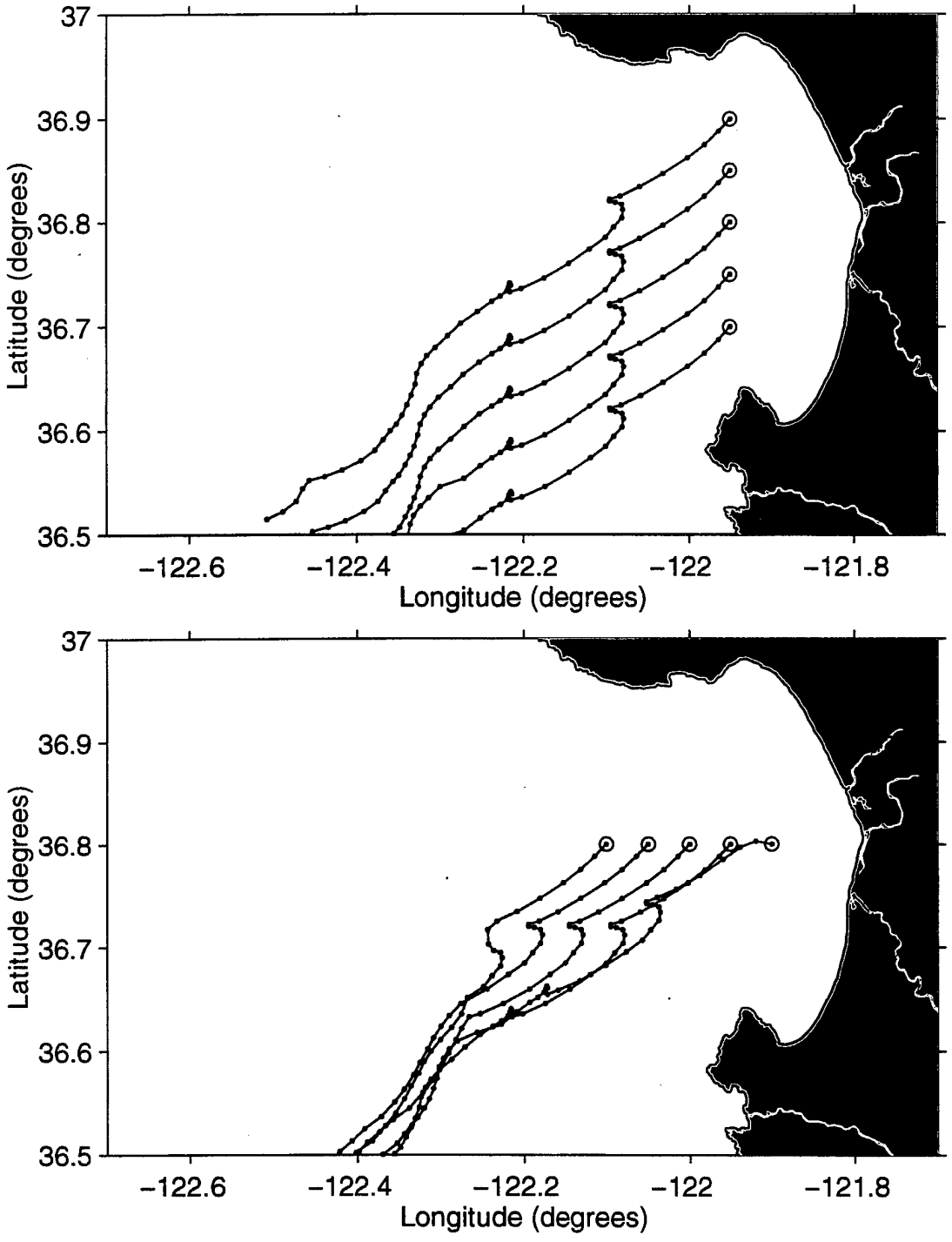


**Figure 46**. Trajectories for selected LEs produced from OSSM using NOAA circulation model currents with a three percent wind. 96 hours plotted (each symbol represents two hours). Upper panel displays LEs along 121.95°W. Lower panel displays LEs along 36.8°N.

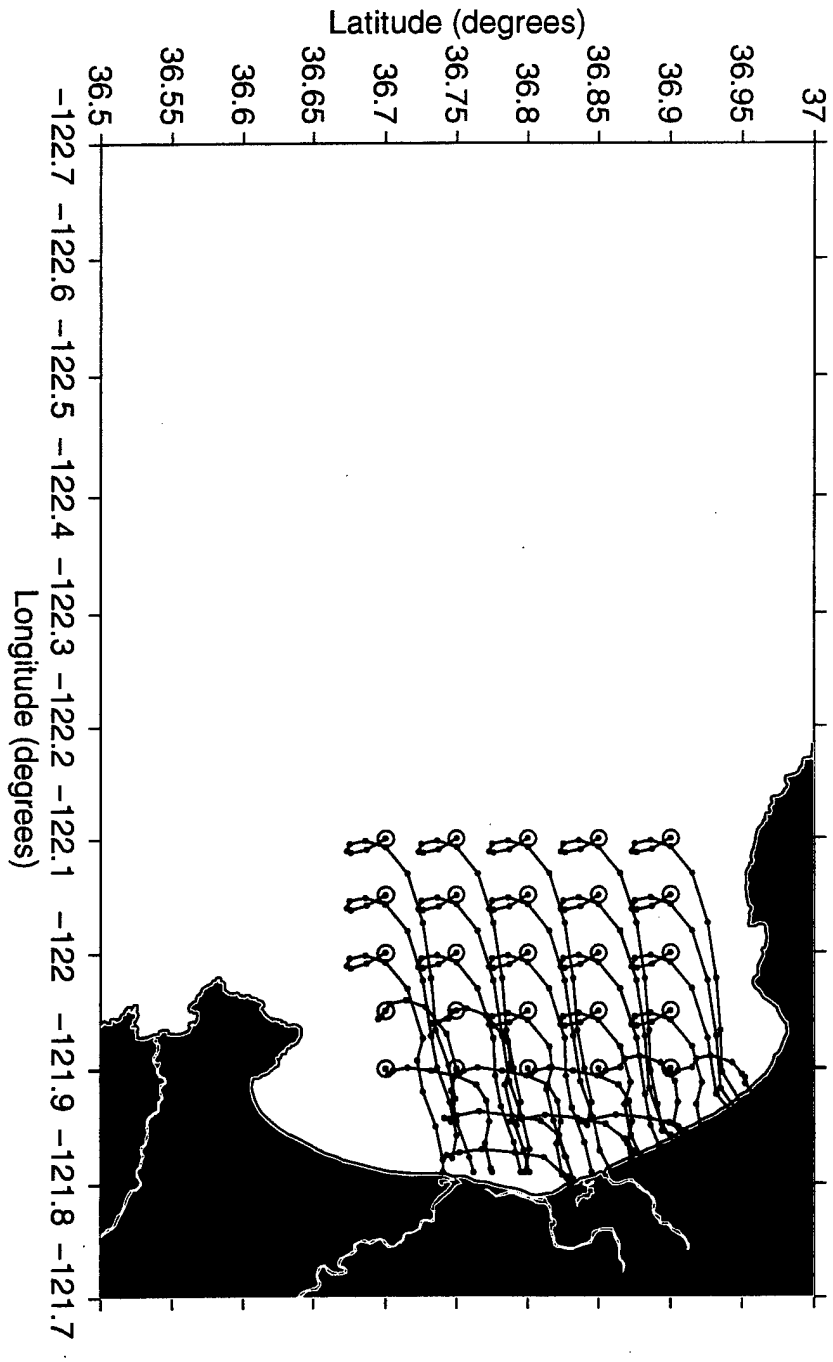


**Figure 47**. Trajectories for all 25 LEs produced from OSSM using canonical-day time file currents with a three percent wind. 46 hours plotted (each symbol represents two hours).

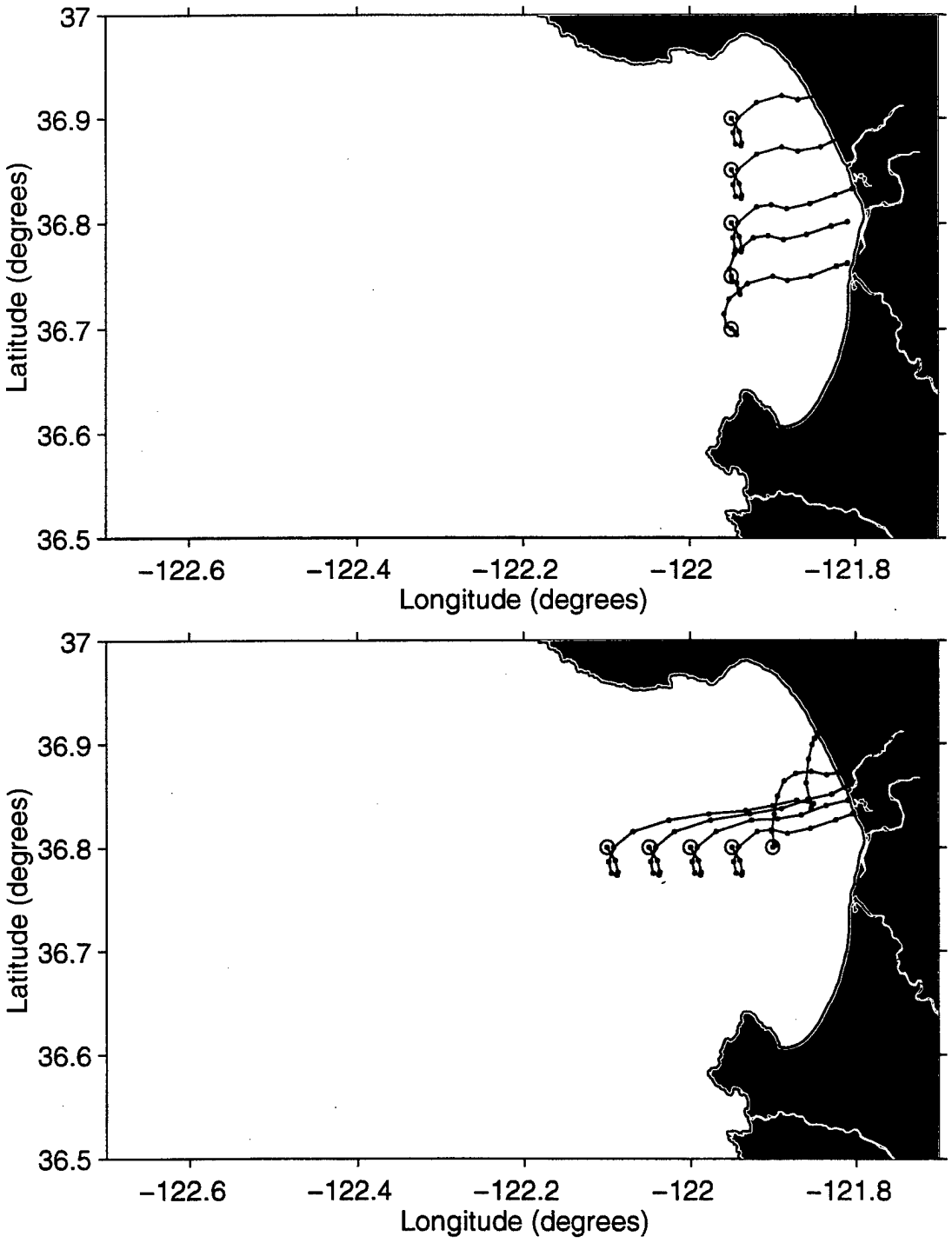


**Figure 48**. Trajectories for selected LEs produced from OSSM using canonical-day time file currents with a three percent wind. 46 hours plotted (each symbol represents two hours). Upper panel displays LEs along 121.95°W. Lower panel displays LEs along 36.8°N.

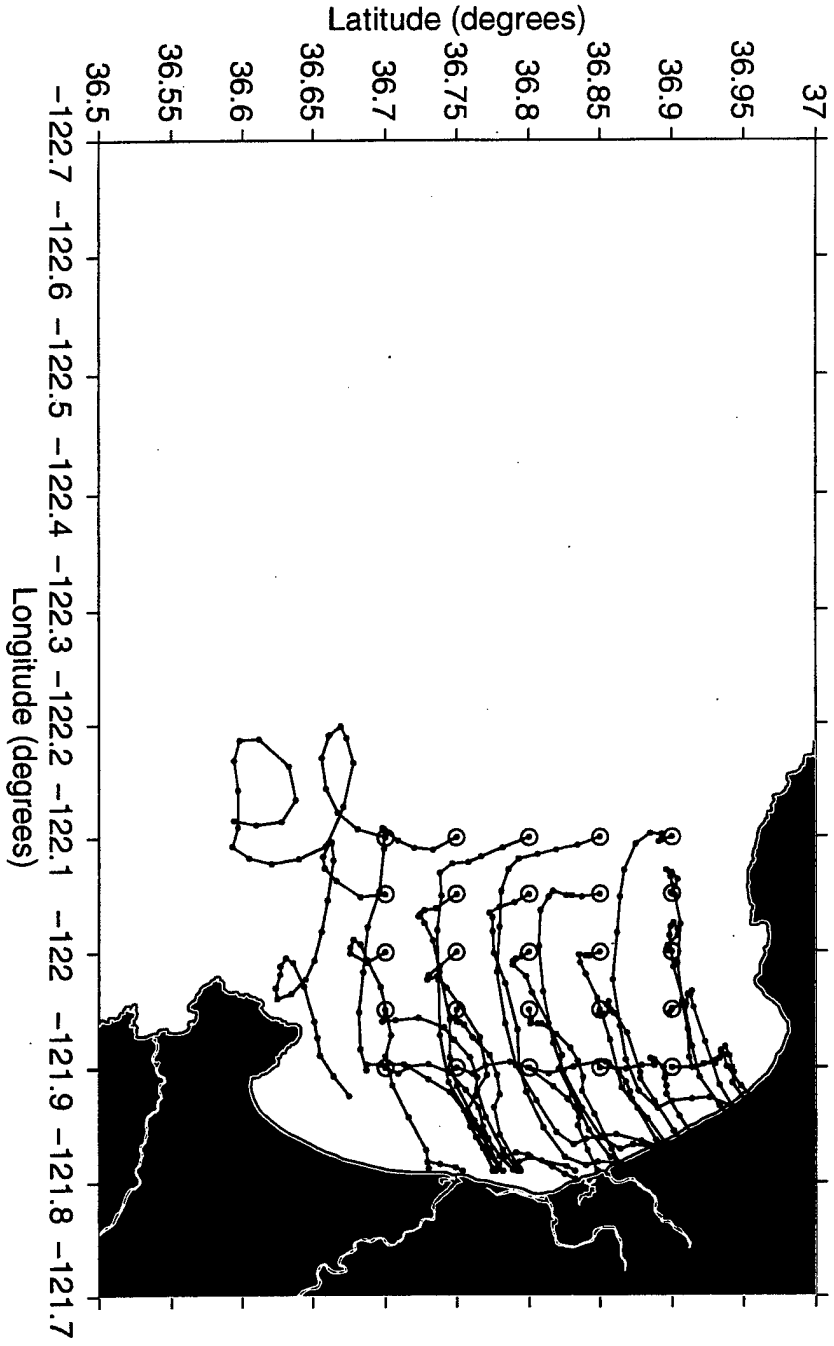


**Figure 49**. Trajectories for all 25 LEs produced from OSSM using canonical-day grid currents with a three percent wind. 48 hours plotted (each symbol represents two hours).

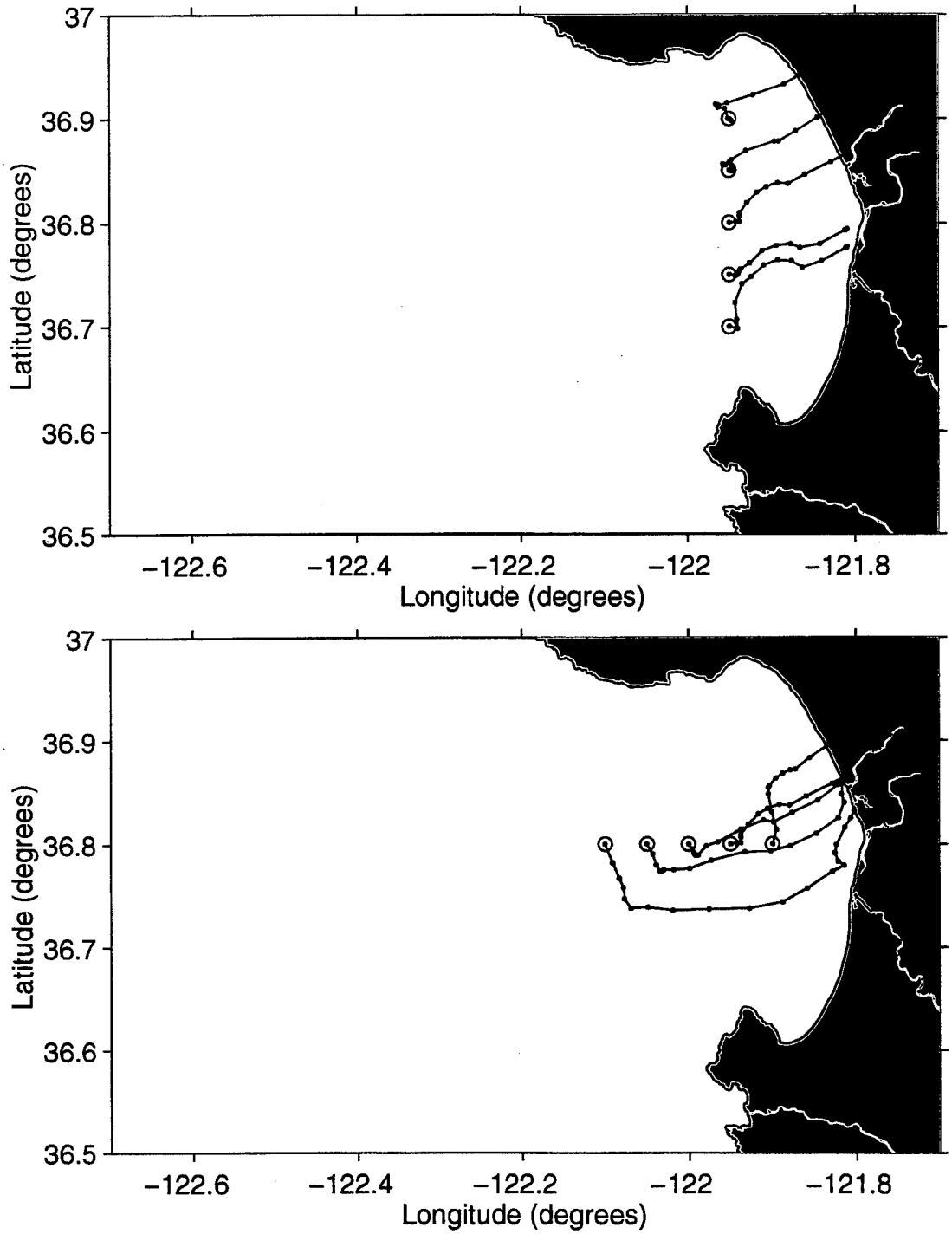


**Figure 50**. Trajectories for selected LEs produced from OSSM using canonical-day grid currents with a three percent wind. 48 hours plotted (each symbol represents two hours). Upper panel displays LEs along 121.95°W. Lower panel displays LEs along 36.8°N.

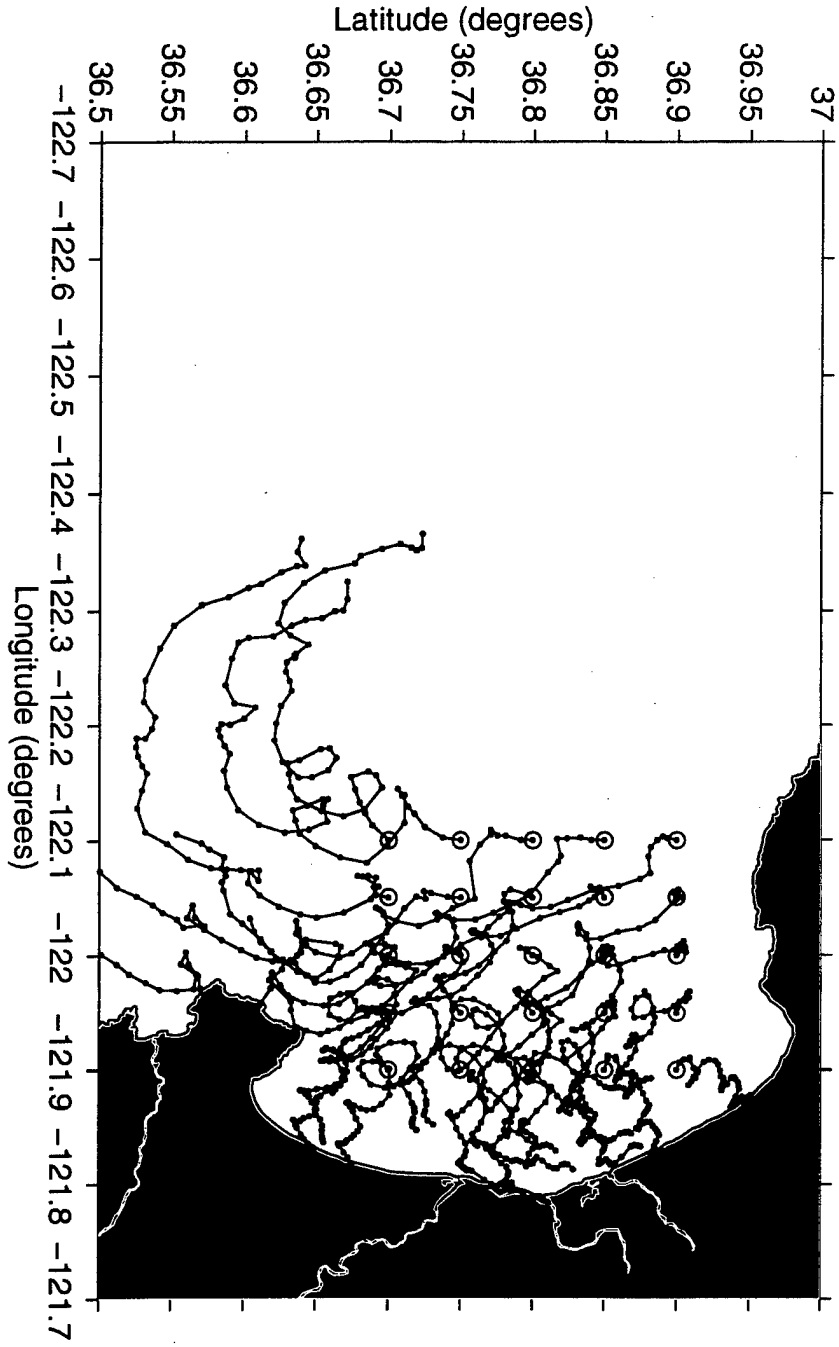


**Figure 51**. Trajectories for all 25 LEs computed from HF radar-derived surface current maps with a one percent wind, released at 0000 PDT. 96 hours plotted (each symbol represents two hours).

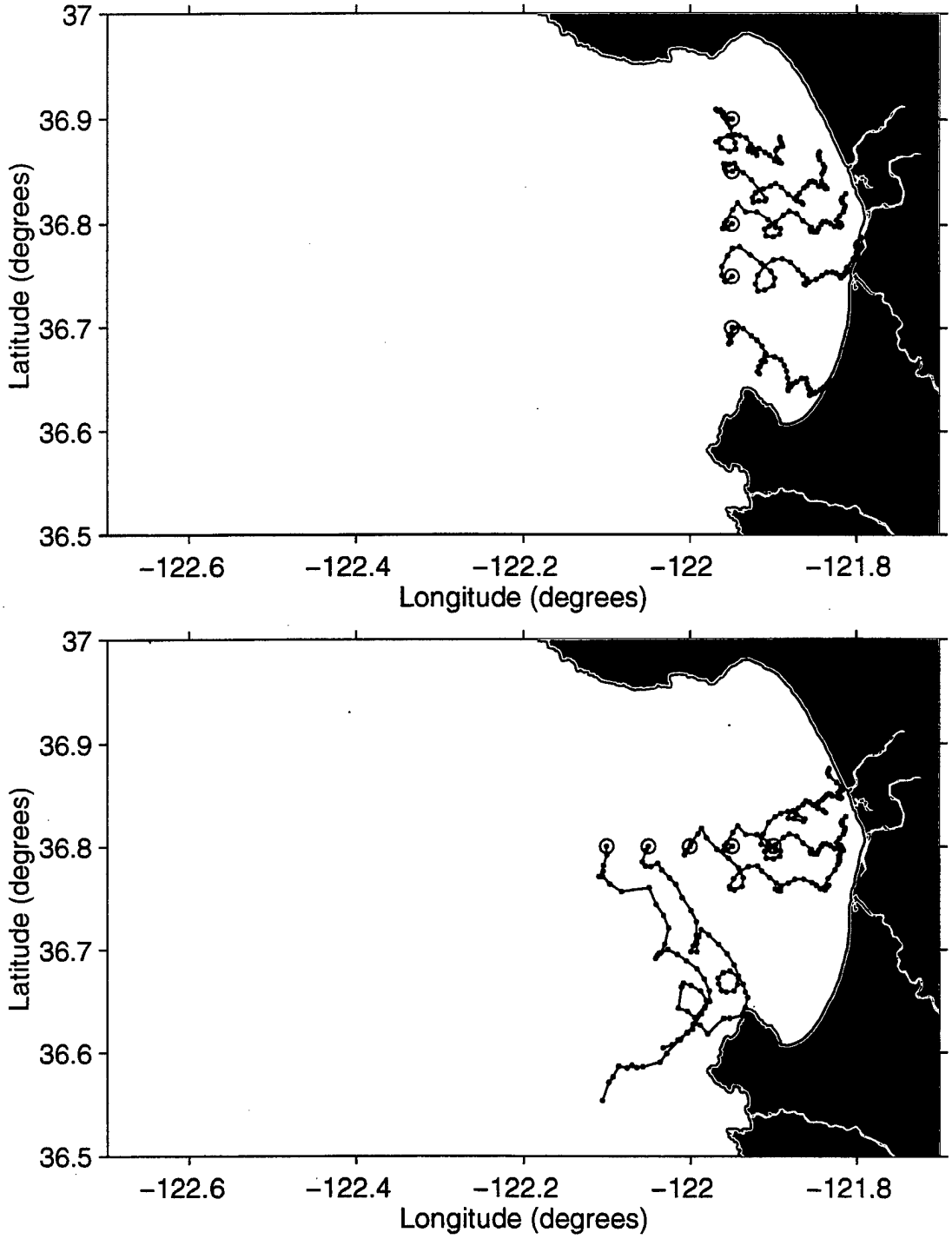


**Figure 52.** Trajectories for selected LEs computed from HF radar-derived surface current maps with a one percent wind, released at 0000 PDT. 96 hours plotted (each symbol represents two hours). Upper panel displays LEs along 121.95°W. Lower panel displays LEs along 36.8°N.

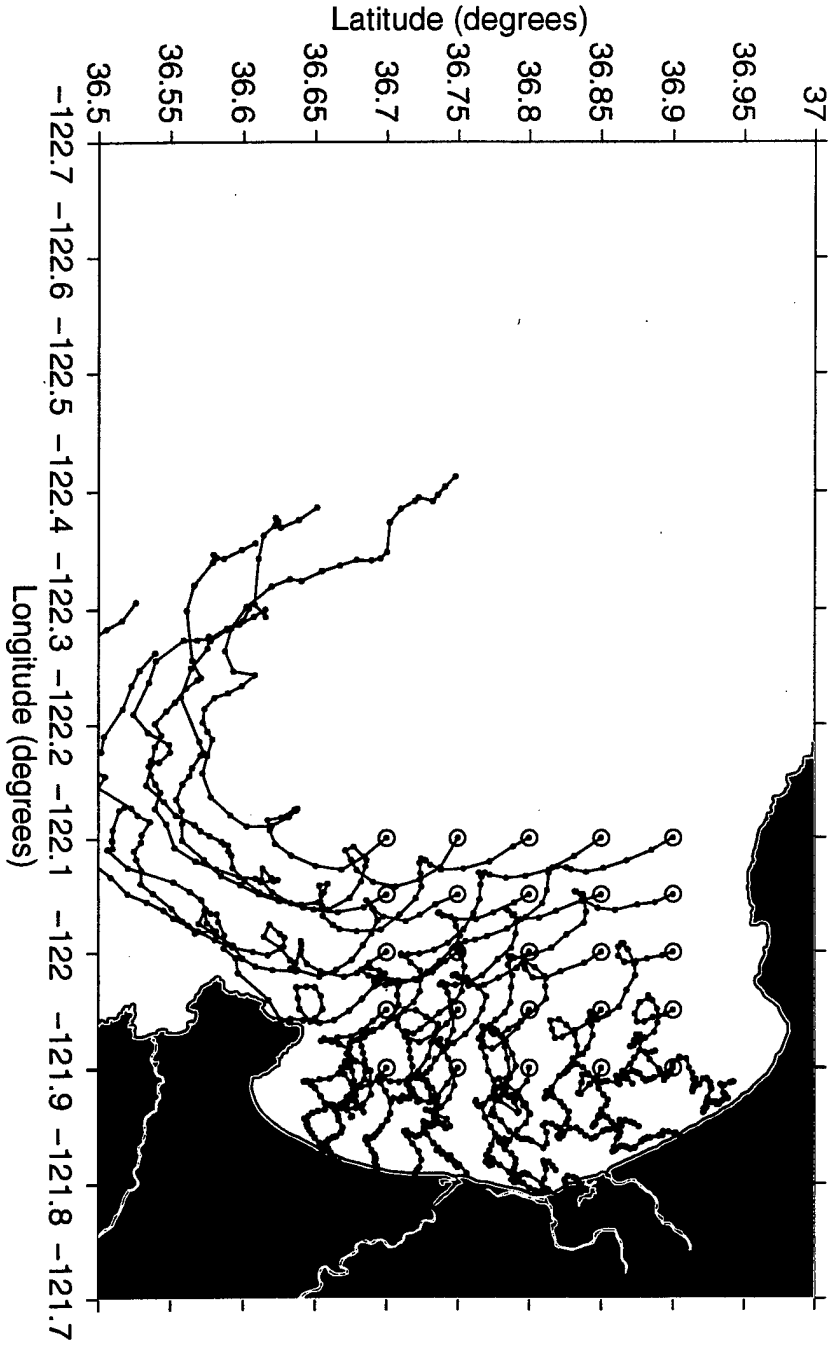


**Figure 53.** Trajectories for all 25 LEs computed from HF radar-derived surface current maps with a one percent wind, released at 1600 PDT. 96 hours plotted (each symbol represents two hours).

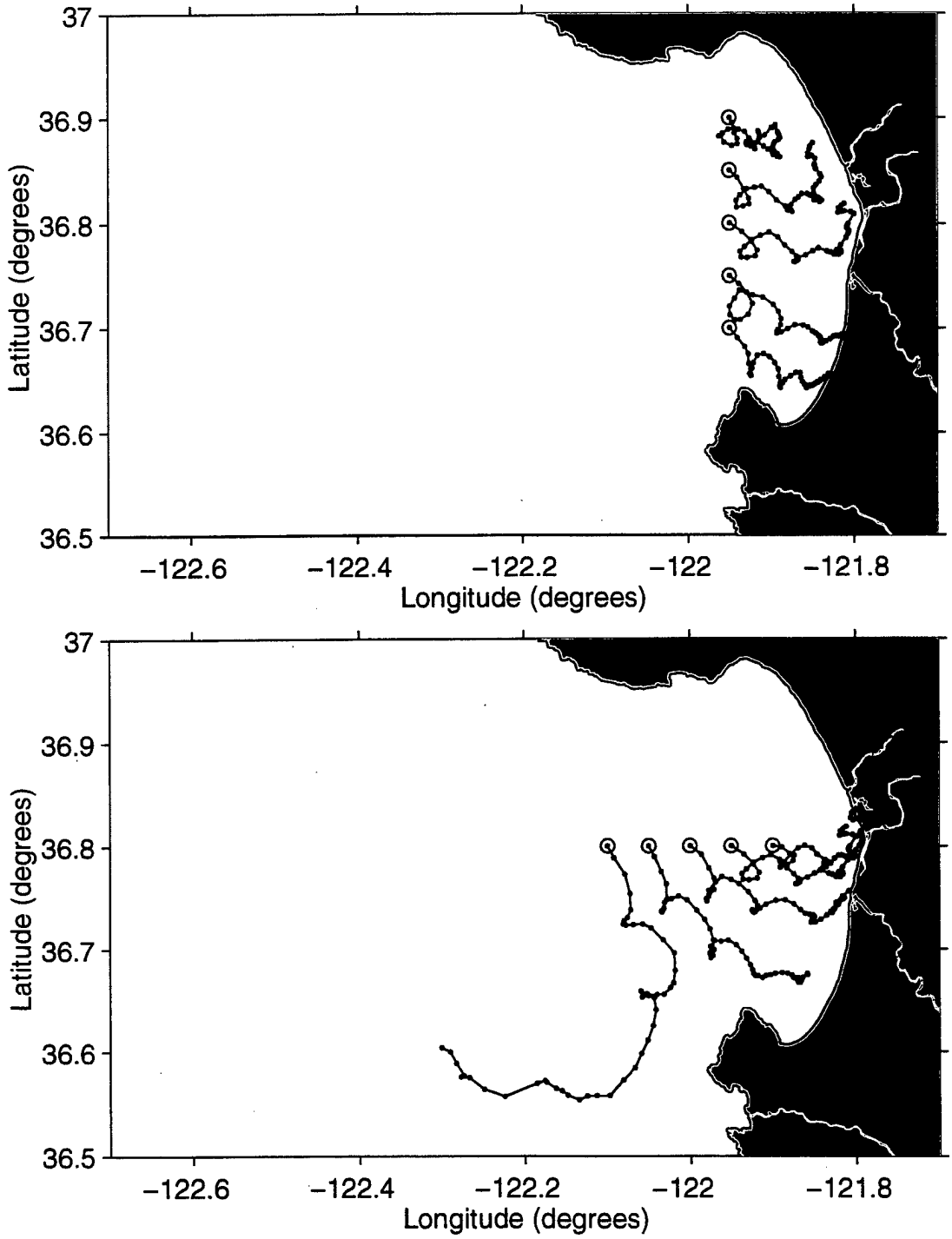


**Figure 54**. Trajectories for selected LEs computed from HF radar-derived surface current maps with a one percent wind, released at 1600 PDT. 96 hours plotted (each symbol represents two hours). Upper panel displays LEs along 121.95°W. Lower panel displays LEs along 36.8°N.

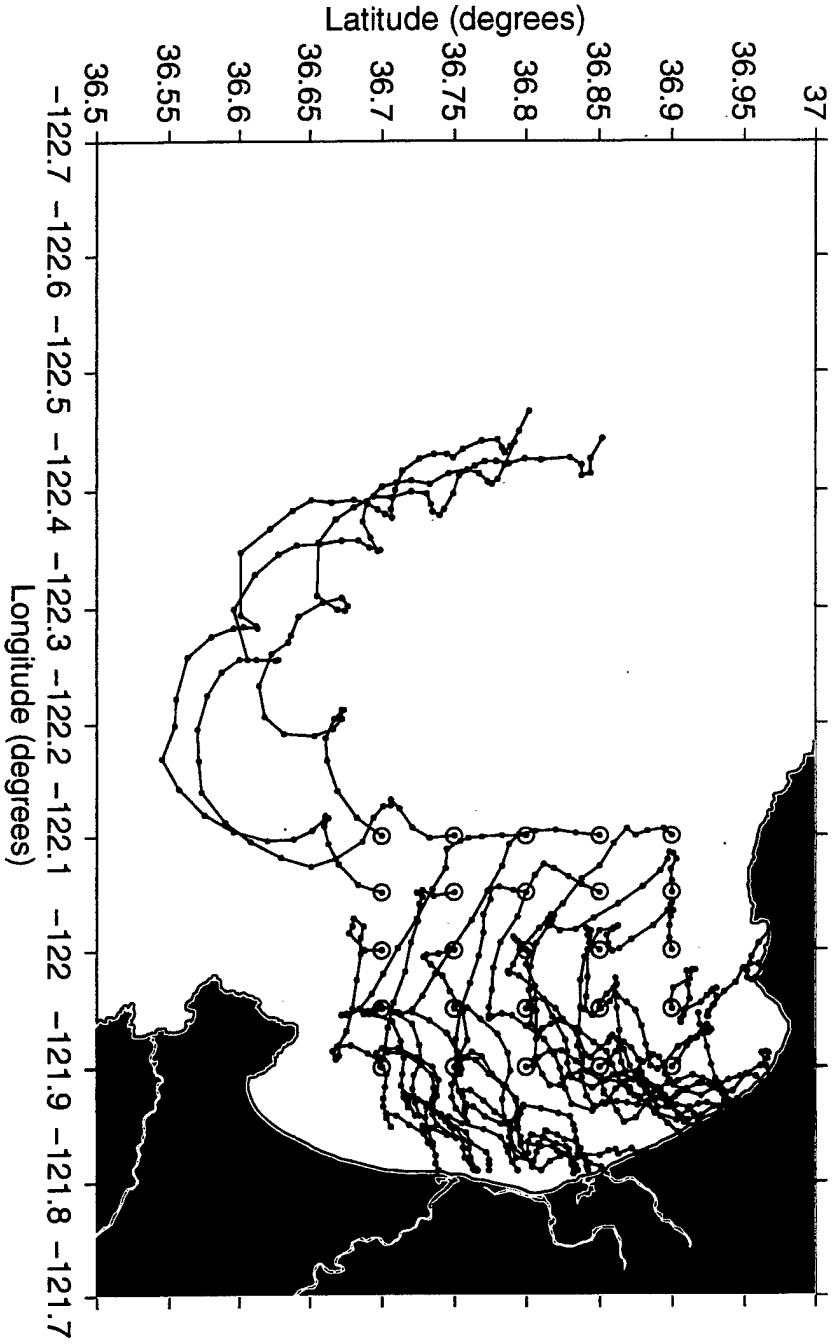


**Figure 55.** Trajectories for all 25 LEs produced from OSSM usng canonical-day grid currents with a one percent wind, released at 0000 PDT. 96 hours plotted (each symbol represents two hours).

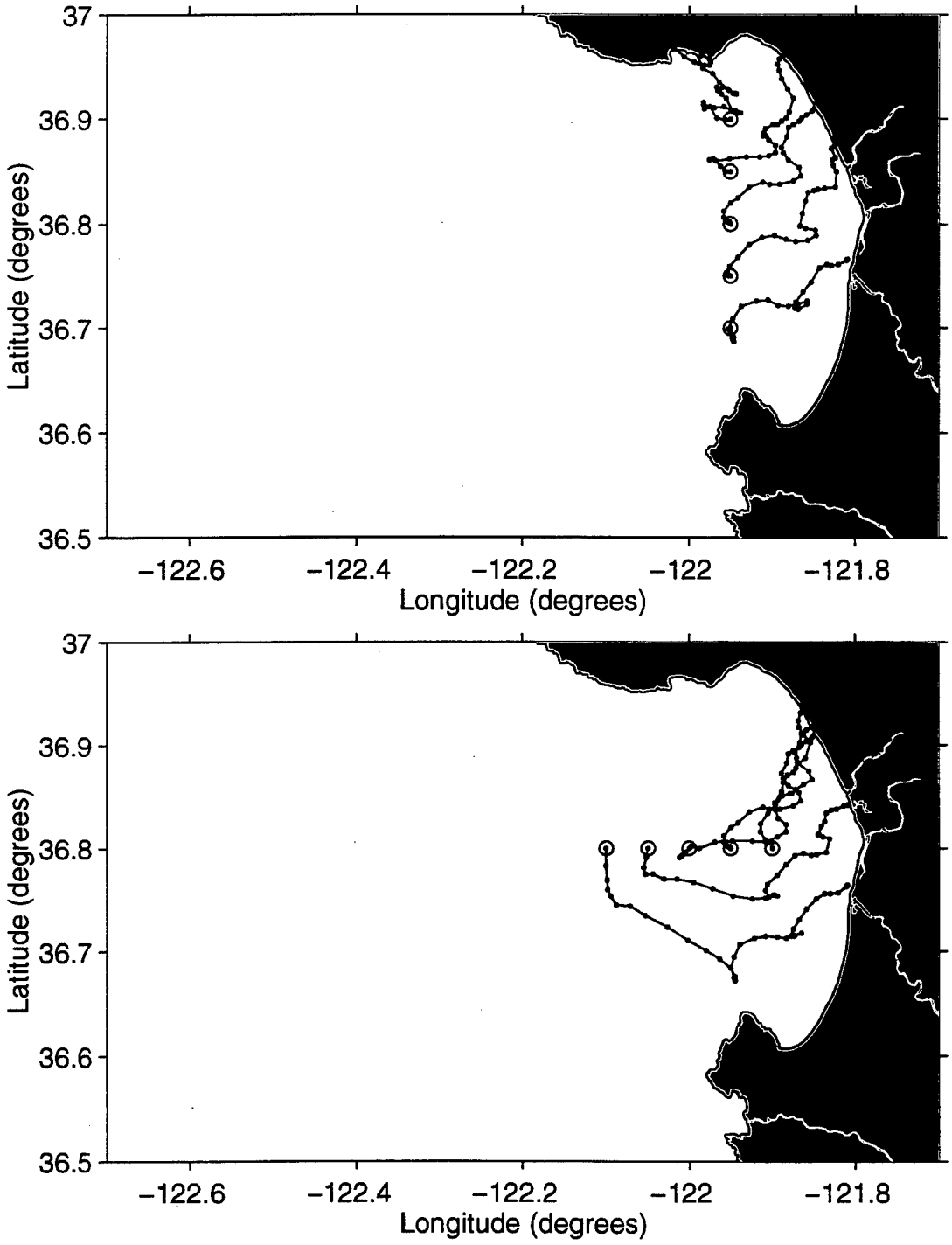


**Figure 56**. Trajectories for selected LEs produced from OSSM using canonical-day grid currents with a one percent wind, released at 0000 PDT. 96 hours plotted (each symbol represents two hours). Upper panel displays LEs along 121.95°W. Lower panel displays LEs along 36.8°N.

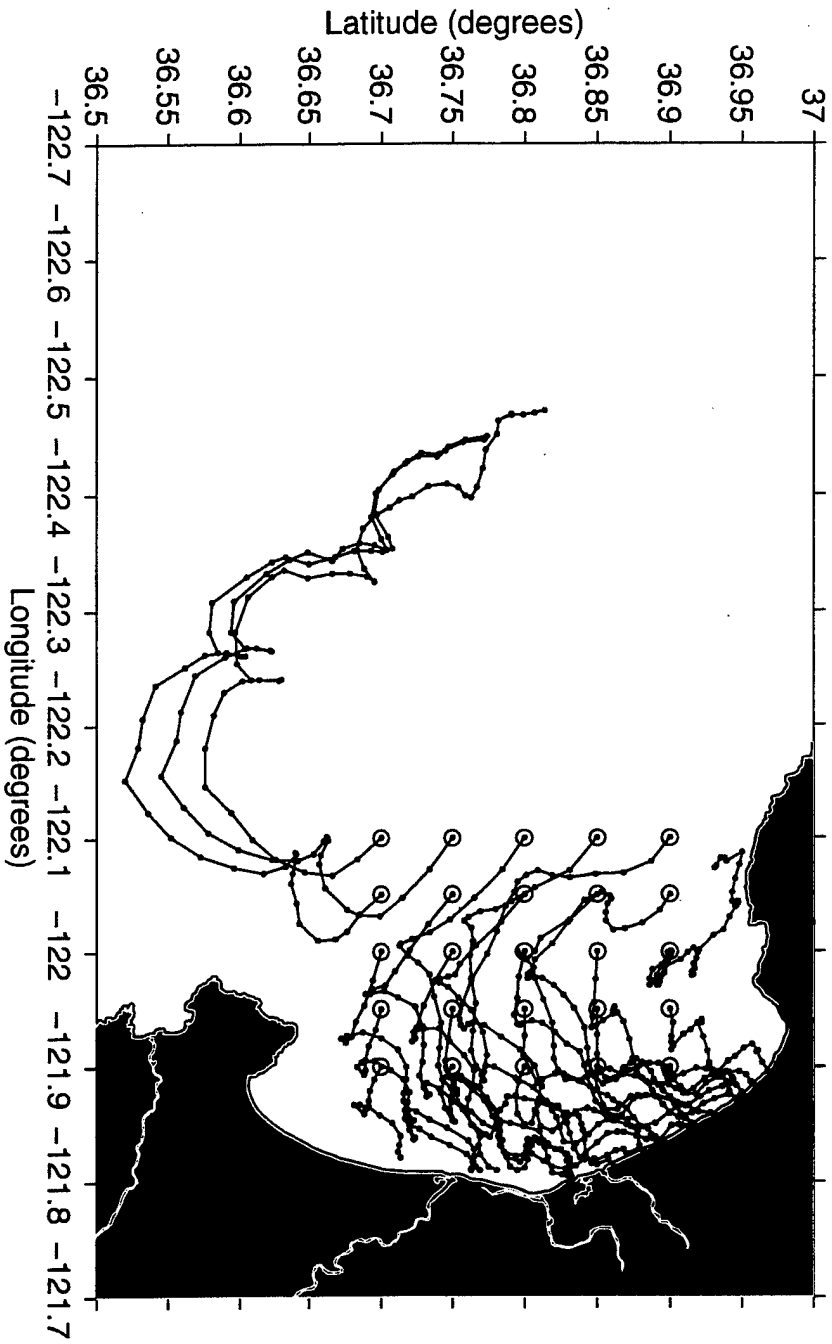


**Figure 57**. Trajectories for all 25 LEs produced from OSSM usng canonical-day grid currents with a one percent wind, released at 1600 PDT. 96 hours plotted (each symbol represents two hours).

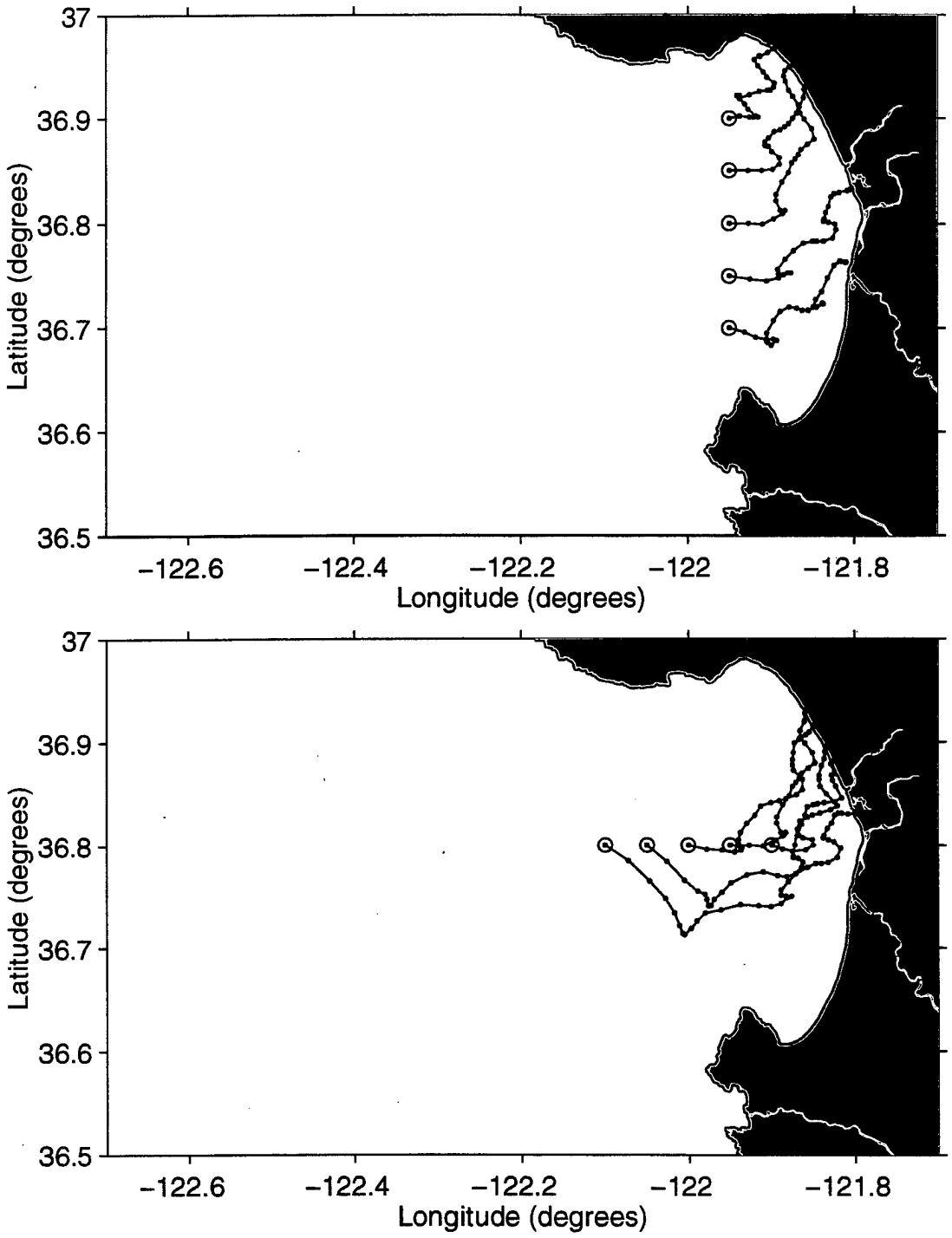


**Figure 58.** Trajectories for selected LEs produced from OSSM using canonical-day grid currents with a one percent wind, released at 1600 PDT. 96 hours plotted (each symbol represents two hours). Upper panel displays LEs along 121.95°W. Lower panel displays LEs along 36.8°N.

# V. SUMMARY AND RECOMENDATIONS

## A. SUMMARY

This study was conducted to examine a possible use of 2-D coastal surface currents from an HF radar network. Due to the environmentally sensitive nature of the Monterey Bay National Marine Sanctuary, oil spill response monitoring was examined in order to evaluate the present state of trajectory analyses in this open ocean coastal environment and to suggest ways to better incorporate modern observational data.

### 1. General Overview

Oil spill monitoring and prediction of oil movement is the responsibility of NOAA/HAZMAT which uses the On-Scene Spill Model (OSSM) and the surface current output from the NOAA circulation model in order to obtain an initial or first-guess idea of where the spilled oil will go. The trajectory results from this initial prediction were evaluated against trajectory results using various surface current products generated from direct surface current data obtained from an HF radar network. First, a copy of the OSSM code, a digitized map of Monterey Bay's coastline, and the output from the NOAA circulation model was obtained. Next, the databases were searched for good HF radar coverage during a time period also containing wind observations of a strong summertime sea breeze signal. The period selected was 9-14 September 1994. Then, trajectories generated from OSSM under various current, wind and element release times were compared to trajectories calculated directly from HF radar-derived surface current maps of the Bay.

Cases examined were currents only, currents with three percent winds and currents with one percent winds but with different element release times. The different currents used to generate trajectories in OSSM were the NOAA circulation modeled current and currents produced from canonical-day averaged HF radar-derived surface current maps, in a time file format and grid format. The circulation model current represents the NOAA/HAZMAT first-response trajectory fields. The current provided was a constant southwestward flow. The other two current fields represented attempts to incorporate direct HF radar-derived surface currents into OSSM. The first was an attempt to reduce the HF radar 2-D current maps into a time file due to the ease in which OSSM can incorporate this type of data. The HF radar-derived surface currents initially were averaged into twelve canonical-day maps. Then, the currents inside the Bay were reduced to an average u- and v-component for each hour. This time file was applied over the entire Bay to produce a temporally varying but spatially constant pattern. The second type of HF radar-generated current was a direct conversion of the canonical-day current maps into an OSSM grid format. This required a more complicated model run, which consisted of manually starting and stopping OSSM every two (model) hours to re-initialize trajectory locations and change the current grid. A more realistic temporally varying 2-D spatial current pattern was created.

### 2. Basic Results

The currents used in OSSM greatly effect the resultant trajectories. The NOAA circulation modeled currents, even with a three percent wind factor included, produced trajectories which all exited the Bay to the southwest. Any prediction based on this

would be a mistake. The use of products generated from canonical-day HF radar-derived surface currents in lieu of the real-time HF radar-derived surface currents do produce more realistic trajectories with OSSM. Using the currents which were reduced to a simple time file shows that trajectories of oil elements released inside Monterey Bay remain in the Bay, but these trajectories do not capture the mesoscale features present in the Bay. Although more time consuming, using the currents reduced to grids provided the most realistic pattern of trajectories. Even though the grids were based on an average of just one week of data, they adequately represented the typical summertime current pattern in the Bay. The trajectories corresponded well to the trajectories obtained using actual surface current maps and captured the mesoscale features present inside and outside the Bay.

Although an examination of different currents in OSSM was the primary focus, the cases also examined the wind effect and sensitivity to release time on the trajectories. In Monterey Bay particularly, the movement due to the wind is of the same order as the surface currents. The wind is dominated by the sea breeze circulation which has a 2-D pattern as well and cannot be adequately estimated by the use of just one wind source. OSSM defaults to incorporating three percent of the wind velocity as an additional factor, besides surface currents, in the prediction of oil movement. This "rule of thumb" represents wind-driven wave factors such as Stokes drift as well as the differential oil-water slip. It is estimated, however, that if the HF radar-derived surface currents are used as the current input to OSSM, this wind effect is probably less than three percent as many of the effects this factor represents are already inherent in the direct surface current

measurements. With no winds, the trajectories do not beach; with one percent wind, they beach within three to four days; with three percent wind, they beach within two to three days. Finally, releasing the oil elements either at midnight (no sea breeze) or in the afternoon (strongest sea breeze) shows the initial trajectory is greatly effected as is the precise time and location of the final beaching.

## B. RECOMENDATIONS

The use of HF radar-derived surface current data provides a more realistic picture of oil spill trajectory analyses in Monterey Bay than using the output from the NOAA circulation model. Even though the result obtained from use of the circulation model is meant to be a first-guess prediction of oil movement, it provides a false sense of security that discharged oil will leave the Bay whereas the actual surface current patterns as well as the strength of the sea breeze circulation within the Bay will actually lead to oil beaching within a few days.

This study concentrated on the summertime current and wind pattern in Monterey Bay. In wintertime, both the surface currents and sea breeze patterns are different. An examination of a seasonal deployment of an HF radar network in winter for the Bay or for another open ocean coastal environment should be conducted.

Trajectories generated directly using the HF radar-derived surface current patterns show that elements released outside of the mouth of Monterey Bay tend to escape. Even with a three percent wind factor included, these are either caught in the anticyclonic eddy feature located well off shore of the Bay or in the strong southward flowing California

Current. This suggests that oil elements can escape being a problem in Monterey Bay if released only 50 miles offshore.

Finally, the trajectories examined in this study do not include the specific oil characteristic factors which influence oil movement, evaporation and dissipation. The incorporation of these parameters is the most significant feature of the NOAA On-Scene Spill Model. It is important, therefore, to develop better methods of incorporating direct surface current measurements, such as those collected using an HF radar network, into OSSM. Although realistic results were obtained using the current grids, the procedure is too manually intensive. Possibly future versions of OSSM will be able to incorporate an ability to ingest complicated temporally varying 2-D current and wind patterns.

## LIST OF REFERENCES


Barrick, D. E., Evans, M. W., Weber, "Ocean Surface Currents Mapped by Radar," *Science*, VOL. 198, NO. 4313, pp. 138-144, 1977.

Barrick, D. E., "The Role of the Gravity-Wave Dispersion Relation in HF Radar Measurements of the Sea Surface," *IEEE Journal of Oceanic Engineering*, VOL. OE11, NO. 2, pp 286-292, 1986.

Bakun, A. and Nelson, C. S., "The Seasonal Cycle of Wind-Stress Curl in Subtropical Eastern Boundary Current Regions," *Journal of Physical Oceanography*, VOL. 21, pp. 1815-1834, 1991.

Battisti, D. S. and Clarke, A. J., "A Simple Method for Estimating Barotropic Tidal Currents on Continental Margins with Specific Application to the M2 Tide off the Atlantic and Pacific Coasts of the United States," *Journal of Physical Oceanography*, VOL. 12, pp. 8-16, 1982.

Boyer, K. F., *Characterization of OSCR HF Radar Data in Monterey Bay*, Master's Thesis, Naval Postgraduate School, Monterey, CA, 1997.

Chelton, D. B., "Seasonal Variability of Alongshore Geostrophic Velocity off Central California," *Journal of Geophysical Research*, VOL. 89, NO. C3, pp. 3473-3486, 1984.

Davis, R. E., "Drifter Observations of Coastal Surface Currents During CODE: The Method and Descriptive View," *Journal of Geophysical Research*, VOL. 90, NO. C3, pp. 4741-4755, 1985.

Foster, M. D., *Evolution of Diurnal Surface Winds and Surface Currents for Monterey Bay*, Master's Thesis, Naval Postgraduate School, Monterey, CA, 1993.

Galt, J. A., "A Finite-Element Solution Procedure for the Interpolation of Current Data in Complex Regions," *Journal of Physical Oceanography*, VOL. 10, pp. 1984-1997, 1980.

Galt, J. A., "Trajectory Analysis for Oil Spills," *Journal of Advanced Marine Technology Conference*, VOL. 11, pp. 91-126, 1994.

Gill, A. E., *Atmosphere-Ocean Dynamics*, Academic Press, 1982.

Han, G., Hansen, D. V. and Galt, J. A., "Steady-State Diagnostic Model of the New York Bight," *Journal of Physical Oceanography*, VOL. 10, pp. 1998-2020, 1980.

Hsu, S. A., *Coastal Meteorology*, Academic Press, 1988.

Melton, D. C., *Remote Sensing and Validation of Surface Currents from HF Radar*, Master's Thesis, Naval Postgraduate School, Monterey, CA, 1995.

Neal, T. C., *Analysis of Monterey Bay CODAR-Derived Surface Currents, March to May 1992*, Master's Thesis, Naval Postgraduate School, Monterey, CA, 1992.

Nuss, W. A., *Coastal Meteorology Science Plan*, ONR NPS-MR 96-001, 1996.

Overstreet, R. and Galt, J. A., *Physical Processes Affecting the Movement and Spreading of Oils in Inland Waters*, NOAA / HAZMAT Report 95-7, 1995.

Paduan, J. D., Petruncio, E. T., Barrick, D. E., and Lipa, B. J., "Surface Currents Within and Offshore of Monterey Bay as Mapped by a Multi-Site HF Radar (CODAR) Network," *Proceedings, IEEE Fifth Working Conference on Current Measurement*, pp. 137-142, February, 1995.

Paduan, J. D., Pickett, M. H., and Cook, M. S., *Comparison of Drifting Buoy and HF Radar (CODAR) Ocean Surface Currents in Monterey Bay*, NOAA Rep. MBNMS 96-01, 1996.

Paduan, J. D. and Rosenfeld, L. K., "Remotely Sensed Surface Currents in Monterey Bay from Shore-Based HF Radar (CODAR)," *Journal of Geophysical Research-Oceans*, VOL. 101, NO. C9, pp. 20669-20686, 1996.

Petruncio, E. T., *Characterization of Tidal Currents in Monterey Bay from Remote and In-Situ Measurements*, Master's Thesis, Naval Postgraduate School, Monterey, CA, 1993.

Petruncio, E. T., *Observations and Modeling of the Inertial Tide in a Submarine Canyon*, Ph.D. Dissertation, Naval Postgraduate School, Monterey, CA, 1996.

Pond, S. and Pickard, G. L., *Introductory Dynamical Oceanography*, 2ed, Pergamon Press, 1989.

Rosenfeld, L. K., Schwing, F. B., Garfield, N., and Tracy, D. E., "Bifurcated Flow from an Upwelling Center: a Cold Water Source for Monterey Bay," *Continental Shelf Research*, VOL. 14, NO. 9, pp. 931-964, 1994.

Stewart, R. H. and Joy, J. W., "HF Radio Measurements of Surface Currents," *Deep-Sea Research*, VOL. 21, pp. 1039-1049, 1974.

Strub, T. P., Kosro, P. M., and Huyer, A., "The Nature of the Cold Filaments in the California Current System," *Journal of Geophysical Research*, VOL. 96, NO. C8, pp. 14,743-14,768, 1991.

Stull, R. B., *An Introduction to Boundary Layer Meteorology*, Kluwer Academic Press, 1988.

Torgrimson, G. M., *On-Scene Spill Model*, NOAA Technical Memorandum NOS OMA 12, 1984.

## INITIAL DISTRIBUTION LIST

No. Copies

1. Defense Technical Information Center . . . . . 2
   8725 John J. Kingman Rd., STE 0944
   Ft. Belvoir, VA 22060-6218

2. Dudley Knox Library . . . . . 2
   Naval Postgraduate School
   411 Dyer Rd.
   Monterey, CA 93943-5101

3. Dr. Robert Bourke (Code OC/Bf) . . . . . 1
   Department of Oceanography
   Naval Postgraduate School
   Monterey, CA 93943-5000

4. Dr. Jeffrey Paduan (Code OC/Pd) . . . . . 1
   Department of Oceanography
   Naval Postgraduate School
   Monterey, CA 93943-5000

5. Dr. Mary Batteen (Code OC/Bv) . . . . . 1
   Department of Oceanography
   Naval Postgraduate School
   Monterey, CA 93943-5000

6. LCDR Margaret Smith . . . . . 1
   Naval Pacific Meteorology and Oceanography Center West
   PSC 498 Box 2
   FPO AP 96536-0051

7. Glen Watabayashi . . . . . 1
   NOAA Hazmat
   7600 Sand Point Way
   NE Seattle, WA 98115

8. Andrew DeVogelaere . . . . . 1
   Monterey Bay National Marine Sanctuary
   Research Coordinator
   299 Foam St., Suite D
   Monterey, CA 93940